

**DESIGN AND DEVELOPMENT OF COMPACT AND
HIGH-PERFORMANCE ANTENNA FOR THE
INTEGRATION OF WIRELESS POSITIONING SYSTEM**

Thesis Submitted for the Award of the Degree of

DOCTOR OF PHILOSOPHY

in

Electronics and Communication

By

Sneha

Registration Number: 41900165

Supervised By

Dr. Praveen Kumar Malik (23314)

Electronics and Communication (Professor)

Lovely Professional University



L OVELY
P ROFESSIONAL
U NIVERSITY

Transforming Education Transforming India

LOVELY PROFESSIONAL UNIVERSITY, PUNJAB

2023

DECLARATION

I, hereby declare that the presented work in the thesis entitled “**Design and Development of Compact and High-Performance Antenna for the Integration of Wireless Positioning System**” in fulfillment of the degree of **Doctor of Philosophy (Ph.D.)** is the outcome of research work carried out by me under the supervision Dr. Praveen Kumar Malik, working as Professor, in the Electronics and Communication Engineering of Lovely Professional University, Punjab, India. In keeping with the general practice of reporting scientific observations, due acknowledgments have been made whenever the work described here has been based on the findings of other investigators. This work has not been submitted in part or full to any other University or Institute for the award of any degree.

Name of the scholar: Sneha

Registration No.:41900165

Department/School: Electronics and Communication Engineering

Lovely Professional University,

Punjab, India

CERTIFICATE

This is to certify that the work reported in the Ph. D. thesis entitled “**Design and Development of Compact and High-Performance Antenna for the Integration of Wireless Positioning System**” submitted in fulfillment of the requirement for the reward of the degree of **Doctor of Philosophy (Ph.D.)** in the department of Electronics and Communication Engineering, is a research work carried out by Sneha,41900165, is a bonafide record of his/her original work carried out under my supervision and that no part of the thesis has been submitted for any other degree, diploma or equivalent course.

(Signature of Supervisor)

Name of supervisor: Dr. Praveen Kumar Malik

Designation: Professor

Department/School: Electronics and Communication

University: Lovely Professional University,
Jalandhar Punjab

ABSTRACT

Communication has always been a part of human evolution. The ever-changing world of technology has always necessitated the ongoing improvement and refinement of communication systems. The Internet has ushered in a completely new age for communication standards. Connecting individuals to gadgets and devices to other devices on a global scale is part of modern communication. Automation of society with the help of sensors is in demand and it can be fulfilled by using IoT with the help of its data communication network system. The sensor era demands cheap and compact devices. Among all the IoT technologies, “LPWAN is wireless wide-area connectivity for low-powered battery-operated devices, which can communicate with less bitrate over a wide range”. It receives huge demands from researchers and industrialists, as it gives wings to the automation world, which is full of sensors, and it fits perfectly for data communication in a smart world. For our thesis work, the NB-IoT and LoRa technologies were chosen because of their huge demands, their characteristics, and the wide area of application of these technologies in a real-time environment.

Any wireless communication system needs antennas, and microstrip antennas are often the best choice for Internet of Things (IoT) applications because they are small, flexible, and easy to design. The multiband, compact, and lightweight antenna is highly required in this automation era, where sensors can communicate and act accordingly. The literature survey is performed on antenna technology used for this LPWAN technology. The antenna specifications are studied, and then the designing process starts with slot technology, meandered, and fractal technology. For both technologies, the efficient planar and compact antennas are designed using HFSS software and fabricated, and their results are measured and cross-checked with the simulated ones. We have also designed two more antennae with some other antenna technology as slotted and fractal designs to achieve broadband characteristics with compact size. The gain and isolation need to improve as the fractal design consists of two port feed systems. In comparison to the existing antenna, the proposed antenna has a low profile, is lightweight, compact and has better gain and radiation characteristics. LoRa antenna is well implemented in the real-time scenario and found better connectivity than the available monopole antenna.

The purpose of this thesis is to develop a compact antenna for low-power IoT technologies specifically NB-IoT and Long-Range technology. A square-slotted circular patch monopole antenna with square slots, symmetric slotted monopole, and fractal geometry MIMO antenna is proposed for NB-IoT communication. The antenna which is square-slotted covers the B1 and B3 bands of NB-IoT and can perform in a multi-antenna environment. The antenna that has a symmetric slot structure covers the B1 band of NB-IoT and a Fractal antenna covers the B1, B3, and B5 bands of NB-IoT. The dimension of the antenna is 30mm x 60mm in size, allowing it to be printed on the NB-IoT module and thereby reducing the overall size of the NB-IoT communication system. The designed antenna is compatible with NB-IoT applications. When compared to existing designs in the literature, the proposed concept is innovative in terms of simplicity of production, size, and gain. The antenna was created using HFSS software and a 1.6mm thick FR4 substrate. The designed antenna was also built and tested in the lab, and the results from the lab measurements and the software simulations were very similar. The test results show that it covers both bands with satisfactory antenna performance. The characteristics of the antenna were analyzed and found suitable for the NB-IoT applications. NB-IoT technology can coincide with all generations of mobile networks and also solve the problems of coverage and consumption. It can also be implemented in all the latest mobile communication devices like cellular phones, IoT module devices, and other chipset devices. NB-IoT also works with the mobile network architecture that is already in place. This gives NB-IoT communication extra security and privacy features. For, LoRa Technology, a meandered-dipole planar antenna is designed, and the antenna is implemented in a real-time environment to verify its performance. The antenna latency is reported to be less than the standard monopole antenna used for LoRa Module devices of the brand Arduino. The fabricated antenna results are in good agreement with the designed antenna. The achieved gain at the operating band is more than 0.5 dB and the radiation efficiency of the antenna is more than 75% for the complete operating band from 861 MHz to 871 MHz. The designed antenna is implemented with LoRa connectivity and communicates the data up to 8 km in line-of-sight communication, more than 1 km in urban environments, and approximately 250 m of connectivity in building areas. The characteristics of the antenna were analyzed and found suitable for the LoRa applications. Future studies can

focus on increasing the range of LoRa in high-traffic areas by adding more gateways along its route. The 433MHz frequency can be combined with the LoRa antenna to make it multi-band and universal in India. In this case, the LoRa antenna is only used to send data, but in the future, it could be used with many sensors to make the environment smarter, such as smart lighting or a smart agriculture system. The bandwidth can also be improved by adding meta surface ground structure to both antennas.

ACKNOWLEDGEMENT

Throughout the writing of this dissertation, I have received a great deal of support and assistance. First and foremost, I would like to express my deep and sincere regards to my supervisor, Prof. Dr. Praveen Kumar Malik for providing me with the opportunity, support, and freedom to carry on this research work. His passion, guidance, and discipline have been indispensable to my growth as a researcher and as a person over these past three years. I am especially grateful for his devotion to his students' education and success. I wish to acknowledge the infrastructure and facilities provided by the Electronics and Communication Department, Lovely Professional University, and the Research Department to guide me on a timely basis regarding norms and guidelines.

I would like to pay my special regards to Prof. Dr. Manoj Kumar Meshram and Mr. Rahul Dubey for their technical support in the Microwave Department of the Indian Institute of Technology (BHU) Varanasi, Uttar Pradesh.

Last, but not least I would express my sincere gratitude to my family for their love, sacrifice, and moral support without their continued support this work would never have been possible.

25-Oct-2023

Table of Contents

S. No	Topic	Page. No
	Title Page	i
	Declaration	ii
	Certificate	iii
	Abstract	iv
	Acknowledgment	vii
	Table of Contents	viii
	List of Tables	xi
	List of Figures	xii
	List of Appendices	xvi
1	Chapter 1 Introduction	1
1.1	Introduction	1
1.2	Low power wide area network technologies	3
1.2.1	Narrow Band IoT	3
1.2.2	Long-Range technology	5
1.3	Motivation	8
1.4	Objective	9
1.5	Thesis outlines	9
1.6	Summary	10
2	Chapter 2 State of the art	11
2.1	Introduction	11
2.2	Literature review	12
2.3	Summary	20
3	Chapter 3 Design, fabrication, and measurement of NB-IoT Antennas	22
3.1	Introduction	22
3.2	Design procedure of MPA	23
3.3	Square-slotted monopole antenna	25

3.3.1	Introduction	25
3.3.2	Design procedure of square-slotted patch antenna	25
3.3.3	Parametric studies	27
3.3.4	Results and discussion	30
3.4	Symmetric slotted monopole antenna	36
3.4.1	Introduction	36
3.4.2	Design procedure of square-slotted patch antenna	36
3.4.3	Results and discussion	39
3.5	Fractal antenna	43
3.5.1	Introduction	43
3.5.2	Design procedure of square-slotted patch antenna	43
3.5.3	Results and discussion	44
3.6	Summary	49
4	Chapter 4 Design, fabrication, and measurement of ultra-wideband antenna	50
4.1	Introduction	50
4.2	Proposed design detail	51
4.3	Results and discussions	51
4.4	Summary	57
5	Chapter 5 Design, fabrication, and measurement of LoRa antenna	58
5.1	Introduction	58
5.2	Proposed design detail	59
5.2.1	Design strategy	59
5.2.2	Antenna geometry	60
5.2.3	Meander line theory and equivalent circuit diagram	60
5.3	Simulations and measurement results	63
5.4	Summary	69
6	Chapter 6 LoRa antenna implementation	70
6.1	Introduction	70
6.2	LoRa Network Setup	70

6.2.1	Requirements	70
6.2.2	Arduino UNO	70
6.2.3	LoRa Module SX1276	71
6.2.4	Software Arduino IDE	72
6.3	Implementation of LoRa connectivity	73
6.4	Summary	78
7	Chapter 7 Conclusion and Future Scope	79
7.1	Introduction	79
7.2	Conclusion	79
7.3	Future Scope	82
	Bibliography	84
	Appendices	100
	List of publication	110
	List of conference	111
	List of patents	112

List of Tables

S. No	Table Name	Page No.
1.1	Frequency Band of LoRa Technology for a Different Country	7
3.1	Comparison table with the antennas published in recent years	33
3.2	The comparison table of all the designed antennas at various steps	39
3.3	Comparison of the final designed antenna with another available antenna for IoT technology	42
3.4	Comparison of the final designed antenna with another available antenna for IoT technology	48
4.1	Comparison of the proposed antenna with other antennas published in recent years	56
5.1	Comparison of the proposed antenna with other antennas published in recent years	66

List of Figures

S. No	Figure Name	Page No.
1.1	Attributes of NB-IoT as presented in 3GPP	3
1.2	Different fields where the NB-IoT can be applicable	4
1.3	3GPP Frequency Spectrum Band Used in NB-IoT	5
1.4	LoRa network communication	6
1.5	Various applications where LoRa can be implemented	7
3.1	Microstrip patch antenna basic design process	23
3.2	The NB-IoT antenna structure (a)top (b) bottom	26
3.3	Designing steps of cropped patch antenna to reduce the size and improve performance	26
3.4	Simulated $ S_{11} $ of antenna for change of dimension and design of NB-IoT Antenna	27
3.5	$ S_{11} $ Plot of circular square slotted patch antenna for different values of width of feed line varies from 3mm to 7mm	28
3.6	$ S_{11} $ Plot of circular square slotted patch antenna for different values of square slot sizes varies from 10mm to 14mm.	29
3.7	$ S_{11} $ Plot of circular square slotted patch antenna for different values of radius of circular patch varies from 15mm to 19mm	29
3.8	$ S_{11} $ Plot of circular square slotted patch antenna for different values of slot designed in-ground length(above) and width (below) both vary as mentioned in the graph	30
3.9	Snapshot of fabricated antenna top (a) and bottom (b) view	31
3.10	Fabricated antenna with vector network Analyzer for $ S_{11} $ measurement	31
3.11	The $ S_{11} $ Vs Frequency of the proposed antenna	32
3.12	The realized gain vs. frequency graph of the proposed antenna	32
3.13	The simulated total efficiency graph	33
3.14	The antenna in an anechoic chamber	35

3.15	The simulated and measured radiation pattern of the proposed antenna in (a) E-Plane and (b) H-Plane at 2 GHz	35
3.16	The Basic Patch Antenna	37
3.17	The Reflection Coefficient of Basic Patch	37
3.18	The final design (a) top and (b) bottom view of the antenna	38
3.19	The design steps (progress) of the proposed patch antenna	38
3.20	Comparative reflection coefficient of antenna a, b, c, d, and e	39
3.21	Fabricated antenna top (a) and bottom (b) view	40
3.22	Fabricated antenna with vector network analyzer for $ S_{11} $ measurement	41
3.23	The simulated and measured $ S_{11} $ vs. frequency graph	41
3.24	The radiation pattern of the proposed antenna in (a) E- Plane (b)H-Plane at 2.1 GHz.	42
3.25	Design steps involved in the Patch design	43
3.26	The dimension of the patch antenna	44
3.27	Reflection coefficient of final designed antenna resonating at 2.09GHz	45
3.28	The simulated gain-frequency band of the designed antenna	46
3.29	Fabricated antenna top (a) and bottom (b) view.	46
3.30	Fabricated antenna with VNA for $ S_{11} $ measurement.	47
3.31	The simulated and measured $ S_{11} $ versus frequency graph.	47
3.32	The Simulated and measured Radiation pattern of the proposed antenna in (a) E-Plane and (b)H-Plane at 2.1 GHz.	48
4.1	(a)Top view of the patch antenna and (b) Bottom view of the patch antenna	51
4.2	The reflection coefficient graph for the ultra-wideband frequency range	52
4.3	The simulated gain versus frequency graph	53
4.4	The simulated total efficiency of the proposed design for the ultra-wideband	54
4.5	Snapshot of fabricated antenna top (a) and bottom (b) view	54

4.6	Fabricated antenna with vector network Analyzer for $ S_{11} $ measurement and in an anechoic chamber for pattern measurement	55
4.7	The simulated and measured reflection Coefficient plot ($ S_{11} $ Vs Frequency) of the proposed antenna.	55
4.8	The measured (E-plane and H-plane) co-polarization and cross-polarization at 3.5GHz for the designed antenna.	56
5.1	Flowchart for antenna designing Strategy	59
5.2	Configuration of the proposed LoRa antenna	60
5.3	Basic meander- line in (a) and its equivalent circuit diagram (b)	62
5.4	The equivalent electrical circuit of the proposed antenna	62
5.5	Snapshot of the fabricated antenna (a) top and (b) bottom	64
5.6	Fabricated antenna with VNA for $ S_{11} $ measurement.	64
5.7	The simulated and measured reflection coefficient graph ($ S_{11} $ vs. Frequency) of the proposed antenna	65
5.8	The simulated gain Vs frequency graph of the proposed antenna Co-polarization(black) and cross-polarization(blue)	65
5.9	The antenna is placed in an anechoic chamber for gain and pattern measurement (a) the antenna is placed in an anechoic chamber (b) horn and fabricated antenna at 5.2 m distance	68
5.10	The radiation pattern comparison of the proposed antenna in (a) E-plane and (b) H-plane at 868 MHz	68
6.1	Arduino UNO Chip	71
6.2	The LoRa Module (EByte E32-868T30S SX1276 868MHz) (a)Module (b)Module with a proposed antenna	71
6.3	Arduino Software window with the program used to address the device	72
6.4	Final Circuit assembly with Laptop, LoRa Module, UNO R3 SMD Atmega328P Board, jumping wires, and reference antenna (one is as transmitter and another one as receiver).	73
6.5	The connection between Arduino and LoRa Module (868MHz)	75

6.6	First experiment- Connectivity for Line of sight (a)receiver set up (b) Map where the experiment (Tx-Transmitter and Rx-Receiver) performed	76
6.7	Second experiment- Connectivity in an urban environment (a)receiver set up (b) Map where the experiment (Tx-Transmitter and Rx-Receiver) performed	76
6.8	Third experiment- Setup for In-building connectivity (a)receiver set up (b) Map where the experiment (Tx-Transmitter and Rx- Receiver) performed	77
II.1	Ansys HFSS simulation procedure for Antenna designing	104
II.2	PCB prototyping machine by eleven labs	105
II.3	The photograph of the VNA is used to measure the return loss of the antenna.	107
II.4	VNA Setup for $ S_{11} $ parameter measurement and $ S_{11} $ parameter representation.	107
II.5	The photograph of the reference antenna and antenna under test in an anechoic chamber.	108
II.6	Block Diagram representation of Antenna-Measurement System	109

List of Appendices

S.no	Appendix	Page No.
I	List of abbreviations	100
II	Antenna design and measurement tools	103

CHAPTER 1

INTRODUCTION

1.1 Introduction

The ever-changing world of technology has always necessitated the ongoing improvement and advancement of communication systems. The Internet has ushered in a completely new age for communication standards. Connecting individuals to gadgets and devices to other devices on a global scale is part of modern communication. More characteristics, such as fast data rates, effective communication, less traffic, and the convenience of using a variety of applications, are required by users of wireless devices. Our expectations of the wireless system rise as these characteristics get more advanced daily. Even scientists are aware of these realities, and they suggest the Internet of Things (IoT) as the ideal way to manage items wirelessly over long distances. The term "IoT," which refers to the supply chain management system, was first used by Kevin Ashton in 1999 [1]. IoT is based on the idea of "smartness," which is defined as a device's capacity to independently gather and infer information [2]. The Internet, which is defined as a link for sensors or devices that may help connect billions of users from many businesses utilizing various internet technologies, and the Internet of Things are two phrases that can be used to describe the Internet of Things. The second word is "thing," which in this context refers to a machine that can be made sentient [3]. Three categories internet-oriented, things-oriented, and knowledge-oriented have been established by Atzori et al. for the IoT [4]. The networking of things or devices is a topic covered under the Internet-oriented category. Both knowledge-oriented categories deal with information components, such as how to store, manage, and process the information available on the server, whereas the things-oriented category is concerned with generic objects. These categories are occasionally referred to as "The IoT Vision by the ITU, which is defined as any time, anyplace connectivity for everybody; we will now have connectivity for anything." [5].

Among all other IoT technologies, The LoRa WAN is one of the low-power technologies that also provides a wider coverage area. Similarly, the Narrow Internet of Things (NB-IoT) provides a wide range of network services that can help to improve IoT Services. LoRa technology provides low data rate communication over a wider scale area. Any communication is done by the transmission of an RF signal through the antenna. An antenna that can transmit and receive a frequency signal. Additionally, it is essential for achieving compactness while constructing circuits. There are numerous types of antennas available on the market, including PIFA, microstrip patch, and horn antennas [6]. Low-profile antennas are sought after in modern communication systems because of their number of advantages and the broad range of applications. As microstrip antennas have many advantages in planar structure, fabrication cost, portability, and many more as compared to conventional and nonplanar antennas, these are also easy to make and affordable to produce.

Deschamps first proposed microstrip patch antennas in 1953, but they were never put into use. Since then, MPA has drawn attention due to its many benefits, including its lightweight, ease of manufacture utilizing PCB technology, low cost, compact size, and simplicity of microwave circuit integration [7]. They have been widely used in medical, remote sensing, space, television, navigation, military, and civilian applications [8]. Microstrip patch antenna has shape flexibility. Multiple frequency operations can also be possible with some modification in different design technologies. Even both polarizations, circular and linear, can be achieved with modification in design that leads to different resonance modes and different electric field directions. To achieve these properties and to overcome the limitation of microstrip patches as low gain, different types of technologies have been introduced in the designing of microstrip patch antennas. Among them, the major technologies that can work well in these LPWAN are multiple input multiple output technologies, fractal design technologies, array antennas, the introduction of metamaterial concepts, and many more.

1.2 Low Power Wide Area Network Technologies

Among all IoT technologies, LoRa and NB-IoT provide a broad range of connectivity to IoT devices, which can easily communicate less bit of data over a wide range when powered by a low-powered battery. It receives huge demands from researchers and industrialists, as it gives the wings to the automation world which is full of sensors and it fits perfectly for data communication in the Smart world. For our thesis work, the NB-IoT and LoRa technologies are chosen because of their huge demands, their characteristics, and the wide area of application of these technologies in a real-time environment.

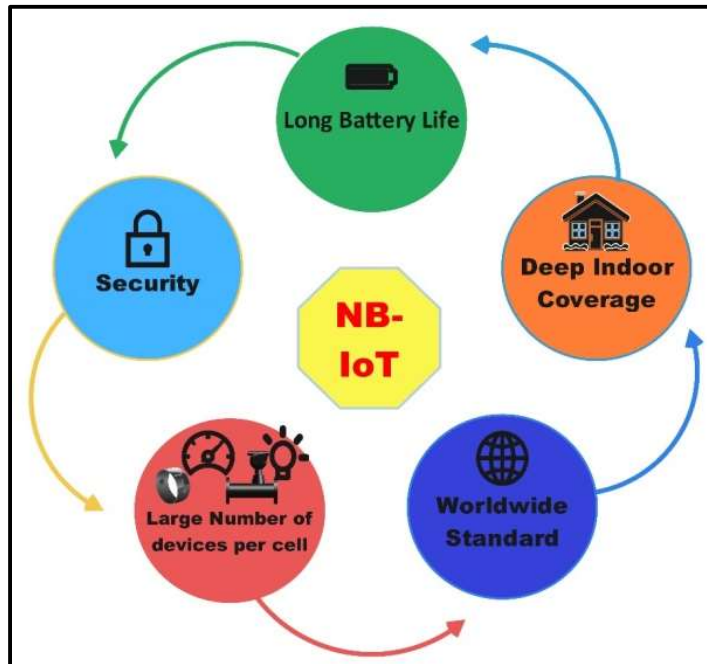


Figure 1.1: Attributes of NB-IoT as presented in 3GPP [10]

1.2.1. Narrow Band IoT

Narrowband IoT technology provides a broad range of connectivity to IoT devices, which can easily communicate a few bits of data over a wide range. The NB-IoT communication needs very little power for data communication, which leads to an increase in the battery life to more than 10 years. Various useful features of NB-IoT make it applicable in many applications that help in automation systems or smart systems. The various features are mentioned in Figure 1.1. NB-IoT technology is developed to fulfill the requirements for a

wide area network, low power consumption devices, and indoor penetration of the signal. NB-IoT is a benefit of the Internet of Things era, where sensor communication is in high demand. NB-IoT technology can be easily merged with mobile network existing technology with some upgradation in software and systems to solve the problem of data communication in wireless sensor networks [9]. In 2015, the 3GPP introduced the NB-IoT. In June 2016, initially, “this technology was known as Cat-NB, and later LTE Cat-NB1 or Cat-N1.

The next version of the Cat-NB is known as Cat-N2 and Cat-NB2 with some advancements and the next upgrade in this technology is named NB-IoT, which is implemented for broader applications” [10]. The specified features or objectives, which are described by 3GPP, are mentioned in Figure 1.1 [11]. They are designed to provide good coverage for both outdoor and indoor applications [12]. The spectrum efficiency and coverage are increased by decreasing the data bandwidth in the NB-IoT communication. They need to communicate the sensors' data, which is only a few bits. The bandwidth spectrum requirement for data communication in NB-IoT is very small compared to general data communication [13].

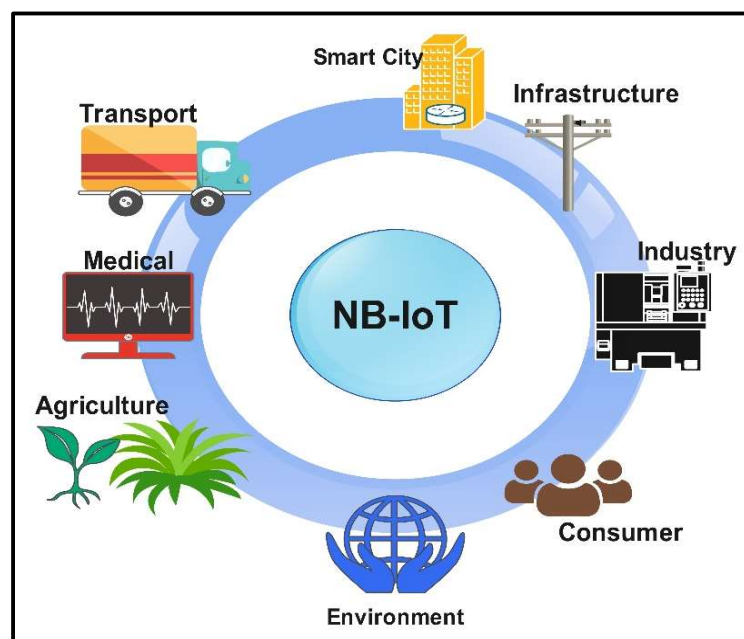


Figure 1.2: Different fields where the NB-IoT can be applicable [10].

NB-IoT technology addresses network layer communication, making it simple to implement and communicate with devices. As shown in Figure 1.2, the simple communication of NB-IoT makes it applicable in almost every smart system for communications. As per the 2019 reports [14], NB-IoT technologies is implemented in 69 Countries for different application with more than 140 employees. NB-IoT utilizes different licensed frequency spectrum mentioned in Figure 1.3, named B1, B3, and B5 which belongs to 2100MHz, 1800MHz, and 850 MHz bands respectively. In the mentioned Figure their uplink and downlink frequency bands are also mentioned and this spectrum is provided by the 3GPP only. It is also predicted as per the report [15], that the NB-IoT technology will occupy almost 60% of the LPWAN communication by 2026, and the rest approximately 40% market will be dominated by SIGFOX and LoRa.

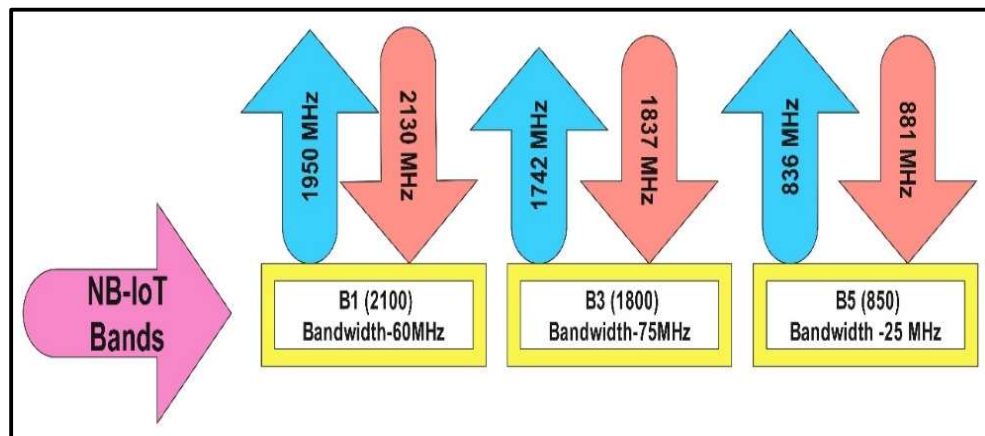


Figure 1.3: 3GPP Frequency Spectrum Band Used in NB-IoT [11].

1.2.2 Long-Range Technology

Long Range (LoRa) is one of the LPWAN (unlicensed open IoT technologies). Its coverage range is good with very low power consumption in data communication, and it can communicate within its network; there is no need for the internet. These features motivate the researcher to work with this technology and work together. Initially, LoRa is a modulation technique that provides a long range of communication at very low power

consumption, and it was developed by two friends, “Nicolas Sornin and Olivier Seller, who lived in France”. But when it comes to reality, they are facing problems with the implementation of this technology. IN 2010, with the help of Francois-Sforza They created a wireless network using LoRa technology in which they used CSS for the data modulation. Using this technology, they have just collected the meter reading data from all the metering devices. When their company Cycleo was acquired by Semtech in May 2012, their collaboration became the LoRa Alliance in February 2015.

In the long-range, data communication is bidirectional as mentioned in Figure 1.4. The internet is required at the server level where the gateways communicate, and the LoRa gateways are connected to thousands of physical devices, including sensors, actuators, trackers, etc., and they communicate with only one frequency hop.

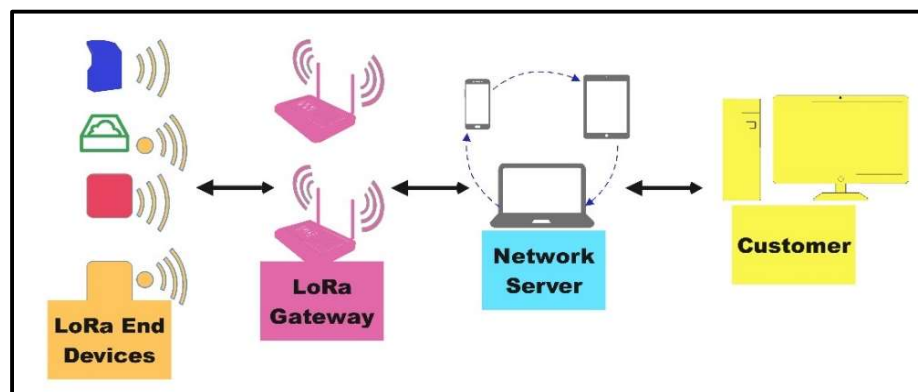


Figure 1.4: LoRa network communication

One of the major advantages of LoRa is its variable transmission properties; “depending on the application's requirements, such as power and delay, some transmission properties, such as spreading factor, coding rate, bandwidth, and transmission power, can be changed to achieve greater efficiency” [18]. The LoRa technology can be very easily implemented in many areas as mentioned in Figure 1.5. Long-range communications also face the problem of interference, scattering, and building interference. The antenna plays a good role in a noisy environment. The requirement for small, lightweight, and good radiation efficiency is the demand for this technology.



Figure 1.5: Various applications where LoRa can be implemented.

Table 1.1 Frequency Band of LoRa Technology for a different country [20].

Country	LoRa Band
India	(865-867) MHz
Europe	433MHz, (863-870) MHz
United States	(902-928) MHz
Asia	923 MHz
South Korea	(920-923) MHz
China	(415-510) MHz, (779-787) MHz
Russia	(864-870) MHz

As mentioned in the literature by many authors, LoRa is implemented in real-time for different applications. As per the authors [16], the LoRa technology is implemented in the urban areas of Italy to find the LoRa connectivity range for data communication. The LoRa

range measurement is also reported in [18–19]. Furthermore, “some of them also measure the latency, packet error rate, packet loss rate, and distortion margin”. The data communication experiment is performed in different scenarios, such as in-building areas, in free space, and line of sight communication. The LoRa technology is allocated with different frequencies for countries as shown in Table 1.1.

1.3 Motivation

Both these, “NB-IoT and LoRa” technologies are LPWAN technologies that provide a wide range with less power consumption, and these things belong to the module and antenna system used for the communication with these technologies, or we can say the antennas used in these technologies. The following are the main requirements of this LPWAN technology to make it more efficient for data communication:

i. Compact transceiver

These two LPWAN technologies require small, planar, and printed antennas that can be accommodated within the LoRa or NB-IoT Module. Isolation needs to be taken care of while designing the printed antenna on the module, as its radiation properties may affect the presence of the module’s lumped element.

ii. Less Power Consumption

The LPWAN technologies are low-power technologies, which means the module used in the communication must be designed to consume less power in data communications. many antenna designing technologies help in designing antennas that may behave as energy harvesters, a transceiver, or sensors.

iii. Optimized Antenna Parameters

Both of these LPWAN technologies require very little bandwidth in data communication so the resonating frequency must be considered accurately while designing the antenna. As the system affects noise the communication by shifting the resonating frequency. For indoor and outdoor application, different radiation pattern is required that also needs to be considered while designing. On these bases, the objective of the thesis is designed.

1.4 Objective

The objective of this thesis is as follows: -

- i. The study, Design, analysis, optimization, and fabrication of wideband microstrip Patch antenna for NB-IoT (800MHz -2.5GHz) Applications using HFSS Software.
- ii. The study, Design, analysis, optimization, and fabrication of small efficient narrowband microstrip Patch antenna for LoRa (865-867) MHz Applications using HFSS Software.
- iii. Testing and real-time implementation of fabricated microstrip patch antenna with the collaboration of the IoT Industry.

1.5 Thesis Outlines

The purpose of this thesis is to develop a compact patch antenna for low-power IoT technologies specifically NB-IoT and Long-Range technology. To accomplish the objectives the thesis is divided into the following chapters.

The thesis starts with the introduction chapters. It explains different LPWAN technologies, their evolution, and their applications. The next Chapter 2 deals with literature surveys related to IoT antennas and the new technology implemented to improve the parameters of IoT antennas for LoRa applications. A comprehensive literature survey using books and various published papers guided me through the entire research work. Various microstrip patch antennas have been designed and analyzed using HFSS software, and after a while, we have designed monopole and slotted monopole for NB-IoT applications and a meandered-dipole antenna for LoRa applications, which are discussed in detail in the next chapters and also provides a detailed explanation of basic design techniques used in antenna design, such as meandered and defected geometries for NB-IoT and LoRa bands. Chapter 6 is about the real-time implementation of a LoRa antenna, in which the LoRa connectivity is verified and the range of the LoRa antenna is tested in a LOS situation, in a building, and on the free ground. In the last chapter, the conclusions drawn from this

research work are explained, and future research work that can be an extension of this work is mentioned.

1.6. Summary

This chapter begins with an introduction to IoT technology and a study of the various LPWAN technologies is performed to ensure the benefits of choosing NB-IoT and LoRa technologies. The research gaps and objectives are discussed in detail. There is a brief discussion of the research conducted for the ensuing chapters. This chapter contains an outline of the research thesis.

CHAPTER 2

STATE OF THE ART

2.1. Introduction

Communication has always been a part of human evolution. The ever-changing world of technology has always necessitated the ongoing improvement and refinement of communication systems. The Internet has ushered in a completely new age for communication standards. Connecting individuals to gadgets and devices to other devices on a global scale is part of modern communication. Automation of society with the help of sensors is in demand and it can be fulfilled by using IoT with the help of its data communication network system. Communication systems in IoT rely heavily on the transmission and reception of data between devices and central hubs or the cloud. Antennas play a crucial role in this process as they are the bridge between the physical world and the digital realm. Antennas are responsible for capturing and emitting radio waves that carry data between IoT devices, enabling them to communicate with each other or with remote servers. The choice of antenna type, design, and placement directly impacts the range, reliability, and efficiency of IoT communication. Whether it's a small, embedded antenna for a low-power sensor node or a high-gain directional antenna for long-range communication, selecting the right antenna is pivotal in ensuring the success of an IoT deployment. Therefore, the synergy between the communication system and the antenna used is vital for optimizing IoT connectivity, enabling real-time data exchange, and ultimately realizing the full potential of the IoT ecosystem. Thus, a harmonious relationship between communication systems and antennas is essential to ensure that IoT devices can communicate effectively, enabling the seamless flow of data that underpins the IoT's transformative potential across various industries. Among all the IoT technologies, “LPWAN is wireless wide-area connectivity for low-powered battery-operated devices, which can communicate with less bitrate over a wide range”. It receives huge demands from researchers and industrialists, as it gives wings to the automation world, which is full of sensors, and it fits perfectly for data communication in a smart world. For the thesis work, the NB-IoT and LoRa technologies were chosen because of their huge demands,

their characteristics, and the wide area of application of these technologies in a real-time environment. Many strategies have been investigated in the literature review to improve the bandwidth, return loss, gain, and directivity of antennas.

2.2. Literature Review

Das et al. (2017), presented an Icosidodecagon-shaped microstrip patch antenna which is fed with a microstrip line. The designed antenna resonates at multiple frequencies. They used the FR4 substrate of 4.4 dielectric constants with loss tangent 2.2 for antenna designing. The presented antenna is applicable for Wi-Fi, WLAN, GPS, and IoT fields [49].

Das et al. (2017), have designed a starfish-shaped microstrip patch antenna that is fed with a microstrip line. This antenna is designed with an FR4 substrate. This antenna is applicable for Bluetooth, Wi-Fi, and WiMAX and enables IoT applications. [50].

Satheesh et al. (2017), studied and designed different slot structures to evaluate their performance and to find an efficient design. In this paper, they have introduced different shaped slots and observed their variation in the shifting of frequency and characteristics of the antenna. Finally, “with the help of U-slots, they get the best result and shift in frequency to 1.5GHz from 2.4GHz and the antenna is miniaturized” [51].

Y.Giay et al. (2018)., designed and evaluated the performance of a microstrip array antenna. In the array design, they have designed a 4-patch structure of the same size, and a microstrip feed structure is designed with the help of designing tools available in HFSS. The proposed design has 6.9 dB of gain [52].

Dardeer et al. (2018)., presented a circular polarized, low-profile array antenna. It is a 2X2 array microstrip antenna that is used to harvest RF energy and is very useful for IoT applications. for the input to the antenna, a Wilkinson power divider is used and designed. It can easily be applied in the IoT field. The dimension of the designed antenna is 54 X 54 X 1.6 mm³. “The designed antenna is fed with sequential feeding at the top of the designed

antenna. The simulated bandwidth of the antenna is 910 MHz at a resonance of 2.5GHz and 360MHz at a resonant frequency of 5GHz for WLAN applications” [53].

Awais et al. (2018) ., presented a novel type of antenna from a rectangular shape antenna to an antenna with rounded corners technique which is fed with a (CPW). The antenna resonates at two frequencies, at 2.4GHz and 3.5GHz giving an ultra-bandwidth of 1.6GHz and 500MHz respectively. This kind of antenna can be useful in Bluetooth, Wi-Fi bands, and 3G, 4G, and 5G applications [54].

K. Shafique et al. (2018) ., presented a new kind of antenna that behaves as a 2.4 GHz RF energy harvester and is used in IoT applications. The proposed rectenna in this paper has efficient behavior. The design is simple and fabricated using FR4 with a dimension of 285 mm X 90mm X 1.6 mm. Therefore, this design is very useful and suitable for the next-generation IoT application The efficiency of the antenna is approx. 98% [55].

Lizzi et al. (2018)., presented a small printed Planar inverted F antenna (PIFA). It resonates at multiple frequencies. This antenna is of low profile and can easily integrate with IoT handheld terminals. The dimension of the design is 40 X 25 X 1 mm³. This is resonating at the L band of frequency (915MHz) and GPSL1 (1.57GHz) and L2 (1.23GHz) bands and can be implemented for Long-Range Communication Technology [56].

Qianyun Zhang et al. (2018)., introduce “a miniature printed inverted F antenna (PIFA)”, and it is placed on the LoRa Module’s PCB. To reduce the PIFA’s working frequency and produce a second resonance to widen the bandwidth, slots are cut into the 1.6 mm-thick board’s surface because there isn’t much room left for antenna deployment. [57].

Shi et al. (2019) ., presented a small RFID tag antenna. The antenna is also implemented and tested in a real-time environment. The tag antenna was tested in an intensive tag scenario and found an accuracy of 98%. they also found that near field frequency is shifted by environmental factors, and the position of tag arrangements such as Stacked tags, and jumbled tags. They also verified the derived formula and found that the average error found in this formula is less than the average error found by the traditional formula. The small RFID tag antenna is very efficient and more accurate than the traditional one [58].

Shahidul Islam et al. (2019) ., presented a microstrip printed antenna of various techniques like inverted S-shape microstrip, rectangular box, capacitive loading, and parasitic patch and investigated their result and performance. This is the meander line antenna which is operated at a 2.4GHz frequency range. By introducing an s-shaped structure in the design “the efficiency of the antenna is improved and with the parasitic patch”, they achieved a high fractional bandwidth of 12.5%. with all such improvements. The simulated gain of the antenna is 1.347dBi [59].

Vamseekrishna et al. (2019) ., presented a microstrip patch antenna that is octahedron-shaped. This antenna is designed with reconfigurable techniques. It is a quadruple-band antenna that resonates at four frequencies of different bands. It can be applied in the field of sensors or microwave sensing IoT applications. From the simulated result, we can say that the fabricated antenna can imply the number of wireless applications as it covers almost all bands S, C, and X bands [60].

Mung et al. (2019) ., presented an antenna with foldable and non-foldable structures. The advantage of the foldable structure is that it can be easily used as a wearable antenna and implemented in the field of medicine. From the fabricated result, it is observed that non-foldable structures show better gain as compared to foldable structure antennae [61].

Sharif et al. (2019) ., presented a small RFID tag antenna. The antenna is also implemented and tested in a real-time environment. it is a novel design made for metallic cans especially. These metallic tags will help in automatic billing and generating alert messages of a shortage of cans. This type of small, low cost and low-profile antenna is so useful for the RFID tag and the novelty of this design is that it uses the metallic can structure as a radiator that improves the gain. They implement these designs to check the real-time performance of this antenna and the antenna can be easily read by a distance of 2.5m in all directions and the reading accuracy of the tag antenna is 98% approximate [62].

Sabban et al. (2019), present compact Ultra-Wideband novel wearable active fractal slot antennas in frequencies ranging from 0.5GHz to 4GHz. The author used the metamaterial concept to enhance the efficiency of the antenna and reduce the size of the antenna. The

mentioned antenna can be used for IoT applications and the medical field as a wearable device [63].

Torre et al., (2019), present the textile-based wearable antenna. That is also implemented with the LoRa technology to check the connectivity distance or to find the range of the antenna. [64].

S. I. Lopes et al. (2019), present a PIFA design compact antenna that can be designed on LoRa module 868GHz. Additionally, they demonstrated LoRa connectivity, which is good up to 4.2 km for Line-of-Sight communication. This design guarantees greater environmental robustness without sacrificing implementation or omnidirectionality. The PIFA has a branch connected to the ground in addition to the branch connected to the radio frequency signal (RF) [65].

F. Ferrero et al. (2019), present a UCA-shaped LoRa antenna. For LPWAN, a 90*30mm terminal is designed to accommodate a dual-band tiny antenna that operates on the 433MHz and 868MHz bands. The utilization of two lumped components placed inside the radiating element as part of a design technique is presented. Electronic parts and a battery are used to build and assemble the optimal antenna. In an anechoic chamber, a measurement is made to evaluate the radiation performance. With a dipolar radiation pattern, the terminal has a total gain of -6dB at 433MHz and -4.5dB at 868MHz, respectively [66].

W. M. Abdulkawi et al. (2019), propose a unique pattern-reconfigurable antenna built on RF MEMS that can guide beams in three different directions. The suggested antenna is constructed on a 1.75 mm thick, RT Duroid substrate with a 2.2 dielectric constant. [67].

A. Birwal et al. (2019), show a novel rectangular patch antenna that is coplanar waveguide (CPW) fed and has a ground plane with a square shape that can be used in current high-tech navigation systems. The antenna is applicable in L-Band applications. The single-feed circularly polarised antenna is easy to integrate with other high-frequency communication equipment has a low profile and is lightweight [68].

Aksha Mushtaq et al., (2020) have designed a microstrip antenna resonating in LoRa Band. the antenna is designed using CST Software and resonates at 433MHz frequency providing a gain of 2 dB, the substrate is FR4. The dimension of the antenna is 210.82 X 164.79 mm². they use the Slot Technique with the microstrip ground plane to improve its Gain. The antenna can be used in LoRa of frequency range 433MHz [69].

Aayush Pandey et al., (2020) have designed “a microstrip Patch antenna with defective ground structure and its resonating frequency is 871 MHz with a bandwidth of 28MHz and gains 0.58dB”. it is applied in the field of IoT with LoRa application [70].

Turke Althobaiti et al., (2020) have proposed an RFID tag antenna for use in IoT applications, which consists of two meander-line structures and a shorting stub. The structure resembles the bow-tie or dipole structure and provides dual polarisation properties. The antenna is designed to be used as a tag antenna in the frequency range of 900MHz [71].

Prem P. Singh et al., (2020) It has designed a planar antenna with two techniques; one with slotted symmetry with parasitic loading and the other with combinational PIN diode switching. With the help of a PIN diode, the antenna resonates at 5 different frequencies in the range of 3.85GHz to 6.01GHz. The corner truncation is also implemented in this design, which leads to the circular polarisation of the proposed design. The antenna offers an average gain of 2.5 dB. It can be used for WLAN, Wi-Max, and IoT applications [72].

Yi Yan et al., (2020) The proposed structure resonates in the RFID frequency range. The band covered by the proposed antenna structure is 902MHz–928MHz. This structure achieves slant polarization, which improves antenna readability. [73].

M. Wang et al. (2020), suggested the patch rectenna to harvest the RF energy in IoT applications. they proposed an antenna with two ports and slots in the shapes of an arrow, a circle, and a rectangle. To transform the RF power collected by the antenna into DC power, a new matching network and a voltage doubler rectifying circuit are created as part of a broadband rectifier. it can be widely used to provide power supply to IoT sensors [74].

Mainsuri et al. (2020), present a smart beam steering antenna at a LoRa frequency of 923 MHz which is an operating frequency in Indonesia. The proposed antenna allows the steering of the antenna beam into 360-degree azimuthal coverage. The principal lobe of the antenna is altered at every 60-degree step. The gain of the antenna is also approximately 8.52 dB. The dimension of the cover casing is 100mm, 200mm, and 90mm with a diameter of 54mm [75].

Sneha et al. (2020), have presented a tri-band metamaterial-based monopole antenna, that can be used for the navigation system at the ground terminal. The proposed antenna covers the L1, L5, and S-band for navigation applications [76].

J. Kulkarni (2020), has proposed the monopole antenna. The proposed antenna operates in the GSM, WLAN, and Wi-MAX bands. It exhibits virtually omnidirectional radiation properties, an overall gain considerably above 4 dB, and a radiation efficiency of at least 80%. This demonstrates that the suggested antenna design is appropriate for use with wireless operations in laptop computers [77].

L. Zhuo et al. (2020), proposed a rectangular tuning stub-equipped U-shaped NB-IoT antenna. By exciting two different operating modes, through stub tuning, the proposed antenna exhibits dual-band properties. On the antenna's ground plate, a large slot in the shape of a U is employed to provide electromagnetic coupling and enable the antenna's broadband properties [78].

S. A. Haydhah et al. (2021), present a small pattern reconfigurable antenna with four radiation patterns is suggested. The antenna's resonance frequency is 868 MHz. The dimension of the antenna with the integrated device is 80mm X 55mm. Two meandering slots and one meandering monopole behave as the radiating components. Utilizing four PIN diodes, pattern reconfigurability is accomplished. The radiation efficiency of the slots was increased by 2.25 dB by eliminating the FR-4 material inside of them [79].

R. Hussain et al. (2021), present an IoT antenna design provided for 5G sub-1 GHz applications that require low power and long-range communications. Wide-band frequency

reconfigurability in the sub-1 GHz range is made possible with the aid of the varactor diode. The frequency ranges covered by the suggested antenna range from 758 to 1034 MHz. The antenna is constructed on an RO-4350 board that has a dimension of 60 X 27 mm². The suggested antenna design stands out for its straightforward biasing circuitry and small, low-profile device with a variety of tuning options [80].

A.Dala et al. (2021), present an implementation of a sensor node antenna capable of long-range (LoRa) communication both underwater and on the water's surface at 868 MHz. A data gateway node may be reached by the sensor node with the buffered antenna at a distance of 160 meters above the water and 6 meters under it. Without a buffered antenna, the communication range of the sensor node over the water surface is only 80 m [81].

C. Rohan et al. (2021), have designed a split ring resonator-based patch antenna used for 900 MHz LoRa applications. In this study, split-ring resonator (SRR) designs are investigated for creating planar antennas with maximum dimensions that are smaller than equivalent monopole designs operating at the same frequency [82].

N.F. Ibrahim et al. (2021), The suggested antenna is designed to support precise localization, and communication needs in the medical, industrial, and military sectors. The patch antenna's modest profile makes it easy to incorporate into garments. “Three textile layers make up the device: a neoprene substrate, and top and bottom polystyrene textiles that have been printed with silver ink [83].

X. Wang et al. (2021), present a textile patch PIFA for LoRa applications. To achieve dual band and wire band features, the radiating plate and ground plane slots were used in the design. To confirm the concept, a prototype covering the two LoRa application operating bands of 433 MHz and 868 MHz was made and measured. The suggested design's SAR is assessed and found to fulfill European norms. A potential choice for LoRa (Long Range) applications is the cloth antenna [84].

F. Mira et al. (2021), have presented a dual-band circularly polarized antenna for LoRa applications. The proposed structure is designed using slotting and stacking techniques that

help in switching the beamwidth of the antenna around 90 degrees and 75 degrees for GPS and Wi-Fi (2.4GHz), frequency bands [85].

W.M. Abdulkawi et al. (2021), introduce a novel single and dual-band patch antenna. The antenna utilizes the square patch structure and four slots in it. The antenna resonates at a frequency band of 2.4 GHz and 2.8 GHz, applicable for IoT applications [86].

H. Singh et al. (2021), proposed a compact antenna for narrow-band -IoT applications. The analysis and evaluation of wideband antenna designs for 5G and NB-IoT applications. The antenna has a folded dipole structure, with a dimension of 35mm X 48mm X 1.62mm, and the ground structure is combined with a metamaterial structure that helps in the gain of the antenna [87].

G. A. Casula et al. (2021), designed a wearable textile antenna that operates at 915 MHz in the UHF frequency range. The suggested architecture is ideal for use because it is small in size and provides excellent isolation. The antenna can be applicable for LoRa and RFID applications [88].

N. A. H. Putra et al. (2021), proposed a square patch antenna for the 924 MHz frequency band. The antenna uses a CSRR to boost gain and reduce antenna size. It is constructed using a Rogers Duroid RT6006 substrate [89].

Z.A.Dayo et al.(2022), The antenna can be used for medical IoT. The antenna utilizes the slot and stub loading technique to improve its efficiency of the antenna. The overall dimension of the antenna is 22mm X 28mm X 1.5mm. The -10dB bandwidth of the proposed structure is 3.65GHz -11.41 GHz [90].

M.Wagih et al. (2022), have presented a broadband Omni directional antenna for LoRa applications. The antenna is well-tested for channel gain and the effect of motion, elevation, and shadowing is also observed with LoRa connectivity. The antenna is designed on a cardboard substrate [91].

R. Hussain et al. (2022), have presented a meandered loop slot line structure. The frequency reconfigurability is achieved using a varactor diode. The suggested antenna has

a minimum bandwidth of 17 MHz over the whole frequency band and resonates over the range of (758-1034) MHz [92].

R. Roges et al. (2022), “have designed an antenna with a dimension of 22mm×34mm×0.5mm. The antenna's simulation and experiment findings are in good agreement, and its operational range features a low VSWR when compared to other antennas operating at the same frequencies, the proposed antenna stands out primarily for its size and performance [93].

A. Mushtaq et al. (2022), proposed array antenna in the current study has dimensions of 159 X 210 X 2.55 mm³ (LoRa band). Further, the gain of an antenna is improved by introducing the T-shaped slots in the patch [94].

S. Robee et al. (2022), present a LoRa patch antenna that works satisfactorily in an environment, in the radiation pattern, bandwidth, and input impedance. The PIFA structure is perfectly matched with the input circuit which improves the efficiency of the antenna [95].

N.Zalfani et al.(2022), presents a miniature printed monopole meander line antenna for the 920 MHz operating band. The meander technology is used to design the antenna. The proposed structure is very small in size 80mm X 50mm and designed on an FR4 substrate. The antenna shows a gain of 1.8dB and an omnidirectional radiation pattern [96].

S. Wang et al. (2022), present a 3X 3 artificial magnetic conductor ISM band dual-band flexible monopole antenna that is suggested. The antenna substrate is made of polyimide, which gives the antenna its bendability and thinness. The double-ring AMC structure's in-phase reflective qualities help the antenna's radiation characteristics [97].

2.3. Summary

From the literature, it is evident that designing an exactly perfect antenna for the communication system in all aspects is an impossible task, but it can be reached to its maximum by incorporating some techniques in antenna design. Several features need to be

considered when designing the antenna, such as bandwidth, multi-band, loss gain, design complexity, size, and efficiency, so research and design work is still ongoing to improve the antenna in terms of these parameters. The research gap in this study lies in the need for the development of compact transceivers for LPWAN technologies with small, planar, printed antennas that ensure proper isolation to avoid interference with the module's lumped element. Additionally, there is a gap in designing modules with reduced power consumption and exploring antenna technologies that can function as energy harvesters, transceivers, or sensors. Lastly, optimizing antenna parameters, including resonating frequency and radiation pattern, to meet the specific requirements of indoor and outdoor. To fulfill this research gap, the majority of this chapter is devoted to a review of the literature on microstrip patch antennas for use in IoT applications especially those associated with L and S-band. Additionally, it inspires the design of multiband microstrip patch antennas with defective and meandering techniques to improve antenna performance. From the literature, it can be concluded that IoT is crucial due to its wide-ranging applications that enhance efficiency, provide valuable insights, improve quality of life, contribute to sustainability, enhance safety and security, optimize supply chains, boost business competitiveness, advance healthcare and agriculture, promote global connectivity, and drive technological innovation. The literature survey confirms that IoT has the potential to profoundly impact various aspects of society and the economy, making it a crucial and transformative technology.

CHAPTER 3

DESIGN, FABRICATION, AND MEASUREMENT OF NB-IoT ANTENNAS

3.1 Introduction

The future of the Internet of Things is LoRa and NB-IoT as their coverage range is very high with good power management. A square-slotted circular patch monopole antenna with square slots, symmetric slotted monopole, and fractal geometry antenna is proposed for the NB-IoT frequency band. The proposed antenna is the size of 30mm x 60mm in size, allowing it to be printed on the NB-IoT module. The designed antenna is compatible with NB-IoT applications in the B1 (2100) MHz, B3 (1800) MHz, and B5 (850) MHz bands". When compared to existing designs in the literature, the proposed concept is innovative in terms of simplicity of production, size, and gain. The antenna was created using HFSS software and a 1.6mm thick FR4 substrate. The designed antenna was also built and tested in the lab, and the results from the lab measurements and the software simulations were very similar.

The contribution of the mentioned work is summarised as follows:

- The antenna has a relatively small dimension as compared to the reported antennas in the literature.
- The antenna mentioned in section 3.3 is square-slotted covers the B1 and B3 bands of NB-IoT and can perform in a multi-antenna environment.
- The antenna mentioned in Section 3.4 that has a symmetric slot structure covers the B1 band of NB-IoT and a Fractal antenna that is discussed in Section 3.5 covers the B1, B3, and B5 bands of NB-IoT.
- The design is also simple, which makes it easy to make, and the antenna's small size makes it likely that it will be placed on the NB-IoT module, which will make the communication module of NB-IoT smaller.

3.2 Design Procedure of MPA [6]

A microstrip patch is constructed using ground, patch, and substrate with a feed. These parameters are given below:

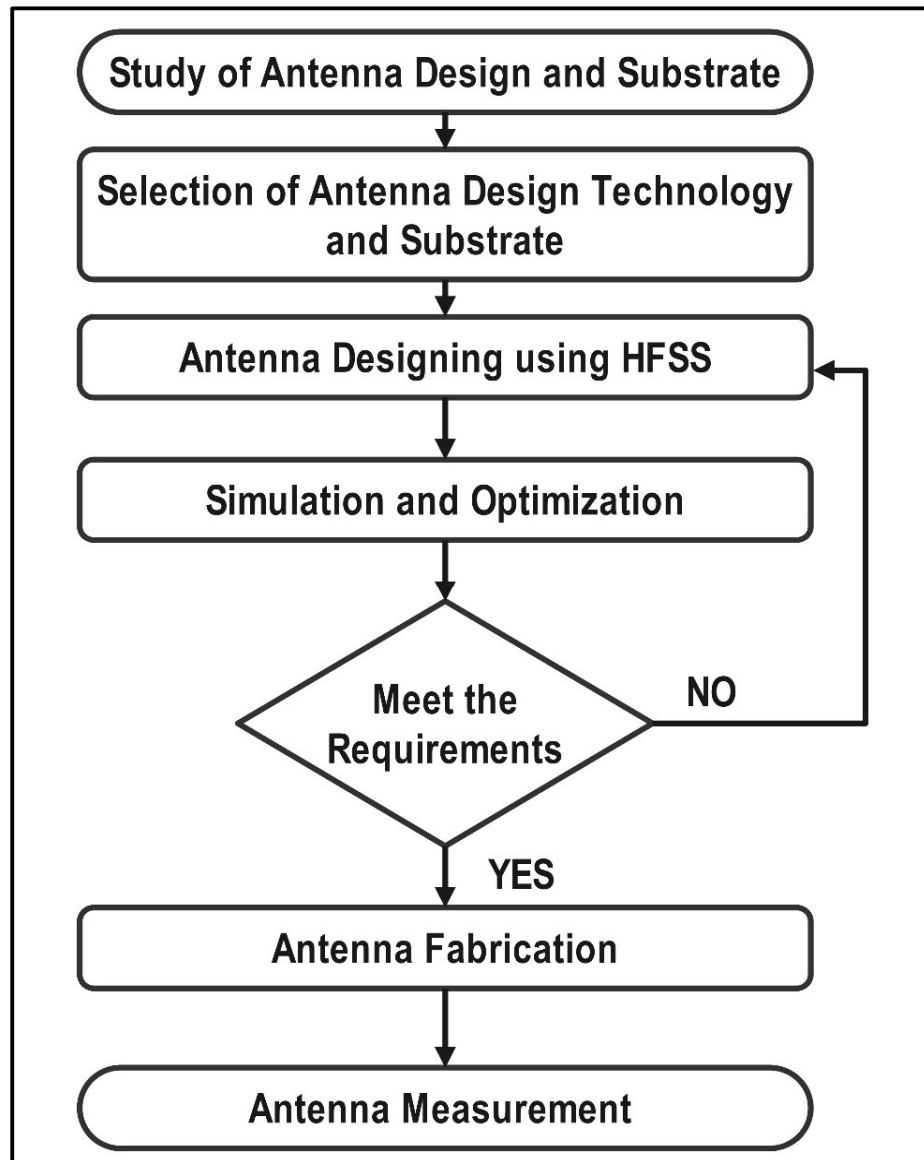


Figure 3.1: Microstrip patch antenna basic design process

- **Dielectric constant (ϵ_r):** “The dielectric constant of substrate material has an important role in antenna designing. But it will affect the performance of the antenna. So, there is a trade-off between the size and performance of the microstrip antenna” [6].
- **Height (h):** In compact communication systems, the profile of the antenna must be low. Hence, the height of the dielectric substrate should be less. As per the application, the above parameter’s values are calculated. The design steps for the microstrip patch antenna are mentioned in Figure 3.1.

a) **Selection of substrate:** The appropriate selection of substrate thickness is more important in antenna design. Due to variations in the thickness of the substrate, there is also a change in the Bandwidth and radiation efficiency of the antenna. The radiation efficiency of the microstrip antenna depends mainly on the permittivity of the dielectric material.

b) **Width of the patch:** The width of the microstrip patch antenna is calculated by the equation, Width = mm

$$W = \frac{c}{2 * f_r} \sqrt{\frac{2}{\epsilon_r + 1}} \quad (3.1)$$

c) **The effective length:** By using equation 3.2, The effective length of the MSA antenna is Length= mm

$$L = \frac{c}{2 * f_r * \sqrt{\epsilon_r}} \quad (3.2)$$

d) **The effective dielectric constant:** Using equation 3.3, the effective dielectric constant can be found

$$\epsilon_{r_{eff}} = \frac{\epsilon_r + 1}{2} + \frac{\epsilon_r - 1}{2} + \left(1 + \frac{12 * h}{W}\right)^{1/2} \quad (3.3)$$

e) **The length extension:** The length extension is

$$\frac{\Delta L}{h} = 0.412 \frac{(\epsilon_{r_{eff}} + 1) \left(\frac{W}{h} + 0.264\right)}{(\epsilon_{r_{eff}} - 0.258) \left(\frac{W}{h} + 0.8\right)} \quad (3.4)$$

f) **The actual length of the patch:** The actual length is obtained by the equation,

$$L_{eff} = L - 2\Delta L \quad (3.5)$$

3.3 Square Slotted Monopole antenna

3.3.1 Introduction

A square-slotted circular patch monopole antenna with square slots is designed, fabricated, and measured. The simulated antenna resonates at 2.1GHz and 1.8GHz, producing an 885 MHz bandwidth (-10 dB) and a gain of more than 4.42 dBi throughout the full bandwidth and omnidirectional radiating pattern.

3.3.2 Design procedure of square slotted patch antenna

The optimized design structure of the proposed NB-IoT antenna with the dimension in mm. The designed prototype is a combination of different parts such as a cropped circular patch, microstrip feedline, lumped port, square slot and slotted ground. The length of the ground has been adjusted to achieve impedance matching with the monopole, and it is connected through a microstrip feed line. To enhance impedance matching and optimize the antenna's radiation efficiency, a slot has been introduced in the ground plane. The designed structure was simulated using the Ansoft High-Frequency Structure Simulator (HFSS). Furthermore, a square slot has been integrated into the patch, resulting in a second resonance frequency within the B3 frequency band. The initial design involves a circular patch monopole antenna that is fed using a microstrip line. It resonates at approximately 2.1 GHz but has a narrow bandwidth limited to the B1 band of NB-IoT.

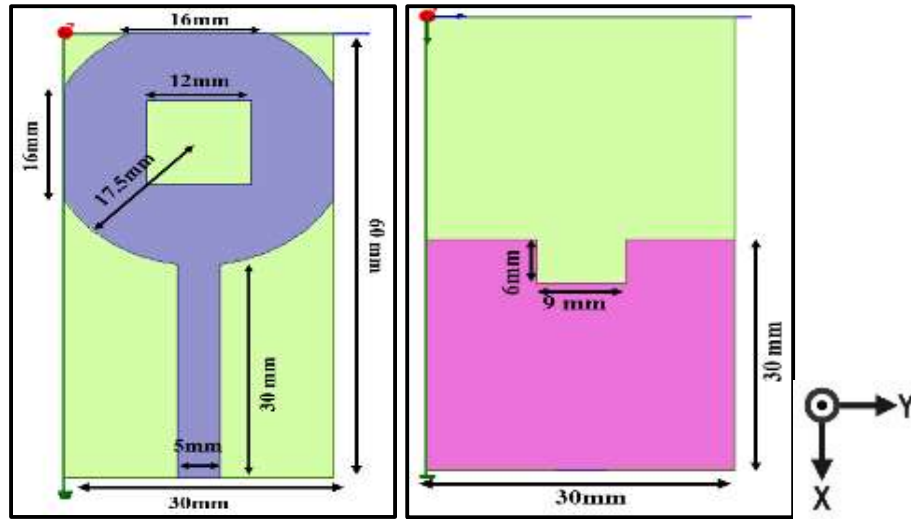


Figure 3.2: The NB-IoT antenna structure (a)Top (b) bottom

Figure 3.3 shows the design procedures. Initially, the circular patch monopole antenna is designed, which is fed with the microstrip line feed, and it resonates around 2.1 GHz but provides a very low bandwidth that covers only the B1 band of NB-IoT. Figure 3.3 (a) resonates at 2 GHz but doesn't give a good resonance as the feedline is mismatched with the patch. To decrease the impedance at the joint, the slot is introduced at the ground, leading to adding inductance and capacitance as mentioned in Figure 3.3 (b). The purpose of this article is to cover both bands B1 and B3 of NB-IoT, so to increase the bandwidth, a square slot is introduced in the upper patch that gives one more resonance at 1.8GHz as mentioned in Figure 3.3 (c), and the last circular patch is cropped to reduce the size by 4mm x 2mm. The affected $|S_{11}|$ (dB) parameter is mentioned in Figure 3.4 as per the design mentioned in Figure 3.3.

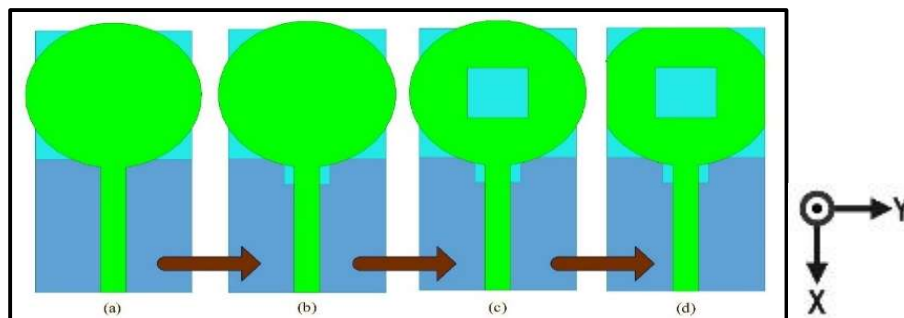


Figure 3.3: Designing steps of cropped patch antenna to reduce the size and improve performance (green-upper patch and grey-ground plane).

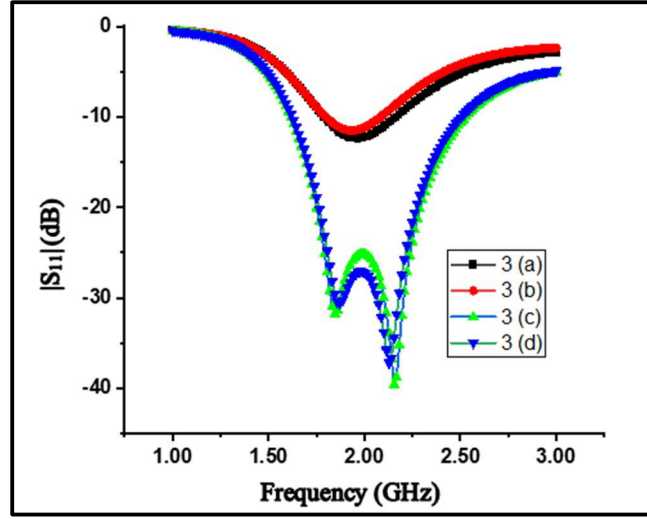


Figure 3.4: Simulated $|S_{11}|$ (dB) of antenna for change of dimension and design of NB-IoT Antenna.

3.3.3 Parametric Studies

A parametric study was performed to optimize the size and performance of the designed antenna. Parameters that affect the performance of the antenna effectively are also determined, and they are as follows:

3.3.3.1 Feed Line Width.

The width of the feed line is inversely correlated with the input impedance of the antenna. When the patch dimension and dielectric substrate are chosen, In the mentioned design, the initial microstrip line width is calculated using equation 3.6 [6] and then it is optimized as per simulated results. In the design, a width of 12 mm is selected, which is a trade-off between the perfect match and bandwidth. We can also find the width dimension by using an online width calculator [99].

Formula to find the width of the feed line [6]

$$Z_c = \frac{60}{\sqrt{\epsilon_{reff}}} \ln \left[\frac{8h}{W_o} + \frac{W_o}{4h} \right], \quad \text{if } \frac{W_o}{h} \leq 1 \quad (3.6)$$

and

$$Z_c = \frac{120\pi}{\sqrt{\epsilon_{reff}} \left[\frac{W_o}{h} + 1.393 + 0.667 \ln \left(\frac{W_o}{h} + 1.444 \right) \right]}, \quad \text{if } \frac{W_o}{h} > 1 \quad (3.7)$$

Where Z_c =characteristics impedance of feed line as we have a 50 ohm connector feed so mostly it will be 50 ohms for a perfect match.

h = height of substrate

ϵ_{reff} =Effective dielectric constant

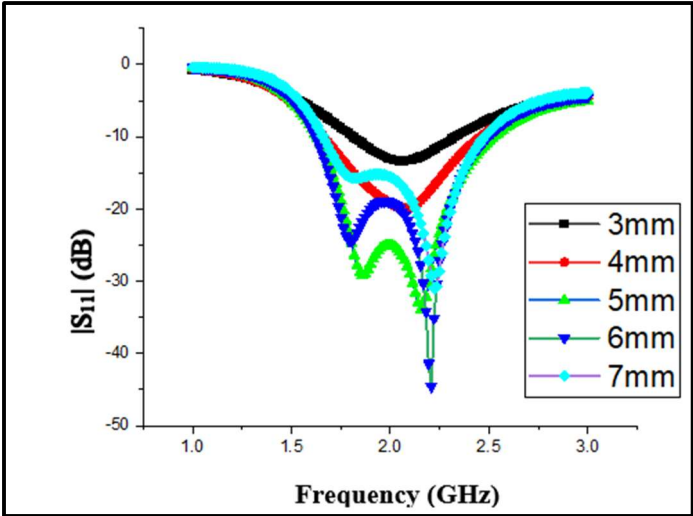


Figure 3.5: $|S_{11}|$ (dB) Plot of circular square slotted patch structure: width of feed line varies from 3mm to 7mm.

3.3.3.2 Width of Square Slot.

The antenna's slot shape deals with the antenna impedance matching and electromagnetic coupling with the patch. From the reflection coefficient graph mentioned in Figure 3.6, it is concluded that the slot size does not affect the resonance frequency but it affects the impedance, because of their small size, it doesn't affect the bandwidth very much [78]. When the patch shape is designed, a change in slot size will affect the current distribution, and the impedance may change, affecting the resonance. Here we have varied the square slot size from 10mm to 14mm and an optimized size of 12mm slot was selected that gives a good response and good impedance match.

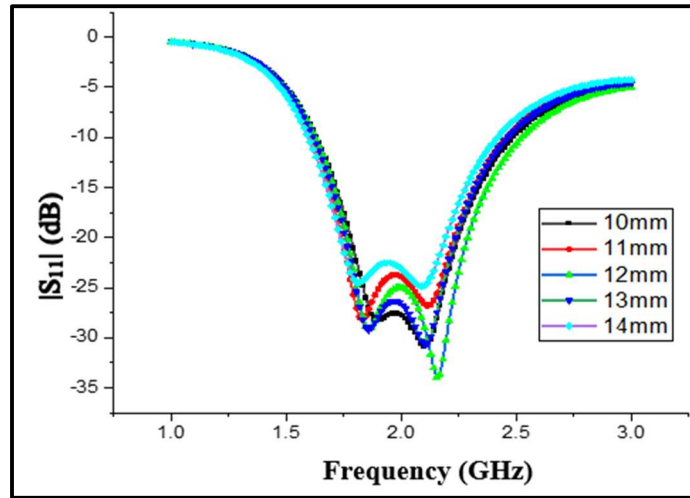


Figure 3.6: $|S_{11}|$ (dB) Plot of circular square slotted patch antenna for different values of square slot sizes varies from 10mm to 14mm.

3.3.3.3 Circular patch radius

With the variation of the radius of the circular patch, the resonant length of the antenna varies, changing the resonant frequency. The variation in resonant frequency is shown in Figure 3.7. As a result, a reasonable radius of 17.5 is selected after optimization as per the size availability of the NB-IoT Module chip and frequency requirements. The parametric study varies from 15mm to 19mm at a step size of 0.5mm.

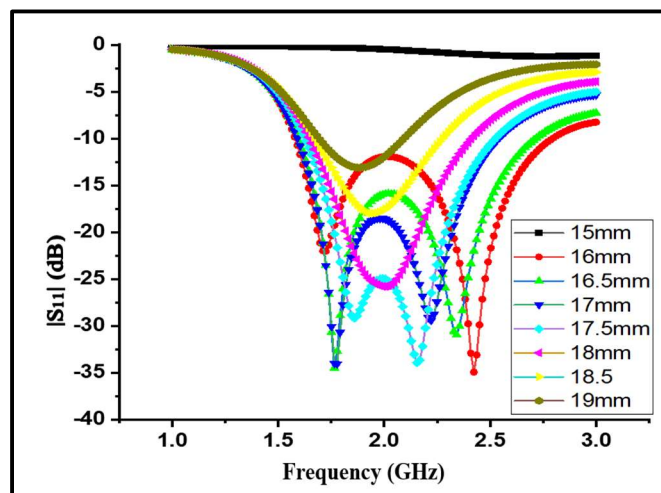


Figure 3.7: $|S_{11}|$ (dB) Plot of circular square slotted patch antenna for different values of radius of circular patch varies from 15mm to 19mm.

3.3.3.4 Dimension of Slot in the Ground Structure

The slot is cut in the in-ground structure at the feed line and antenna connection point. It enhances the impedance matching between the antenna and feedline by improving the coupling between both structures. the coupling exceeds some limit, then it will worsen the performance of the antenna. [100]. The parametric study is combined performed on the length and width of the slot added in the ground structure so that it can be optimized for perfect impedance matching and it came out to be 6 mm X 9 mm after optimization as mentioned in Figure 3.8.

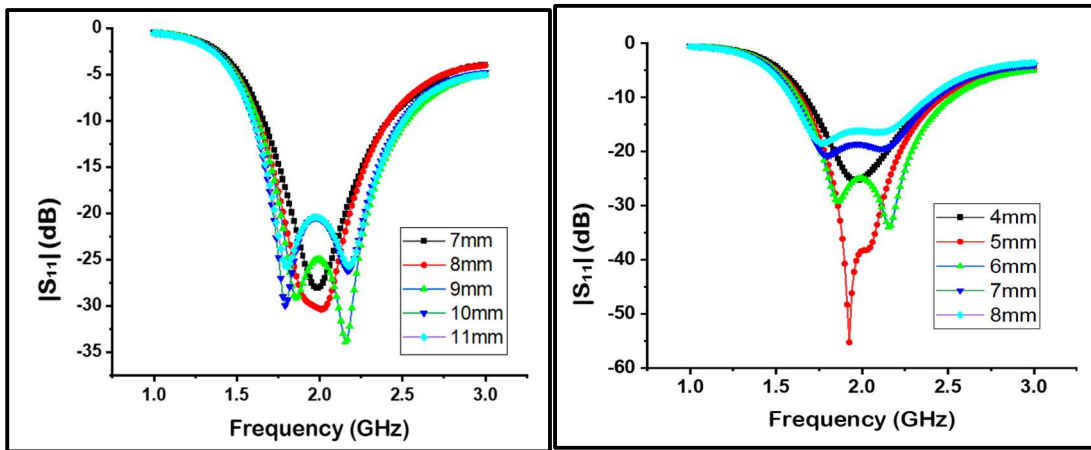


Figure 3.8: $|S_{11}|$ (dB) Plot of the circular square slotted patch (a) length and (b) width both vary as mentioned in the graph.

3.3.4 Results and Discussion

In this section, the Proposed antenna and the performance of the antenna are mentioned in detail. The fabricated antenna is shown in Figure 3.9. The $|S_{11}|$ (dB) parameters are measured using the E8362C PNA Microwave Network Analyzer as shown in Figure 3.10. The $|S_{11}|$ (dB) is shown in Figure 3.11. It can be seen from Figure 3.11 that the bandwidth is from 1.45GHz to 2.6GHz, covering both the B1 and B3 bands of NB-IoT. The fractional bandwidth achieved in this design is 57.5%.

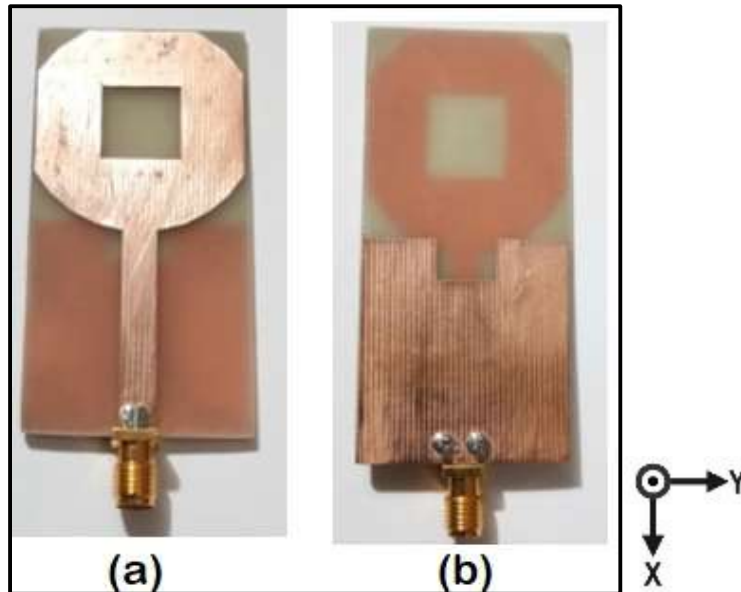


Figure 3.9: Snapshot of fabricated antenna top (a) and bottom (b) view.



Figure 3.10: Fabricated antenna with vector network Analyzer for $|S_{11}|$ (dB) measurement.

The realized gain band graph is also mentioned in Figure 3.12, and it can be concluded from the gain vs. frequency graph that the gain is more than 2dBi for the complete

impedance bandwidth and the peak gain is 5.3 dBi. Figure 3.13, that the radiation efficiency is more than 95% can be seen.

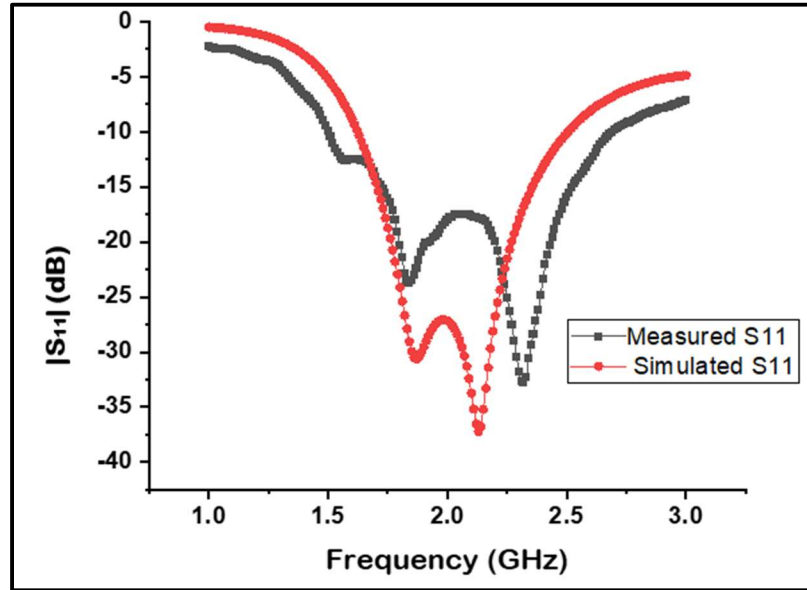


Figure 3.11: The $|S_{11}|$ (dB) vs. Frequency of the proposed antenna.

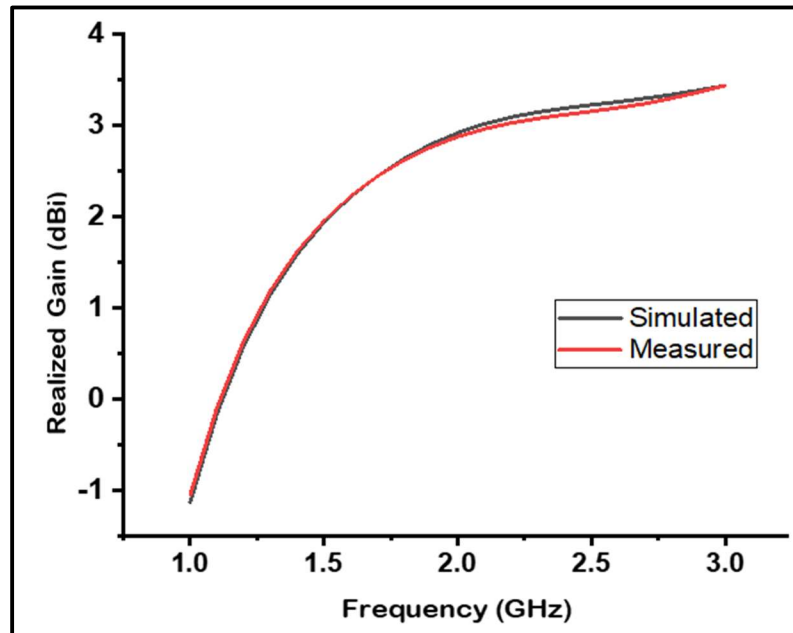


Figure 3.12: The realized gain Vs frequency graph of proposed antenna.

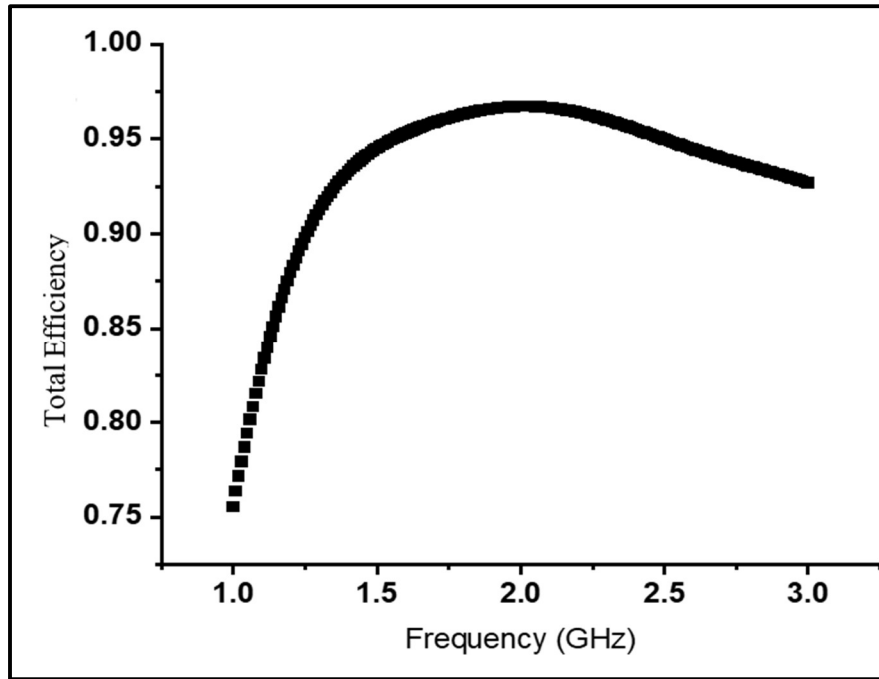


Figure 3.13: The simulated total efficiency graph.

Table 3.1 Comparison table with the antennas published in recent years.

Ref.	Design Complexity or structure	Dimension (mm ³)	Substrate	Frequency Bands (GHz)	Bandwidth (MHz)	Peak Gain (dBi)
[74]	Slotted Patch MIMO	$0.27\lambda \times 0.27\lambda \times 0.009\lambda$	FR4	1.73 & 2.53	30	-3.8
[101]	Slotted patch antenna MIMO	$0.69\lambda \times 0.37\lambda \times 0.01\lambda$	FR4	1.72, 2.18 & 5.5	150	1.97
[76]	Monopole patch metamaterial	$0.22\lambda \times 0.22\lambda \times 0.011\lambda$	FR4	1.1 & 1.6	180	-3.2 & 1.1
[67]	H-shaped reconfigurable	$0.43\lambda \times 0.10\lambda \times 0.01\lambda$	Rogers s5880	1.8	40	5.5
[102]	Switchable slot antenna	$0.64\lambda \times 0.64\lambda \times 0.01\lambda$	FR4	2.4, 3.5	140	2.33, 3.14

[77]	C-shaped conforming BW	$1.25\lambda \times 1.56\lambda \times 0.01\lambda$	FR4	1.8 & 2.4	100	4.4
[68]	L-shaped CPW feed	$0.20\lambda \times 0.20\lambda \times 0.01\lambda$	FR4	1.1 & 2.4	3000	-0.5
[103]	Tuneable rectangular slot	$0.3\lambda \times 0.15\lambda \times 0.007\lambda$	Tin	1.5	400	1
[92]	Meandered slot loaded with varactor diode	$0.06\lambda \times 0.15\lambda \times 0.01\lambda$	RO43 50	0.75 & 1.1	17	-0.35
[86]	Slotted square patch	$0.29\lambda \times 0.29\lambda \times 0.013\lambda$	FR4	2.4	220	3.2
[87]	Folded Dipole	$0.33\lambda \times 0.24\lambda \times 0.01\lambda$	FR4	2.1	100	2
Proposed Design	Circular slotted patch	$0.18\lambda \times 0.26\lambda \times 0.01\lambda$	FR4	1.8 & 2.1	1100	3.45

To showcase the benefits of the designed antenna, a comparative analysis is conducted between the proposed design and an existing design that operates within the same frequency range or is intended for NB-IoT applications. The specific details are presented in Table 3.1. To measure the performance of the antenna, it was placed inside an anechoic chamber, as illustrated in Figure 3.14. The gain measurements were carried out employing the reference gain measurement method. To find out how directed the antenna is, the radiation patterns mentioned in Figure 3.15 show the XY and ZX lines of the radiation pattern, which was calculated at a central frequency of 2 GHz. The simulated radiation pattern is represented by the red color plot, while the measured radiation pattern is depicted by the blue color plot. Based on the analysis, it can be observed that the proposed antenna demonstrates vertical linear polarization and an omnidirectional radiation pattern.

Additionally, the antenna possesses a wide beam width at half power at the central frequency, indicating its ability to radiate energy in Omni directions.

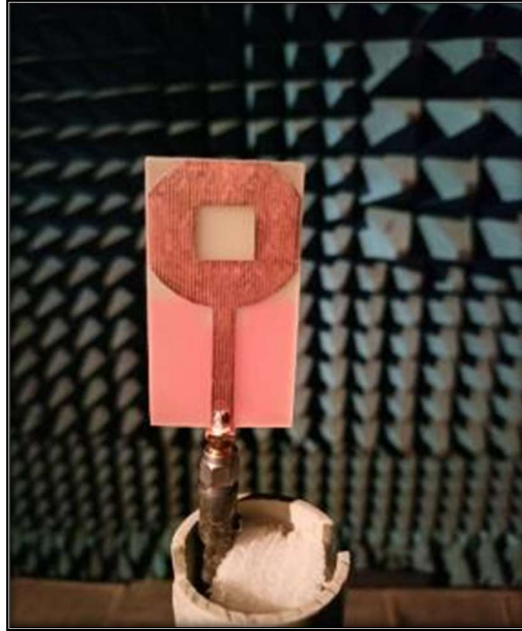


Figure 3.14: The antenna in an anechoic chamber.

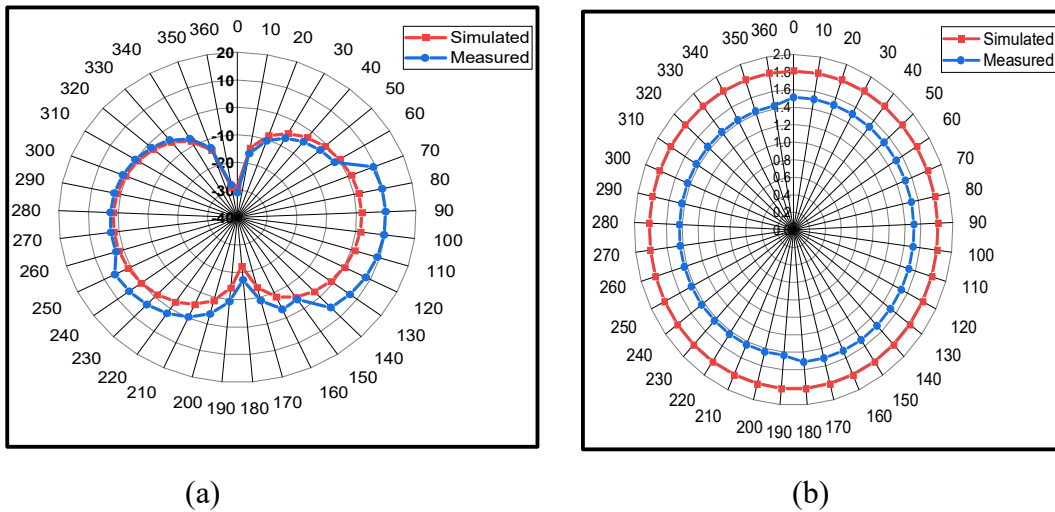


Figure 3.15: The simulated and measured radiation pattern (a) E-Plane (b) H-Plane at 2 GHz.

3.4 Symmetric Slotted Monopole Antenna

3.4.1 Introduction

The symmetric slotted, planar patch monopole antenna on the FR4 substrate is designed. The designed antenna is of dimension 30mm X 30mm which is determined by the dimension available at the NB-IoT Module. It is resonating at 2.09 GHz and provides a good bandwidth of 120MHz. The final design is achieved in a stages design in which one by one we have reduced the resonating frequency using different antenna technologies such as DGS and Slot. The resonating frequency reduces to 2.1GHz from 4.4GHz in the same dimension by using the mentioned design techniques.

3.4.2 Design procedure of symmetric slotted patch antenna

The basic microstrip patch antenna is designed of dimension 15 mm X 25 mm and it is resonating at 4.4GHz theoretically, we can verify this from the mentioned $|S_{11}|$ (dB) graph in Figure 3.17. The simulated antenna design is mentioned in Figure 3.16. The substrate provides mechanical support to the patch antenna. here we used Flame retardant FR4 material of 1.6 mm, the patch antenna of 15 X 25 mm² is designed on the top side substrate, and the ground of dimension 30 mm X 30 mm is designed on the other side or considered as the bottom of the substrate and the dimension of the first antenna is mention in Figure 3.16. The patch antenna is excited with a lumped port through the microstrip feed line. To achieve the required resonating frequency of the antenna we need to increase its resonating length So, the inverted L-shaped slot is introduced in the patch, which helps in reducing the resonating frequency to some extent, one more slot is introduced to the top patch of the antenna that drastically reduced the resonating frequency to the 2.4 GHz.

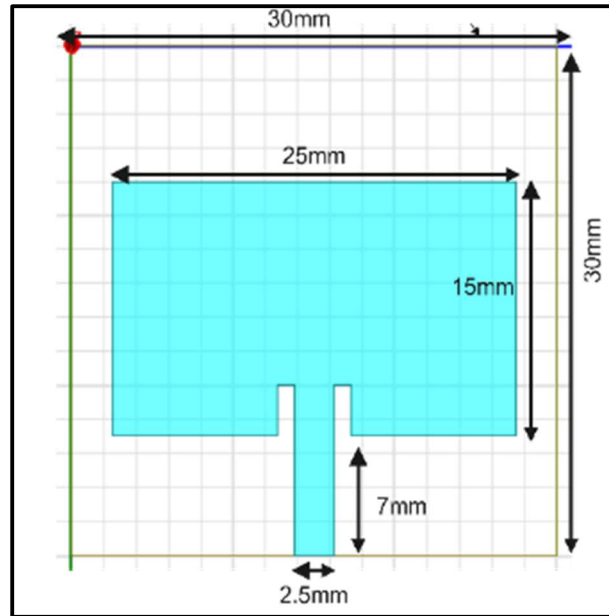


Figure 3.16: The Basic Patch antenna

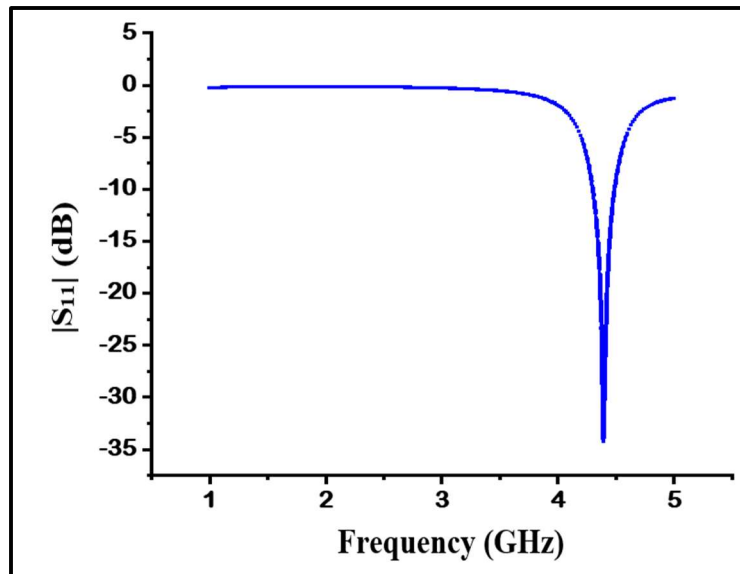


Figure 3.17. The Reflection Coefficient of Basic Patch

For our NB-IoT application, we need a resonating frequency at 2.1 GHz, so again we have added the horizontal slot to the antenna, and antenna 4 is resonating at 2.36 GHz. So, at last, the rectangular-shaped DGS is introduced to the antenna as per surface current so that we can reduce the resonating frequency to 2.1 GHz therefore, step by step by introducing

mirrored slots and DGS structure we have increased the resonating length and reduce the resonating frequency to 2.12 GHz. The step-by-step antenna design is mentioned in Figure 3.19. The final designed antenna is mentioned in Figure 3.18 and its dimensions are $L_p=18.5\text{mm}$, $W_p=25\text{mm}$, $L_f=10\text{mm}$, $W_f=2.5\text{mm}$, $L_s=11\text{mm}$, $W_s=11.5\text{mm}$, $W_1=8\text{mm}$, $L_1=2\text{mm}$, $L_{dgs}=20\text{mm}$, and $W_{dgs}=17\text{mm}$. The patch antenna is fed with an inset microstrip feed line of length 10mm and width of 2.5mm which is optimized to 50 ohms and excited with the lumped port in HFSS. The port is normalized to 50 ohms.

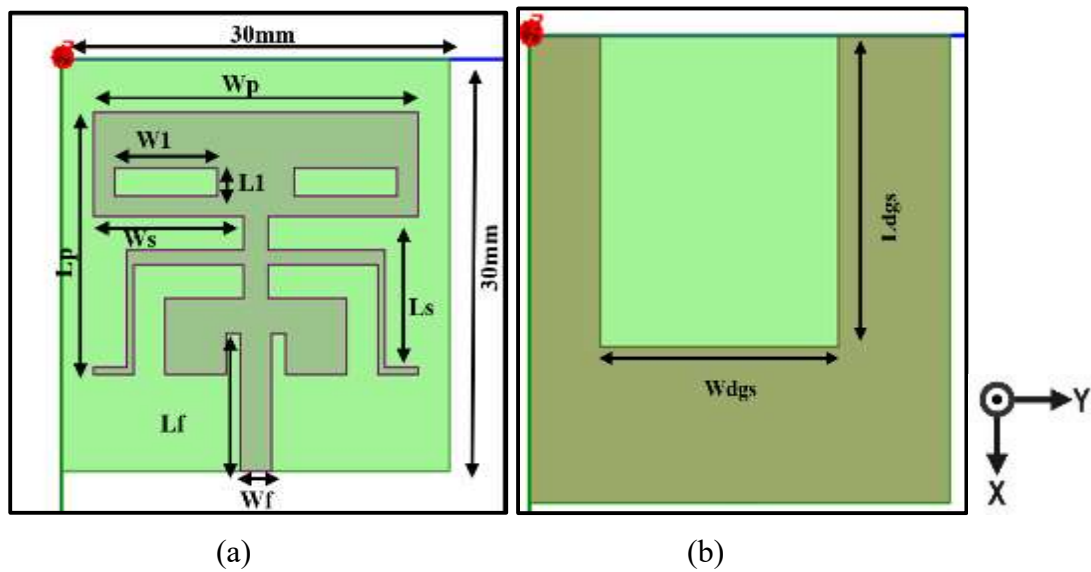


Figure 3.18: The final design (a) top and (b) bottom view of the antenna

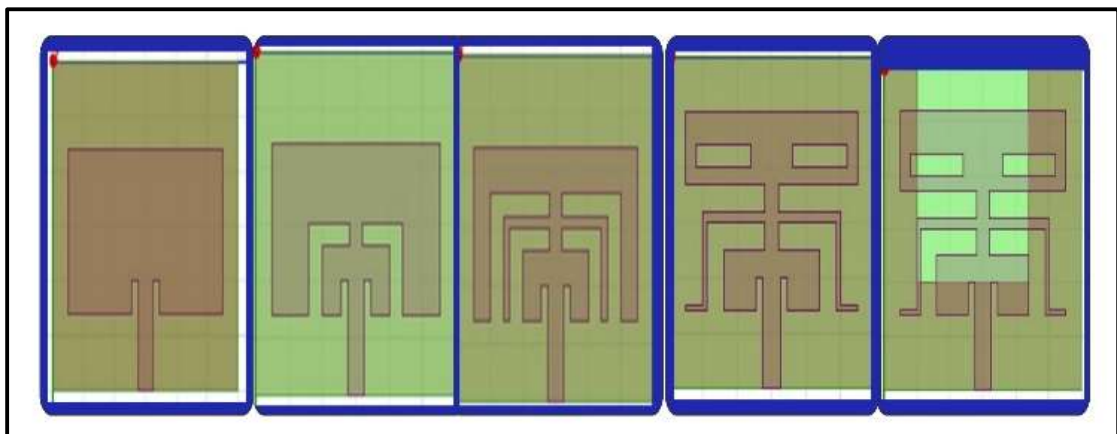


Figure 3.19: The design steps (progress) of the proposed patch antenna.

3.4.3 Results and Discussion

Here in the result section, to study the effect of the designed prototype we have studied its various parameter which is analyzed after stimulation of the designed antenna in HFSS. we have discussed the characteristics of the final designed antenna (e) as mentioned in Figure 3.19 and the shifting of resonant frequency from the antenna (a) to antenna (e) is mentioned in Figure 3.20.

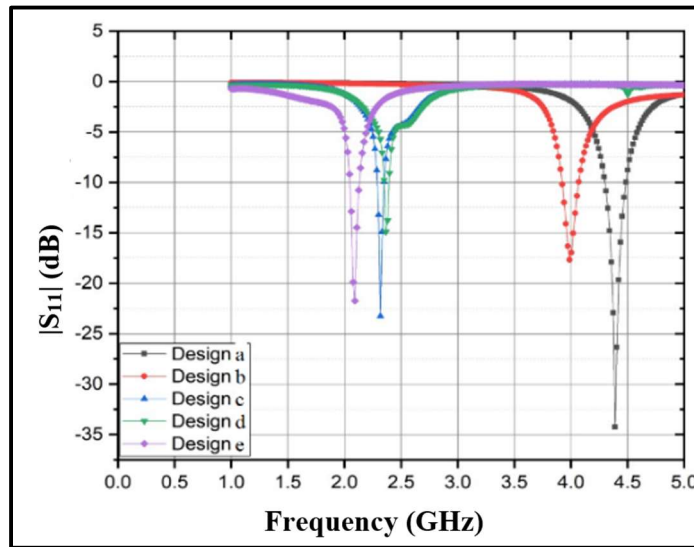


Figure 3.20: Comparative reflection coefficient of antenna a, b, c, d, and e.

Table 3.2 The comparison table of all the designed antennas at various steps.

Design	Resonant frequency	Frequency Range GHz (-10 dB)	Impedance Bandwidth	Gain at the resonating frequency	VSWR at the resonating frequency	Size of Antenna (mm ²)
Design a	4.39GHz	(4.29-4.47)	180 MHz	7.75dBi	1.04	30 X 30
Design b	3.99GHz	(4.06-3.90)	160 MHz	6.27dBi	1.64	30 X 30
Design c	2.4GHz	(2.27-2.45)	180 MHz	3.35dBi	1.06	30 X 30
Design d	2.36GHz	(2.33-2.39)	60 MHz	3.65dBi	1.8	30 X 30
Design e	2.09GHz	(2.12-2.24)	120MHz	2.72dBi	1.01	30 X 30

The fabricated antenna is shown in Figure 3.21. The $|S_{11}|$ (dB) parameters of the fabricated antenna are measured using the E8362C PNA Microwave Network Analyzer as shown in

Figure 3.22. The reflection coefficients are shown in Figure 3.23. It can be seen from Figure 3.23 that the bandwidth is from 1.45GHz to 2.6GHz, covering both the B1 band of NB-IoT. The $|S_{11}|$ (dB) reflection coefficient graph has a good match with the simulated results, while the resonance varies, maybe because of mismatching at the port connectors. All the antenna parameters are concluded in Table 3.2 and Table 3.3. is a brief comparison of our final antenna with a previously designed antenna by other authors which is published.

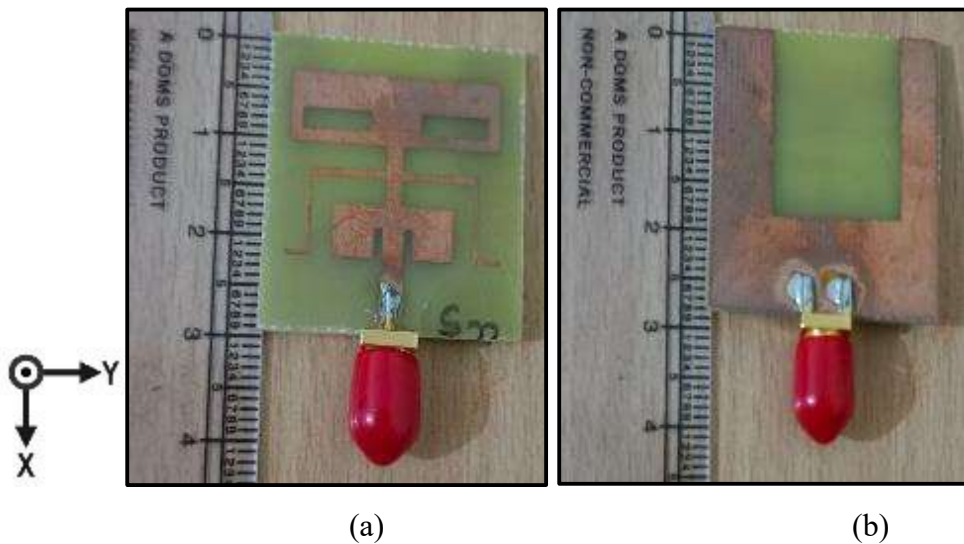


Figure 3.21: Fabricated antenna top (a) and bottom (b) view.

The designed antenna has a slotted patch and DGS fed with a microstrip inset feed line whose width is optimized using the parametric study. The antenna has bandwidth at 120 MHz that corresponds to the Band of NB-IoT (B1 2100). The designed prototype antenna can be used for NB-IoT applications. The gain measurements have been done using the reference gain measurement method. The radiation pattern is calculated at the center frequency of 2.1 GHz and its E-Plane and H-Plane are mentioned in Figure 3.24.



Figure 3.22: Fabricated antenna with vector network Analyzer for $|S_{11}|$ (dB) measurement.

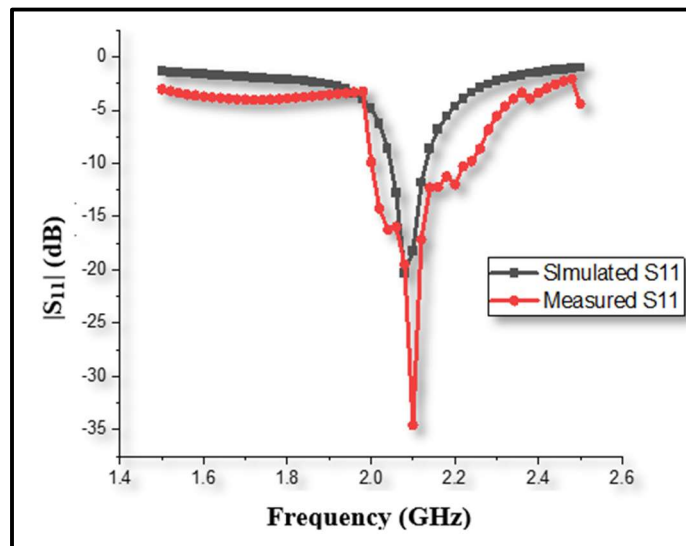


Figure 3.23: The simulated and measured $|S_{11}|$ (dB) versus frequency graph.

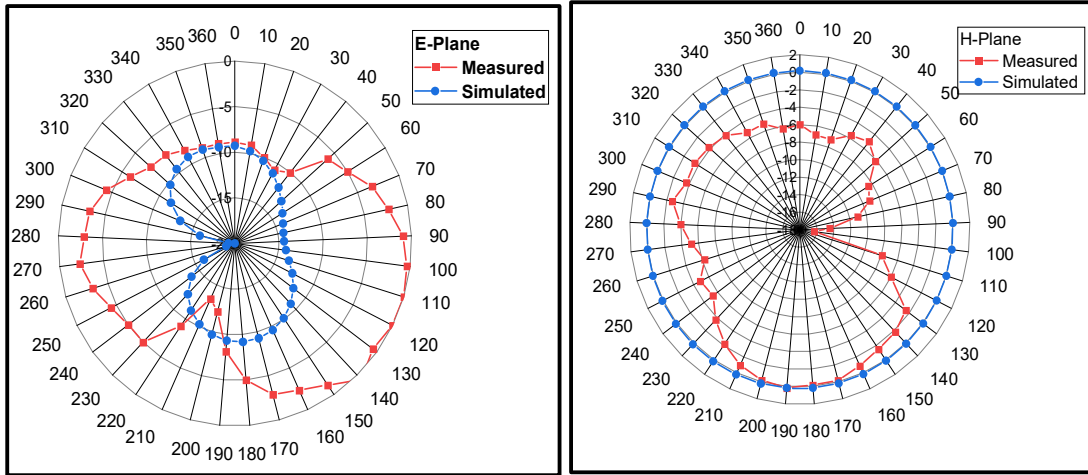


Figure 3.24: The radiation pattern of the proposed antenna in (a) E- Plane (b)H-Plane at 2.1 GHz.

Table 3.3 Comparison of the final designed antenna with another antenna for IoT technology.

Ref	Antenna Design Technology	Substrate Material	Operating Frequency	Dimension(mm ³)	Application
[28]	Rectangular Patch with Slot	FR4	915 MHz 2.45 GHz	0.17λ×0.13λ× 0.009λ	IoT
[52]	Antenna with Array	FV	2.45 GHz	0.44λ×0.32λ× 0.012λ	IoT
[61]	Foldable and non-foldable structure	FR4	2.4 GHz ISM	0.44λ×0.48λ× 0.025λ	IoT
[69]	Patch Antenna	FR4	433 MHz	0.30λ×0.23λ× 0.002λ	IoT
[70]	Patch with DGS	FR4	871 MHz	0.15λ×0.19λ× 0.004λ	LoRa
[106]	Flexible Printed Antenna	Polyamide	868 MHz	0.069λ×0.06λ× 0.005λ	IoT
[107]	UCA & UIT design	FR-4	868MHz	0.10λ×0.23λ× 0.002λ	IoT
[108]	Folded antenna	Copper (PEC)	868MHz	0.08λ×0.28λ× 0.014λ	IoT
[109]	Ring-based slotted structure	FR-4	915MHz 2.45GHz	0.07λ×0.18λ× 0.003λ	IoT
Proposed Antenna	Patch with slot	FR4	2.1GHz	0.21λ×0.21λ× 0.01λ	NB-IoT

3.5 Fractal Antenna

3.5.1 Introduction

A small-size MIMO fractal antenna is designed for NB-IoT applications. The shared patch MIMO antenna is very small in size as compared to the conventional patch MIMO antenna, in which multiple antennae are designed on a substrate depending on the number of ports. The proposed antenna is designed to cover the B1 (2100), B3 (1800), and B5 (800) bands of NB-IoT. The antenna is 20mm x 10mm in size. It resonates at 2 GHz and provides a good bandwidth of 135%. The final fractal design is achieved in four iteration stages of the line and its slant line is at a 45-degree angle. The designed antenna is fed by two complimentary placed microstrip lines, and it is designed and simulated using HFSS. The DGS concept is used to improve the resonance and isolate two-port antennae.

3.5.2 Design Procedure of Fractal Antenna

The patch design steps, which are used to evolve the fractal patch, are shown in Figure 3.25 in steps. The slant line is at 45 degrees and the fractal shape is iterated in three steps. In the last step, the fractal line is shaped into a polygon with five sides. The patch antenna is fed by two microstrip lines which are placed orthogonally, which helps in reducing the dimension and complexity of the antenna. The mutual coupling between the port and patch is improved by increasing the distance between the antenna ports. The substrate provides mechanical support for the patch antenna. Here we used flame retardant FR4 material, of 1.6mm thickness.

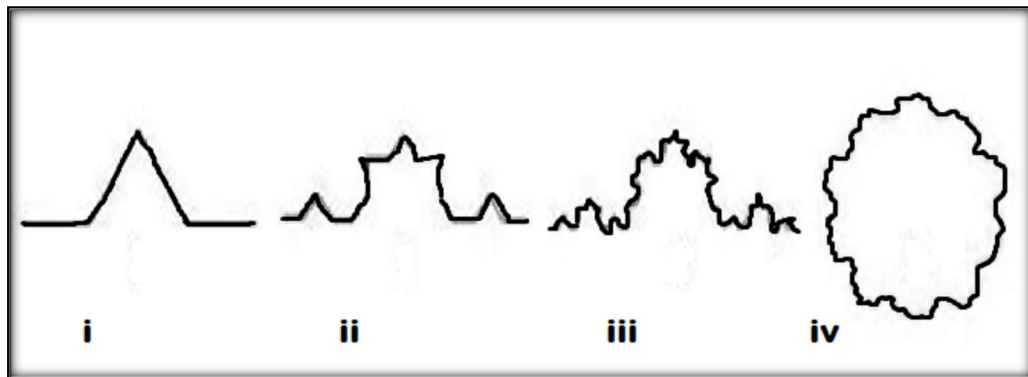


Figure 3.25: Design steps involved in the Patch design

The patch antenna is designed on top of the substrate size of 20 X 10 mm², and the ground is designed on the other side or considered as the bottom of the substrate with the defected ground concept that helps in increasing the effective size of the grounds. The patch antenna is excited with a lumped port through the two microstrip feed lines placed complementary to each other as mentioned in Figure 3.26.

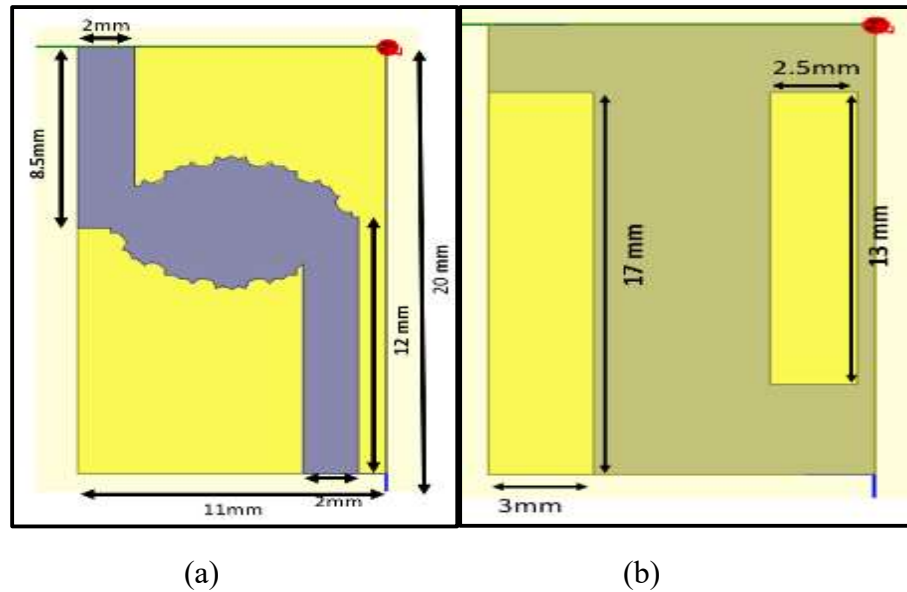


Figure 3.26: The dimension of the patch antenna

3.5.3 Results and Discussion

Here in the result section, to study the effect of the designed prototype we have studied its various parameter which is analyzed after stimulation of the designed antenna in HFSS. The reflection coefficient, $|S_{11}|$ (dB) parameter is mentioned in Figure 3.27 of the final designed antenna the antenna is resonating at 2.05GHz and has an impedance bandwidth of 2 GHz.

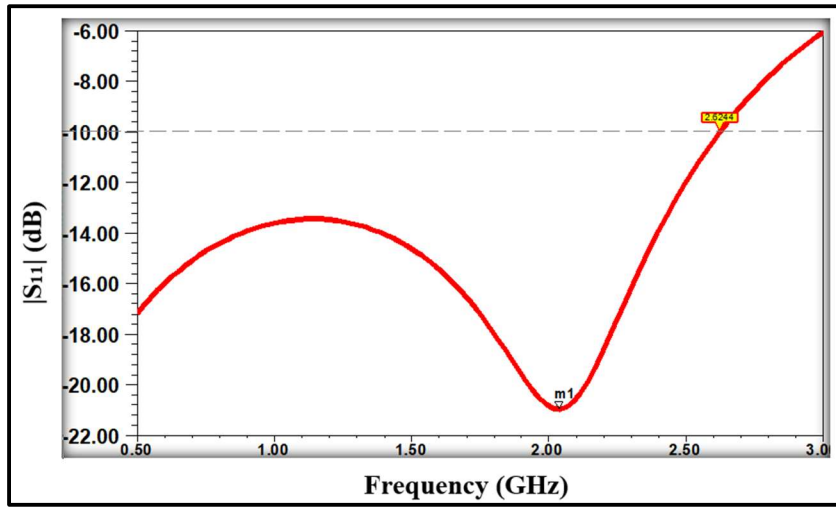


Figure 3.27: Reflection coefficient of final designed antenna resonating at 2.09GHz.

Gain is one of the basic parameters of an antenna that measures the power-delivery capability of the radiator from the transmitter side to the target. Gain describes the maximum intensity of radiation caused by the radiating element when compared with the lossless isotropic antenna, which is provided with the same amount of power. An antenna with a gain of 2 implies that the effective power delivered is twice as when compared to an isotropic radiator. As the dimension of the antenna is very small, the antenna gain is very small at low frequencies and shows 2.15 dBi of gain around 2.1 GHz as mentioned in Figure 3.28. The fabricated antenna is shown in Figure 3.29. The $|S_{11}|$ (dB) parameters of the fabricated antenna are measured using the Microwave Network Analyzer as shown in Figure 3.30. The simulated and measured reflection coefficients are shown in Figure 3.31. It can be seen from Figure 3.31 that the bandwidth is from 100 MHz to 2.6 GHz, covering both the B1, B3, and B5 bands of NB-IoT. The $|S_{11}|$ (dB) reflection coefficient graph has a good match with the simulated results, while the resonance varies, maybe because of mismatching at the port connectors.

The antenna has bandwidth at 2.5 GHz that corresponds to the bands of NB-IoT (B1 2100 MHz), B3 (1800 MHz), and B5 (850 MHz). The designed prototype antenna can be used for NB-IoT applications. The gain measurements have been done using the reference gain measurement method.

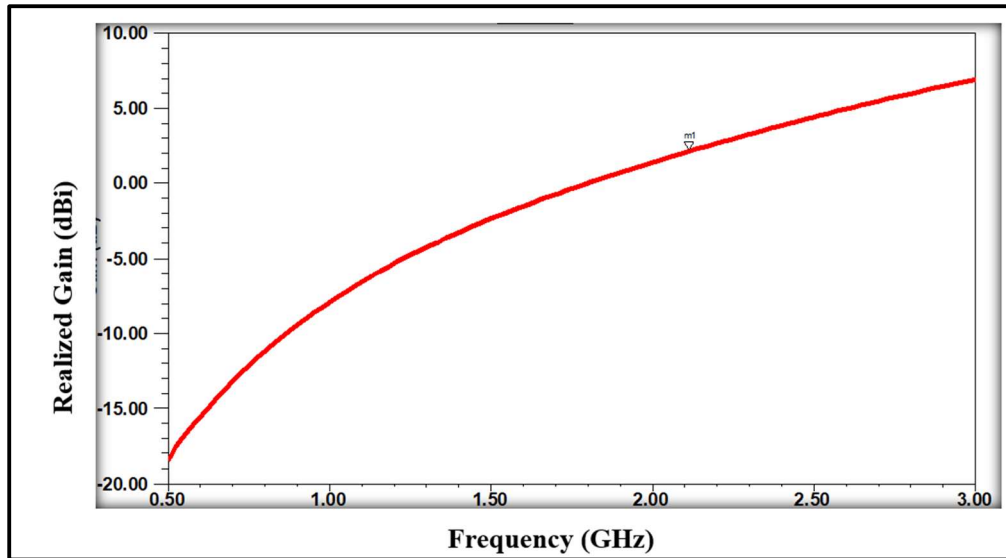


Figure 3.28: The simulated Gain -Frequency band of the designed antenna.

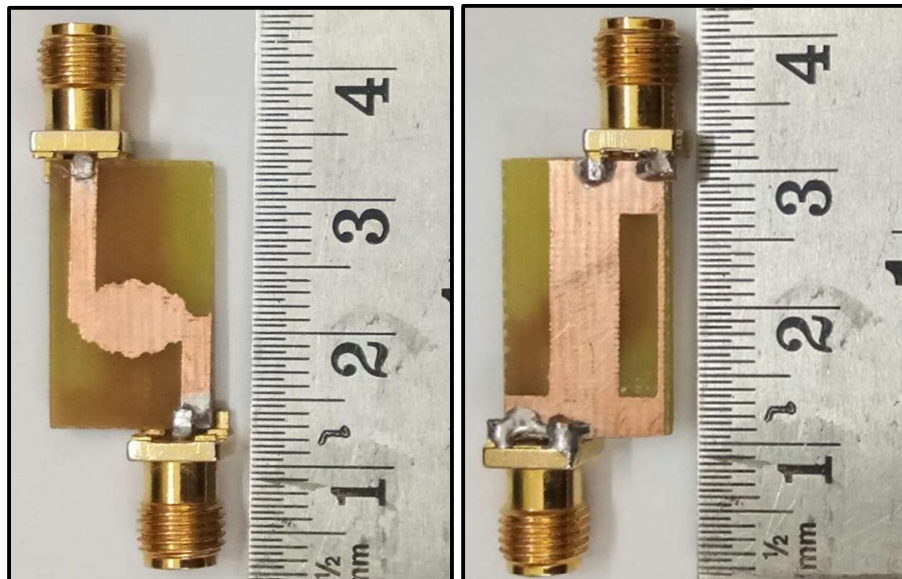


Figure 3.29: Fabricated antenna top and bottom.

The radiation patterns help in finding the directionality of the antenna. The radiation pattern is calculated at the center frequency of 2.1 GHz and its E-Plane and H-Plane are mentioned in Figure 3.32. To substantiate the advantages of the designed antenna, the proposed design is compared with the existing design lying in the same frequency band based on dimension,

operating bands, bandwidth, gain, the substrate used, and design technology, and it is mentioned in Table 3.4.

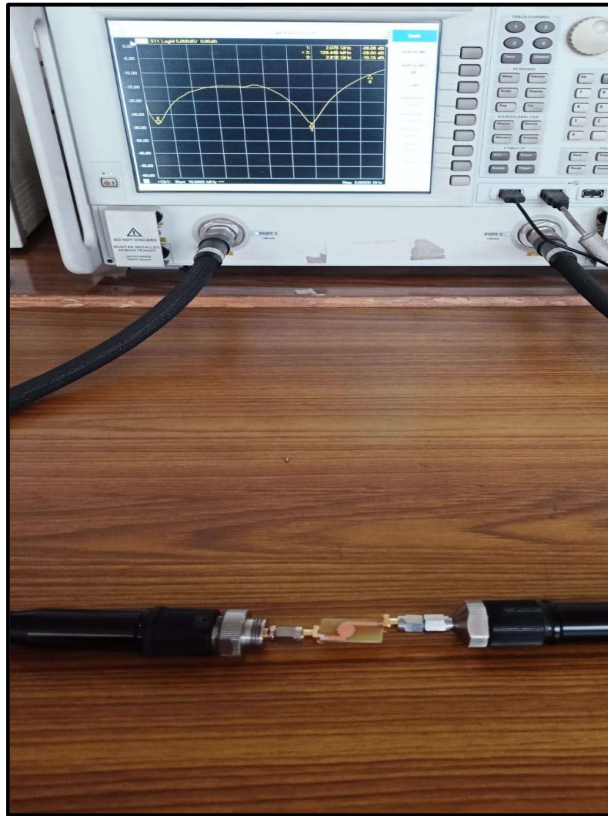


Figure 3.30: Fabricated antenna with VNA for $|S_{11}|$ (dB) measurement.

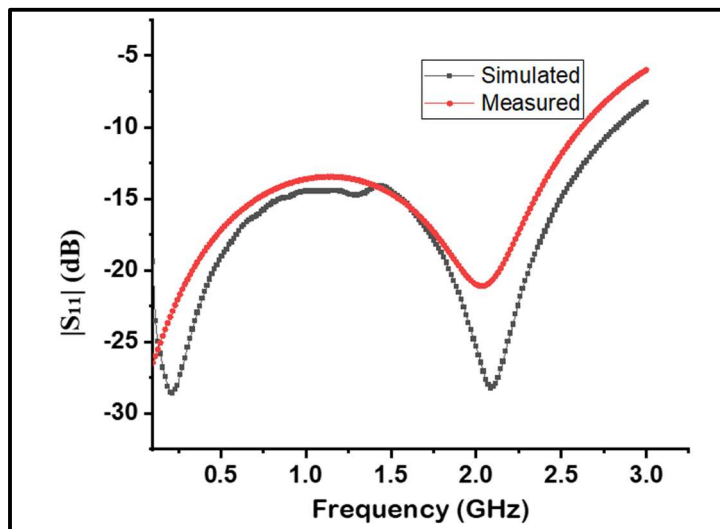


Figure 3.31: The $|S_{11}|$ (dB) versus frequency graph.

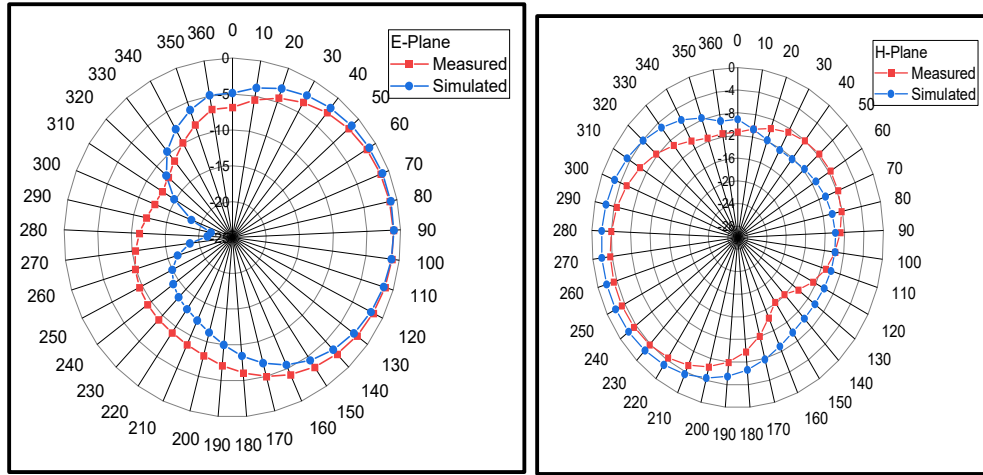


Figure 3.32: The Simulated and measured Radiation pattern of the proposed antenna in (a) E-Plane and (b) H-Plane at 2.1 GHz.

Table 3.4 Comparison of the final designed antenna with another available antenna for IoT technology.

Ref	Antenna Design Technology	Substrate Material	Operating Frequency	Dimension(mm ³)	Application
[18]	Antenna with Array	FV	2.4GHz	0.44λ×0.32λ×0.012λ	IoT
[19]	Patch with DGS	FR4	871MHz	0.15λ×0.19λ×0.004λ	LoRa
[20]	Flexible printed antenna	polyimide	868MHz	0.069λ×0.06λ×0.005λ	IoT
[21]	Rectangular patch with slot	FR4	915MHz 2.45 GHz	0.17λ×0.13λ×0.009λ	IoT
[22]	Patch antenna	FR4	433MHz	0.30λ×0.23λ×0.002λ	IoT
[24]	UCA & UIT design	FR-4	868MHz	0.10λ×0.23λ×0.002λ	IoT
[25]	Folded antenna	Copper (PEC)	868MHz	0.08λ×0.28λ×0.014λ	IoT
[26]	Ring-based slotted structure	FR-4	915MHz 2.45GHz	0.07λ×0.18λ×0.003λ	IoT
[27]	Foldable and non-foldable structure	FR4	2.4GHz ISM	0.44λ×0.48λ×0.025λ	IoT
Proposed antenna	Fractal Design with MIMO	FR4	2.1GHz	0.07λ×0.07λ×0.011λ	NB-IoT

3.6 Summary

In this chapter, a circular cropped, square-shaped slot patch antenna, Symmetric Slotted monopole, and fractal-designed antenna are proposed, designed, and fabricated for the B1, B3, and B5 bands of NB-IoT applications. The test results show that it covers both bands with satisfactory antenna performance. The characteristics of the antenna were analyzed and found suitable for the NB-IoT applications NB-IoT technology can be easily merged with mobile network existing technology with some upgradation in software and systems to solve the problem of data communication in wireless sensor networks [9].

CHAPTER 4

DESIGN, FABRICATION, AND MEASUREMENT OF ULTRA-WIDEBAND ANTENNA

4.1 Introduction

Today the world is rapidly moving towards miniaturization and modernization of technology in the field of electronics and communications. The importance of antenna miniaturization is rapidly growing as communication devices get smaller. An ultrawideband antenna key-shaped patch antenna is a unique design monopole structure. This designed antenna of dimensions 44mm X 44mm X 1.6mm can be used by various wireless technology using different frequencies. The antenna can be used in frequency bands over 2.6GHz -10.6GHz, covering Wi-Fi frequencies at 5.15-5.35 GHz and 5.725-5.825 GHz, and IoT technology.

For wireless communication purposes, monopole patch antenna designs are preferred because of their planarity and they also exhibit wideband properties [110-115]. There is various ultra-wideband (UWB) system and their applications are studied [116-119]. The ultra-wideband systems have very vast applications and use in current broadband communication trends, where high-frequency data is communicated in various application fields like biomedical applications, RFID, wireless sensor networks, the automobile industry, and 5G networking. UWB system has recently for 5G for midrange frequency band (3.3-4.2) GHz and (4.5-5.5) GHz. Microstrip patch antennae are the best-suited antenna for wireless applications because of their planar structure, and simple and cost-effective properties. Although many other techniques are used to improve the performance of patch antennae and also add radiation properties to the resonating structures.

As per literature, [2-9] initially UWB antennas consist of basic shapes of the resonating patch as triangles, rectangles, u shaped and ultra-wideband properties are introduced to them with some enhancement techniques like DGS, Slot, CPW, and many more. Now, days within the UWB system dual notch band and multiband antenna are also designed and implemented as per application requirements [121-123]. For the IoT application and

working module, the monopole structure is a suitable design that exhibits good radiation and wideband properties. Monopole antenna can be easily integrated with other devices or can be printed on PCB, so it is ideally suitable for wireless portable devices, implemented worldwide in many shapes and designs like meandered and PIFA designs [124-128]. Nowadays, the monopole structure is also used for the high gain applications required in GPR, high accuracy positioning systems, and microwave imaging systems, and these antenna designs are integrated with multi-layer technique, electromagnetic band gap structure, and even use DRA concept to increase the gain of the antenna.

4.2 Proposed Design Detail

Different substrates such as High dielectric materials, FR4 substrate, Magneto-dielectric Meta-Materials materials, etc. are used for different designs of an antenna.

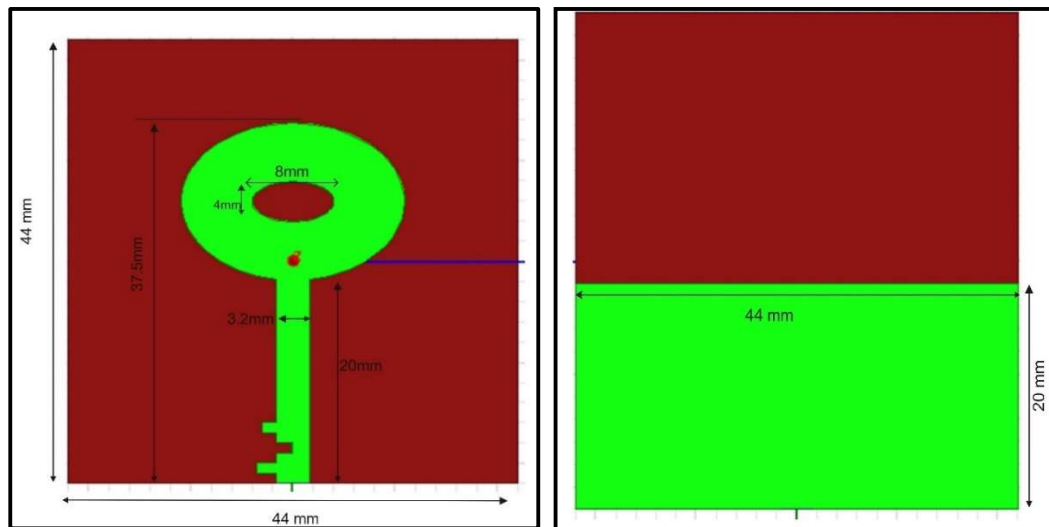


Figure 4.1: (a) Top view and (b) Bottom view of the patch antenna

4.3 Results and Discussions

In this section, the fabricated antenna and simulation and measurement results are mentioned in detail. The simulated reflection coefficient graph is mentioned in Figure 4.2,

and it is directed from the graph that the antenna has an impedance bandwidth of more than 8GHz from 2.5 GHz to 10.7 GHz.

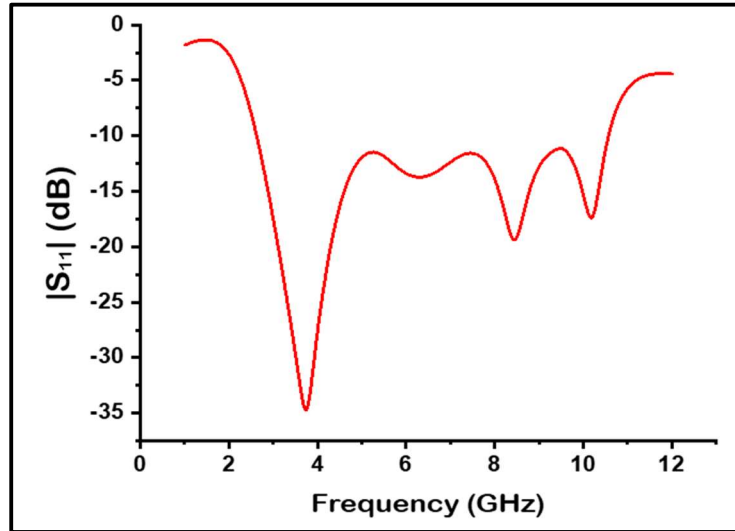


Figure 4.2: The reflection coefficient graph for the ultra-wideband frequency range.

The values of through power are extracted from the VSWR equation 1. From Figure 4.2 it is seen that the value of through power is obtained greater than 99 % for microstrip key-shaped patch antenna, due to $|S_{11}| \text{ (dB)} \leq -10 \text{ dB}$. This deduces that reflected power is only 10 % from the radiating patch.

$$\Gamma = \frac{VSWR-1}{VSWR+1} \quad (4.1)$$

$$\text{Through Power (\%)} = 100(1 - \Gamma^2) \quad (4.2)$$

Where Γ is the reflection coefficient

The values of Return loss are extracted from voltage standing wave ratio (VSWR) according to equation (4.3): which is mentioned in Figure 4.2.

$$RL_{dB} = -10 \log_{10} (1 - \Gamma^2) \quad (4.3)$$

Gain is a quantity that measures an antenna's directional characteristics. A high-gain antenna has directionality and a low-gain antenna has the same power radiation in all directions. Ideally, antennas have equal power in all directions, as happens in isotropic antennas. Power is not created by any antenna; it is redistributed in any direction. For

example, if we consider a directive antenna, its power is focused in a particular direction and it has less power or negative power in other directions.

It is the conservation of energy by the antenna. A high gain antenna has a high range of communication, as in the dish antenna, and a low gain antenna has a lower range, as in the Bluetooth device. From the polarization, we can conclude that the circular part of the key provides a vertical polarization and makes the antenna resonate at a low frequency that is below 5 GHz and gives a gain of 2.8 dBi at 3 GHz, and the feed line key-shaped provides a horizontal polarization at a higher frequency more than 5 GHz with gain 4.8 dBi at 8.8 GHz. The simulated gain Vs frequency graph is shown in Figure 4.3. The simulated total efficiency of the proposed design is mentioned in Figure 4.4. The fabricated antenna, top, and bottom view are shown in Figure 4.5. The reflection coefficient of the fabricated antenna is measured for the ultra-wideband using the E8362C PNA and for the gain and radiation pattern measurement antenna is placed in the anechoic chamber as shown in Figure 4.6.

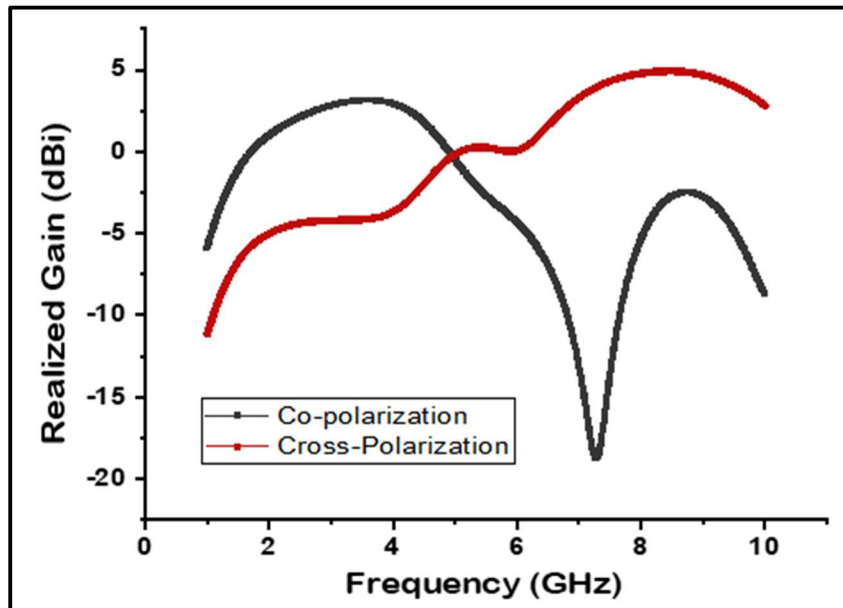


Figure 4.3: The simulated realized gain versus frequency graph.

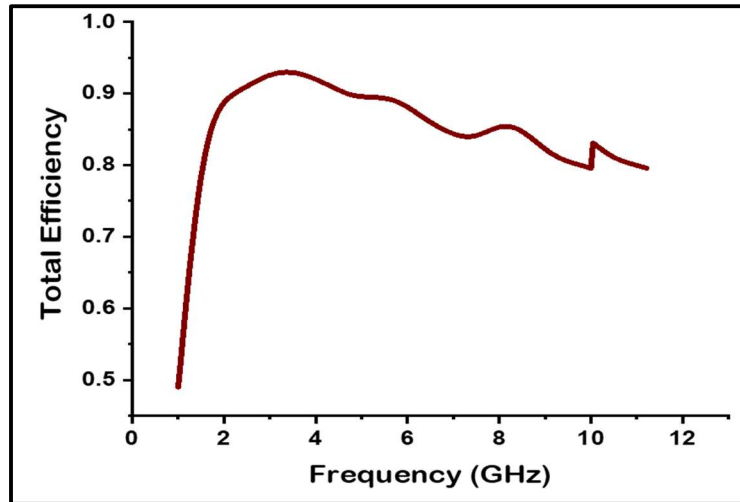


Figure 4.4: The simulated total efficiency of the proposed design for the ultra-wideband.

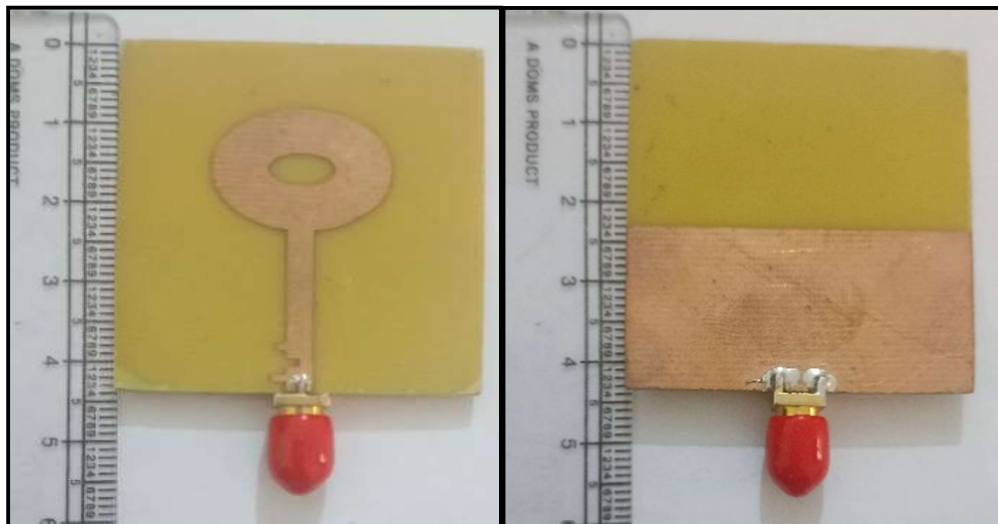


Figure 4.5: Snapshot of fabricated antenna top (a) and bottom (b) view.

The $|S_{11}|$ (dB) parameter is the reflection coefficient, which represents the matching between the port and feed line. It shows, how well the antenna transmits electromagnetic waves. The simulated and measured return losses are shown in Figure 4.7. The measured and simulated radiation pattern of the antenna has been illustrated in Figure 4.8 at 3.5GHz.

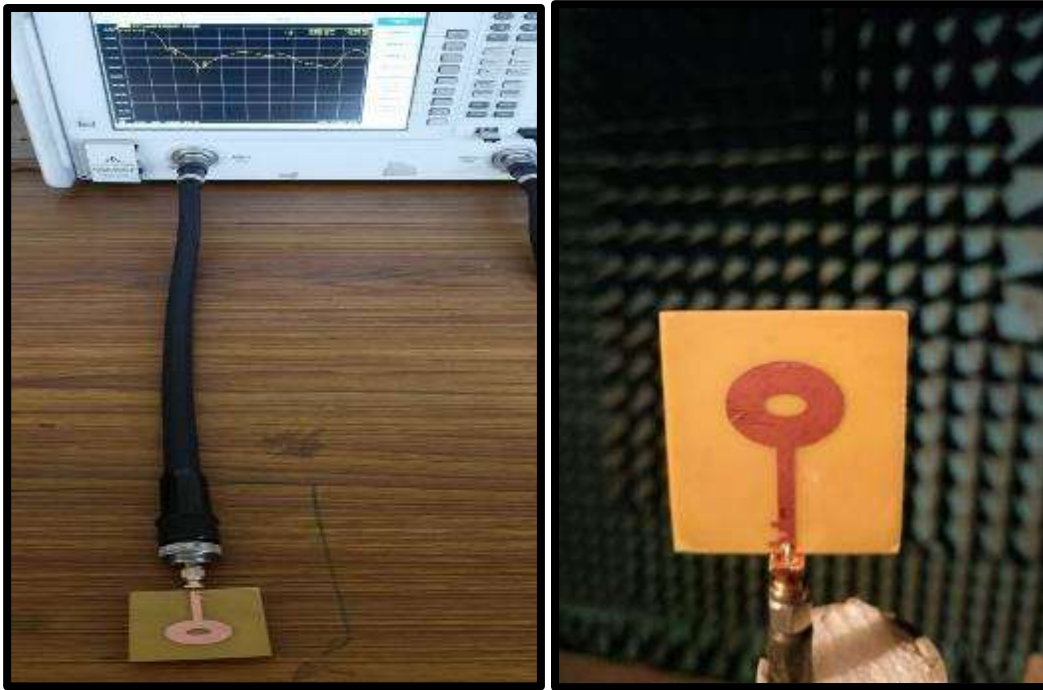


Figure 4.6: Fabricated antenna with vector network Analyzer for $|S_{11}|$ (dB) measurement and in an anechoic chamber for pattern measurement.

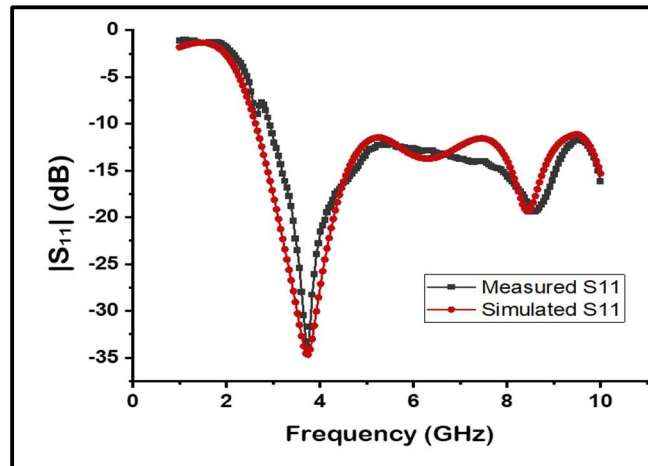


Figure 4.7: The reflection coefficient plot $|S_{11}|$ (dB) Vs Frequency) of the proposed antenna.

To substantiate the advantages of the designed antenna, the proposed design is compared with the existing design lying in the same frequency band based on dimension, operating

bands, bandwidth, gain, the substrate used, and design technology, and it is mentioned in Table 4.1.

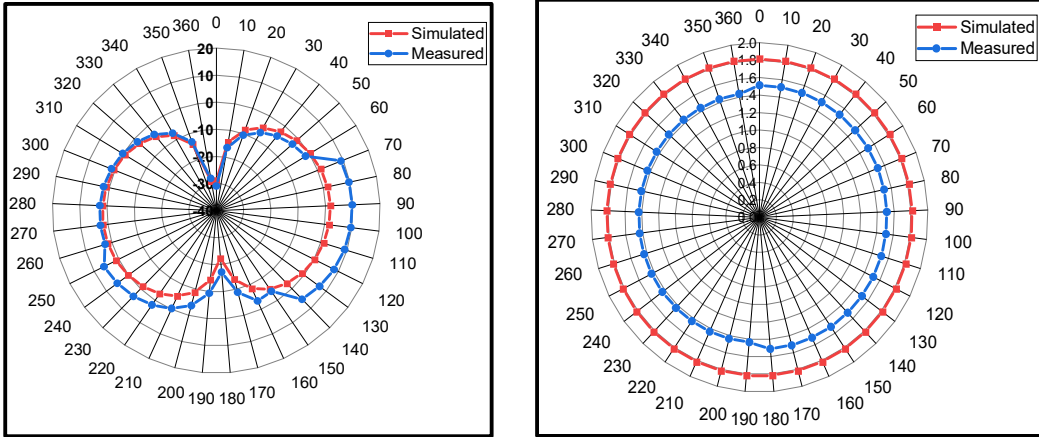


Figure 4.8: The measured E-plane and H-plane at 3.5GHz for the designed antenna.

Table 4.1. Comparison of the proposed antenna with other antennas published in recent years.

Ref	Antenna technology	Substrate	Bandwidth	Size mm ³	Gain (dBi)
[129]	Patch Antenna	FR4	9.2 GHz (3.1-12.3) GHz	9.21λ×6.31λ× 0.042λ	6 (peak)
[130]	Disc monopole antenna	FR4	7.47 GHz (2.69-10.16) GHz	1.08λ×0.9λ× 0.034λ	<8
[131]	PCB printed	FR4	6 GHz (4-10) GHz	0.7λ×0.7λ× 0.037λ	<-5
[132]	Monopole patch	FR4	7.5 GHz (3.1 -10.6) GHz	1.6λ×1.05λ× 0.018λ	-2.36
Proposed Antenna	Key shaped monopole	FR4	9 GHz (2.5 – 11.5) GHz	0.51λ×0.51λ× 0.018λ	5(peak)

4.4 Summary

In this chapter, a key-shaped monopole patch antenna is proposed for UWB IoT applications. The -10 dB impedance bandwidth is from 2.45 GHz to 10.6 GHz and their fractional bandwidth is more than 90% with a radiation efficiency of more than 80% for the bandwidth. It can also be implemented in all the latest mobile communication devices like cellular phones, IoT module devices, and other chipset devices that works in the ultrawideband frequency range. The impedance matching can be improved for higher frequencies to increase the performance of the antenna. Antennas could be designed with polarization purity to enhance the reception at the receiver side and circular polarization may be achieved with the power divider circuit for further work.

CHAPTER 5

DESIGN, FABRICATION, AND MEASUREMENT OF LORA ANTENNA

5.1 Introduction

In this chapter, the designs and develops a planar small-size antenna design for smart IoT communication with LoRa Technology. The design antenna system is best suited for transceiver systems in this automation and sensing era. In the designed antenna, meandered patch, dipole structure, and stub feed techniques are used. A different design approach is employed to get an optimized result. The antenna is made up of a rectangular feed stub to which a connecting wire is attached. The overall dimension of the antenna is 55mm X 55mm X 1.6mm. The antenna is implemented for sensor data communication with the LoRa Module device and Device Interface Arduino platform which is later mentioned in Chapter 7. The antenna is connected as a transmitter and receiver one by one to verify its performance with machine-to-machine communication using the LoRa Module.

The novelty of the proposed work can be summarised as follows:

- i. To overcome the issues of coverage for LoRa devices, the proposed antenna has better coverage than the previously designed antenna and conventional monopole antenna. The proposed antenna meets the requirements for LoRa communication.
- ii. The design is also simple, so there is the ease of fabrication and the small size tends to the placement of this antenna at the LoRa module, which will decrease the size of the communication module of the LoRa device.
- iii. A compact meandered antenna is proposed for LoRa applications. The work cited in [16-20] covered the L bands, but they are not suitable for LoRa communication.
- iv. While optimizing the size of the antenna, a unique meandered design is implemented with the dipole-shaped ground. As per the author's information, such a unique design with a small size and good gain is not achieved in any work.

5.2 Proposed Design Detail

The detailed antenna geometry is discussed in this section, its equivalent circuit is presented, and the design strategy behind optimization is discussed. The designed structure was simulated in Ansoft HFSS, which is based on the FEM method

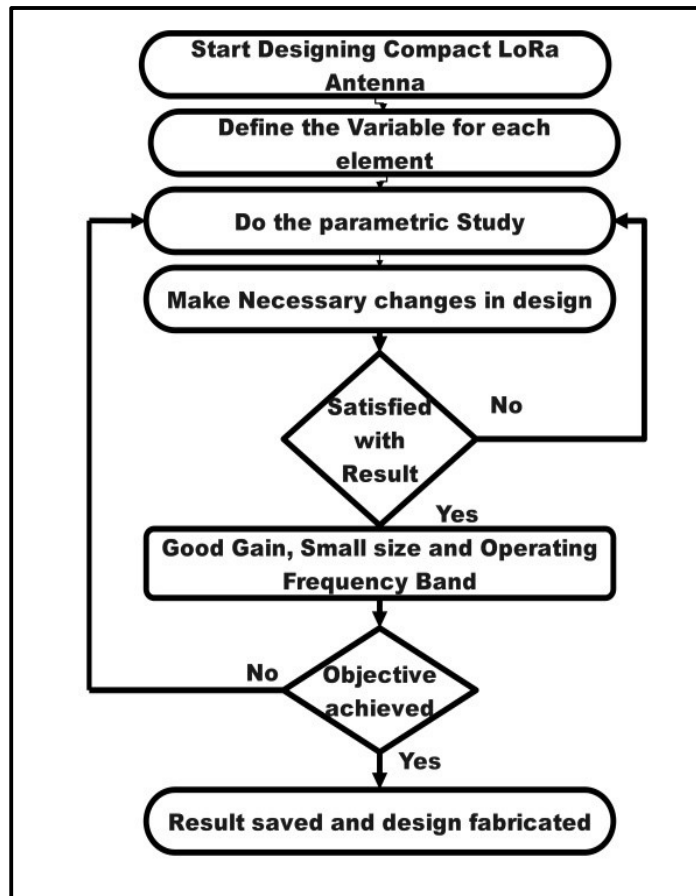


Figure 5.1: Flowchart for antenna designing Strategy

5.2.1 Design Strategy

The technical design strategy for the proposed antenna is briefly described in this section. It is critical to determine the antenna type, material, and thickness before beginning the design process. Because of its excellent performance, the planar meander-line antenna was prioritized, and FR4 epoxy substrate material was used to reduce the antenna's fabrication cost. After that, the appropriate electromagnetic (EM) software was chosen. The antenna

is designed and simulated using version 15.0 of the high-frequency structure simulator (HFSS). The antenna is designed using the technical strategy depicted in Figure 5.1.

5.2.2 Antenna Geometry

The proposed meandered patch antenna consists of the meandered patch and dipole ground. The feed is provided using the rectangular stub between them. The FR4 substrate is the base and mechanical support for the antenna. The overall dimension is 55mm x 55mm, which is optimized after the parametric study. The design mainly consists of a folded meandered line patch, a dipole structure ground, and a stub for feed. The -10dB impedance bandwidth of the proposed antenna is 11MHz from (860–871) MHz, which covers the LoRa spectrum. The gain for the complete band is more than 0.5 dBi.

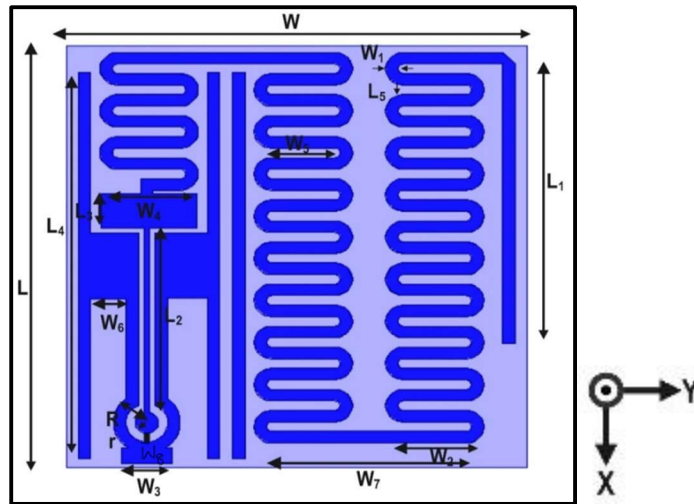


Figure 5.2: Configuration of the proposed LoRa antenna

The proposed antenna design dimensions are the following: $L = 55\text{mm}$, $L_1 = 36\text{mm}$, $L_2 = 22\text{mm}$, $L_3 = 4\text{mm}$, $L_4 = 47\text{mm}$, $L_5 = 0.7\text{mm}$, $W = 55\text{mm}$, $W_1 = 0.8$, $W_2 = 8\text{mm}$, $W_3 = 6\text{mm}$, $W_4 = 11\text{mm}$, $W_5 = 6.4\text{mm}$, $W_6 = 4\text{mm}$, $W_7 = 26\text{mm}$, $W_8 = 0.4\text{mm}$, $R = 3\text{mm}$, $r = 1\text{mm}$. The proposed antenna has both the resonating patch and ground on the top of the substrate with stub as mentioned in Figure 5.2.

5.2.3 Meander line theory and equivalent circuit diagram.

An electrically small antenna is defined as an antenna whose maximum dimension is less than one-tenth of a wavelength [104]. A meander line antenna consists of standing and sleeping lines; both lines together form a turn, and the number of turns helps increase the

efficiency of the antenna. At the same meander, the split increases, and the resonance frequency decreases [105]. A spiral antenna is a development of the fundamental folding antenna and has frequencies significantly lower than single-element antenna resonances of identical length. The efficiency of meander line antennas surpasses that of traditional half and quarter-wavelength antennas. The effectiveness of these antennas relies on the reduction factor of their size, determined by the number of meandering elements per wavelength and the spacing between rectangular loops. In the proposed design, the spacing between the lines is set at 0.7 mm, while the width measures 0.8 mm. By ensuring smooth edges, the impedance matching, and gain of the antenna are significantly enhanced. The meander line antenna consists of both vertical and horizontal components, each playing a distinct role. The vertical meander line functions as an inductor, while the horizontal one serves as a capacitor. A dipole patch antenna that behaves as ground typically consists of a conductive patch (often rectangular or circular) placed over a ground plane with a feedline connected to the patch. The equivalent circuit represents the antenna's impedance, resonance, and radiation characteristics. A meandered structure with two parallel stubs on both sides is a common configuration used in microwave and RF (radio frequency) engineering for various applications, such as impedance matching, filtering, or tuning. To represent this structure with an equivalent circuit, a combination of lumped elements (resistors, capacitors, and inductors) is used to model its electrical behavior. Together, they contribute to the overall performance and characteristics of the antenna. By implementing the meander line design, the antenna achieves improved radiation efficiency compared to traditional half and quarter-wavelength antennas. This enhancement stems from the careful arrangement of the meandering elements and the optimization of the dimensions, specifically the spacing and width between the lines. The smooth edges play a crucial role in minimizing impedance mismatches, resulting in improved performance metrics, such as gain and radiation patterns.

Furthermore, the combination of the inductive and capacitive elements in the vertical and horizontal meander lines allows for better control over the antenna's electrical characteristics.

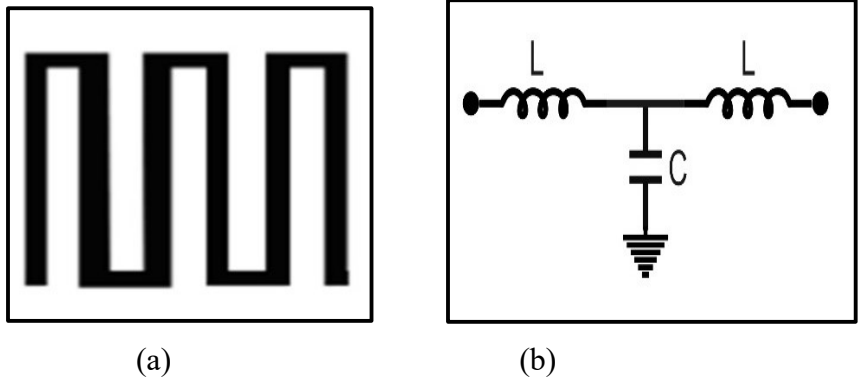


Figure 5.3: Basic meander-line in Figure (a) and its equivalent circuit diagram (b).

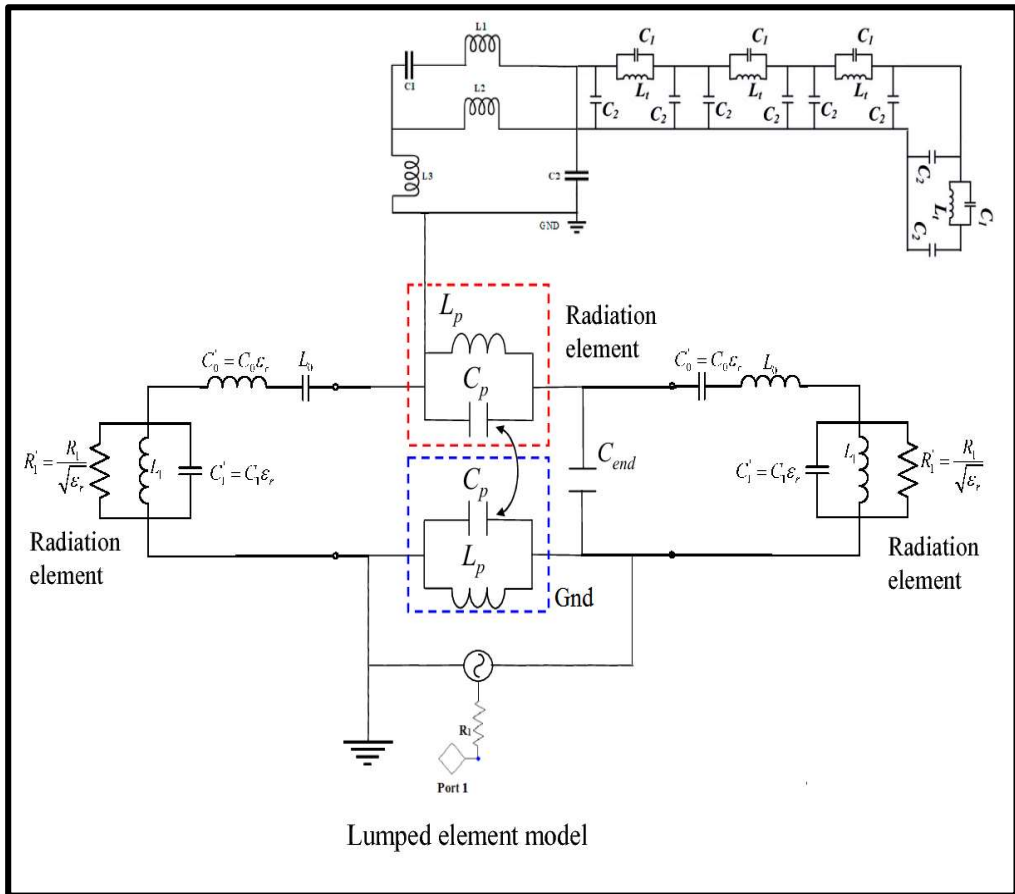


Figure 5.4: Equivalent electrical circuit of the proposed antenna

This arrangement enables the antenna to effectively transmit and receive signals within the desired frequency range. The utilization of these elements ensures optimal utilization of the available space and enhances the overall performance of the antenna system. The proposed meander line antenna design offers enhanced radiation efficiency when compared to traditional half and quarter-wavelength antennas. Through careful optimization of the meandering elements and dimensions, along with the utilization of inductive and capacitive components, the antenna achieves improved impedance matching, gain, and overall performance. The equivalent circuit diagram of the basic meander line is shown in Figure 5.3, where L and C are lumped elements. The equivalent circuit diagram of the proposed design is mentioned in Figure 5.4.

5.3 Simulations And Measurement Results

This section provides a detailed explanation of the fabricated antenna, along with the simulation and measurement results. Additionally, the design includes the development of a connecting cable and the implementation of impedance-matching techniques. The effectiveness of impedance matching is primarily influenced by the width of the meandered line and ground plane. Figure 5.5 showcases the top (a) and bottom (b) of fabricated antennas. To assess the performance of the fabricated antenna, the $|S_{11}|$ (dB) parameters are measured using a Network Analyzer model number ZNLE6, as depicted in Figure 5.6. The return losses, both simulated and measured, are displayed in Figure 5.7. Notably, the antenna's bandwidth is from 860 MHz to 871 MHz, encompassing the 868 MHz bands associated with LoRa technology.

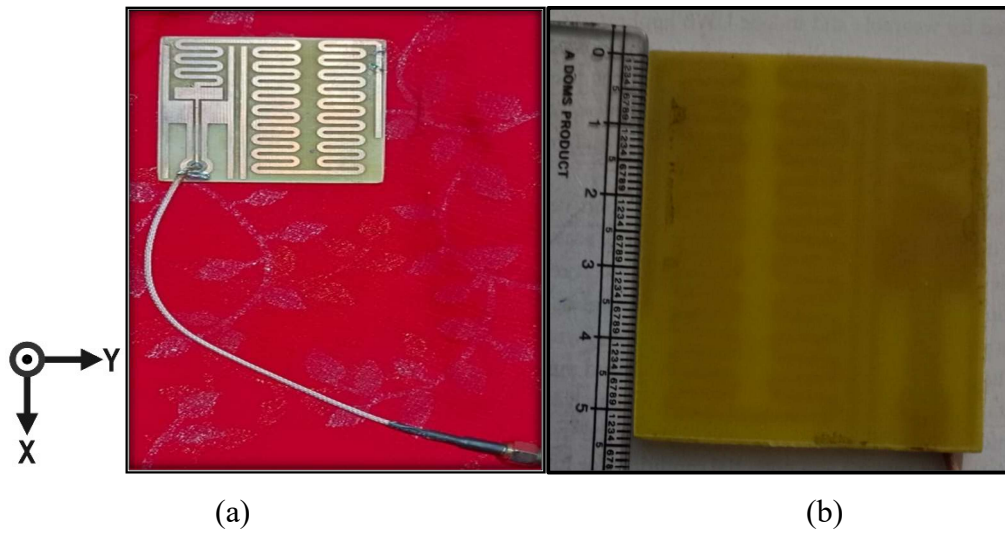


Figure 5.5. Snapshot of the fabricated antenna (a) top (b) bottom

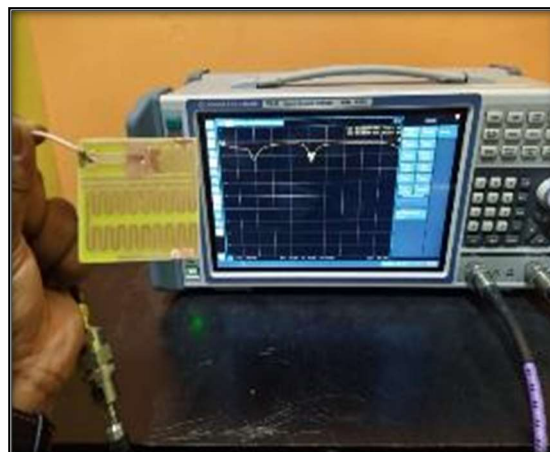


Figure 5.6: Fabricated antenna with Vector Network Analyzer for $|S_{11}|$ (dB) measurement.

The simulated gain band is also mentioned in Figure 5.8, which represents the co-polarization and cross-polarisation bands. To substantiate the advantages of the designed antenna, the proposed design is compared with the existing design lying in the same frequency band or for the LoRa applications based on dimension, operating bands, bandwidth, radiation efficiency, gain, the substrate used, and design complexity, and it is

mentioned in Table 5.1. The radiation pattern helps in determining the directionality of the antenna.

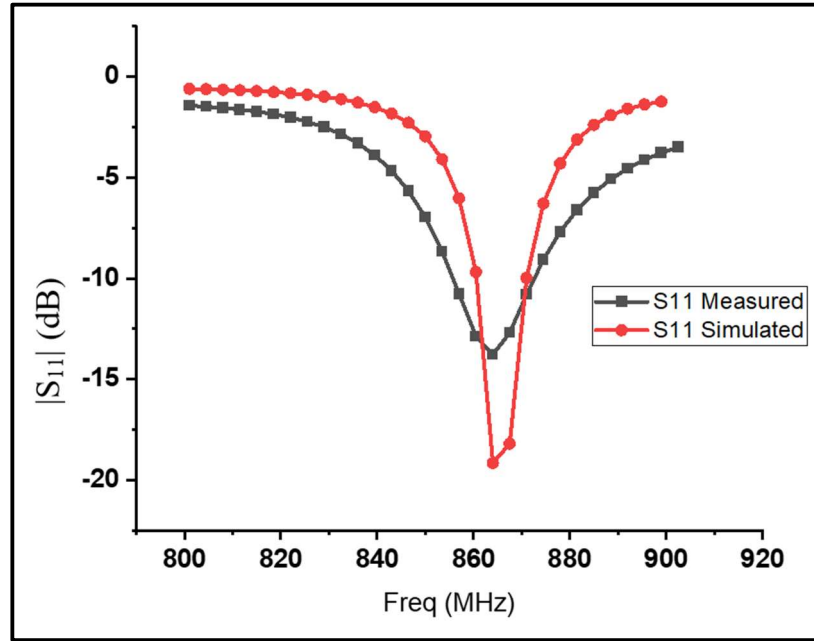


Figure 5.7: The simulated and measured $|S_{11}|$ (dB) Vs Frequency of the proposed antenna.

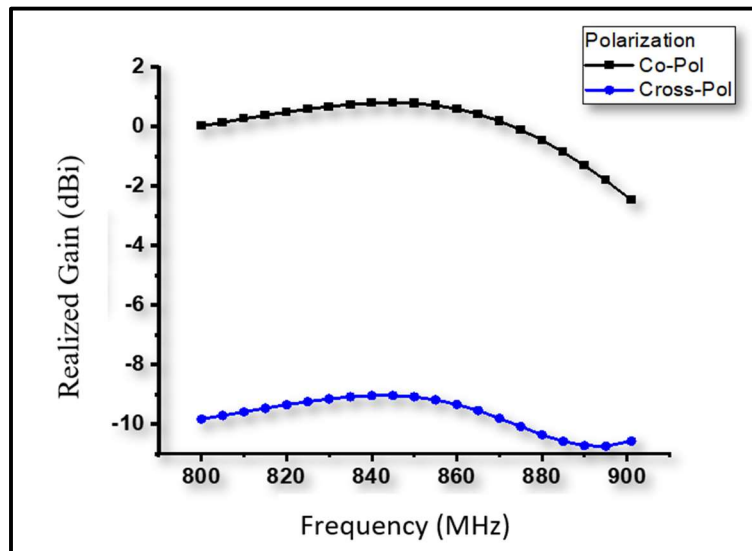
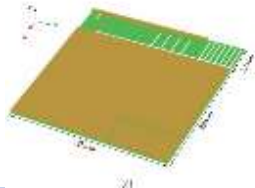
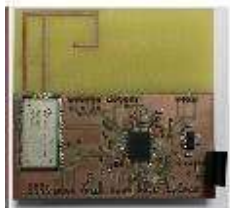
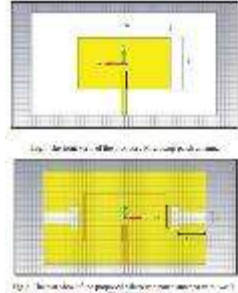

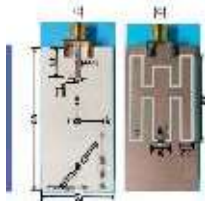



Figure 5.8: The simulated gain Vs. frequency graph of proposed antenna Co-polarization(black) and cross-polarization(blue).

Table 5.1. Comparison table: proposed antenna with antennas published in recent years.

Ref	Dimension Mm ²	Substrate	Frequency (MHz)	Bandwidth	Vias or a shorting pin	Design	Gain dBi
[57]	$0.17\lambda \times 0.14\lambda$	FR4	410	40MHz	yes		-6
[65]	$0.267\lambda \times 0.2\lambda$	PCB	868	20MHz	no		NA
[69]	$0.15\lambda \times 0.11\lambda$	FR4	433	6MHz	No		2.19
[66]	$0.29\lambda \times 0.1\lambda$	FR4	868	2MHz	No		-4.3
[80]	$0.10\lambda \times 0.07\lambda$	RO-4350	868	10MHz	yes		0.96
[81]	$0.34\lambda \times 0.20\lambda$	FR4	868	23MHz	no		NA

[82]	$0.07\lambda \times 0.07\lambda$	FR4	912	60MHz	yes		NA
[83]	$0.43\lambda \times 0.31\lambda$	Silver Ink sheet	868	32MHz	yes		NA
[84]	$0.12\lambda \times 0.24\lambda$	Textile	433	30MHz	no		1.25
[85]	$0.72\lambda \times 0.72\lambda$	RF35	2400	100MHz	yes		6.5
[91]	$0.28\lambda \times 0.46\lambda$	Cardboard	868	50MHz	no		NA
Proposed Antenna	$0.15\lambda \times 0.15\lambda$	FR4	868	11 MHz	No		0.5

The gain is measured by using the reference technique and the reference antenna in a ridge horn antenna placed in an anechoic chamber at a distance of 5.2m from the test (proposed) antenna as mentioned in Figure 5.9. The radiation pattern is calculated at the frequency of 868 MHz and its E-plane and H-plane are mentioned in Figure 5.10. From the radiation, it is observed that the maximum radiation is at an angle of 36 degrees in the theta plane, and it is because of the direction of the field radiated from the antenna.

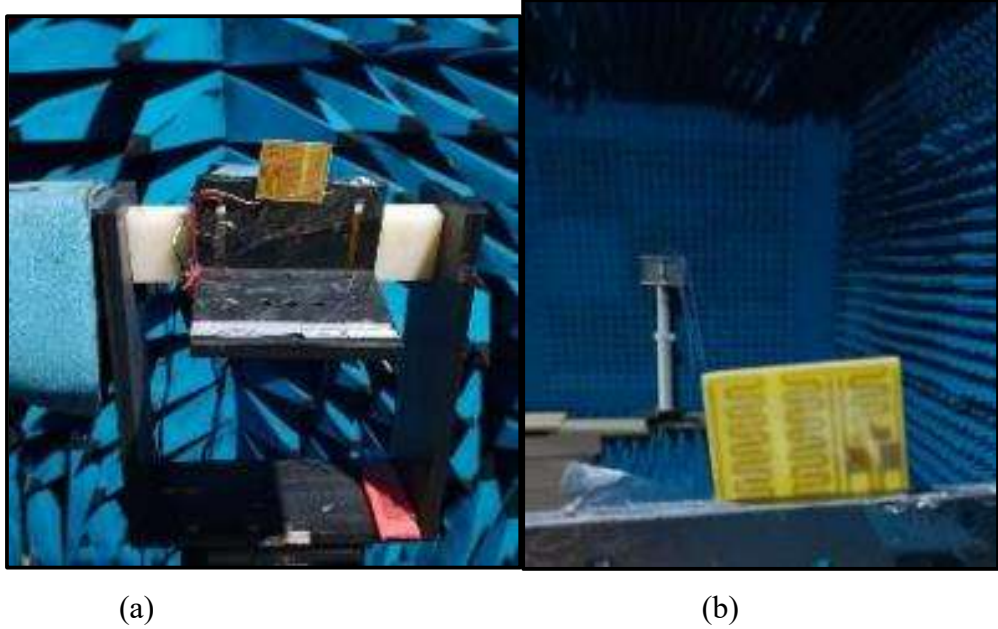


Figure 5.9: The antenna in an anechoic chamber for gain and pattern measurement (a) the antenna in an anechoic chamber (b) horn and fabricated antenna at 5.2m distance.

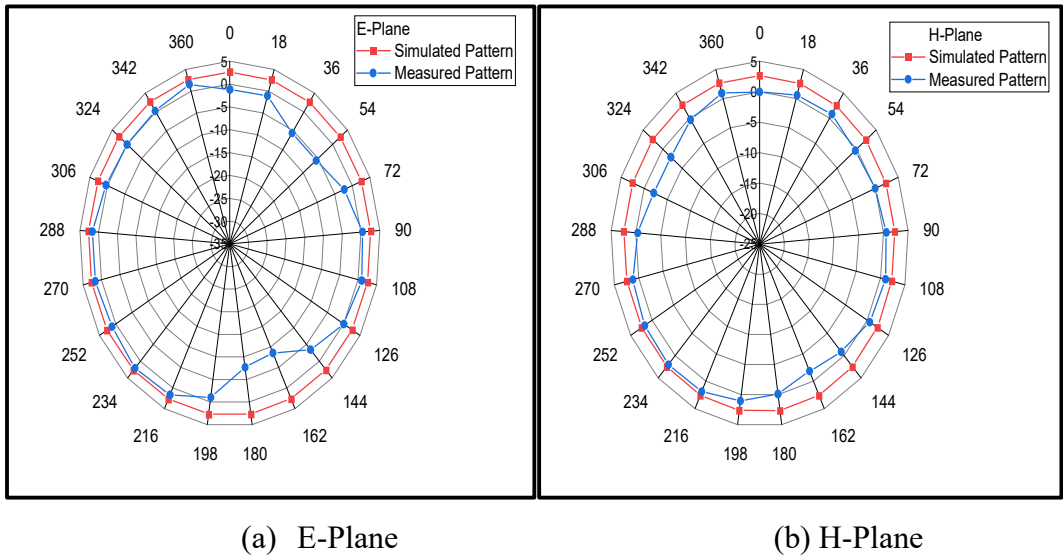


Figure 5.10: The radiation pattern comparison of the proposed antenna in (a) E-Plane (b)H-plane at 868 MHz

5.4 Summary

In this chapter, a meandered-dipole planar antenna is proposed for a long-range application, and the antenna is implemented in a real-time environment to verify its performance. The antenna latency is reported to be less than the standard monopole antenna used for LoRa Module devices of the brand Arduino. The test results show that it covers both bands with satisfactory antenna performance. In future work, it is anticipated that the presented circuit will be reduced in size and that forms and dimensions will be designed to facilitate building deployment. In this case, the antenna should be redesigned with the new materials and size constraints in mind.

CHAPTER 6

LORA ANTENNA IMPLEMENTATION

6.1 Introduction

The proposed LoRa antenna is connected to a LoRa module for data communication. The Arduino IDE software is used to address both LoRa devices and data communication is performed between them. The proposed antenna is considered a transmitter in the first case and a receiver in the second case. As a receiver, it gives a better range of connectivity as it has an omnidirectional radiation pattern. All this communication setup is discussed in detail in this chapter.

6.2 LoRa Network Setup

6.2.1 Requirements

There are many things required for this LoRa connectivity setup as follows:

- i. Arduino UNO
- ii. LoRa Module SX1276 868 MHz
- iii. Jumper Wire for connections
- iv. Bread Board (70mm X 60mm)
- v. USB Cable
- vi. Arduino Software
- vii. Two Laptop

6.2.2 Arduino UNO

According to [133], “Arduino is an open-source electronics platform. Arduino boards can read inputs from a Twitter message, a finger on a button, or a light on a sensor and turn it on”. As a result, such as starting a motor, turning on an LED, or posting something online [133]. The board must have the program, to do so and for that purpose, Arduino is needed. The Arduino Software (IDE), is based on the Wiring programming language Processing. “The board features 6 analog pins, and 14 digital pins, and is programmable using It can be powered by the USB cable or by an Arduino IDE through a type B USB cable. Although it accommodates voltages between 7 and 20 volts, an external 9-volt battery is preferred” [134].

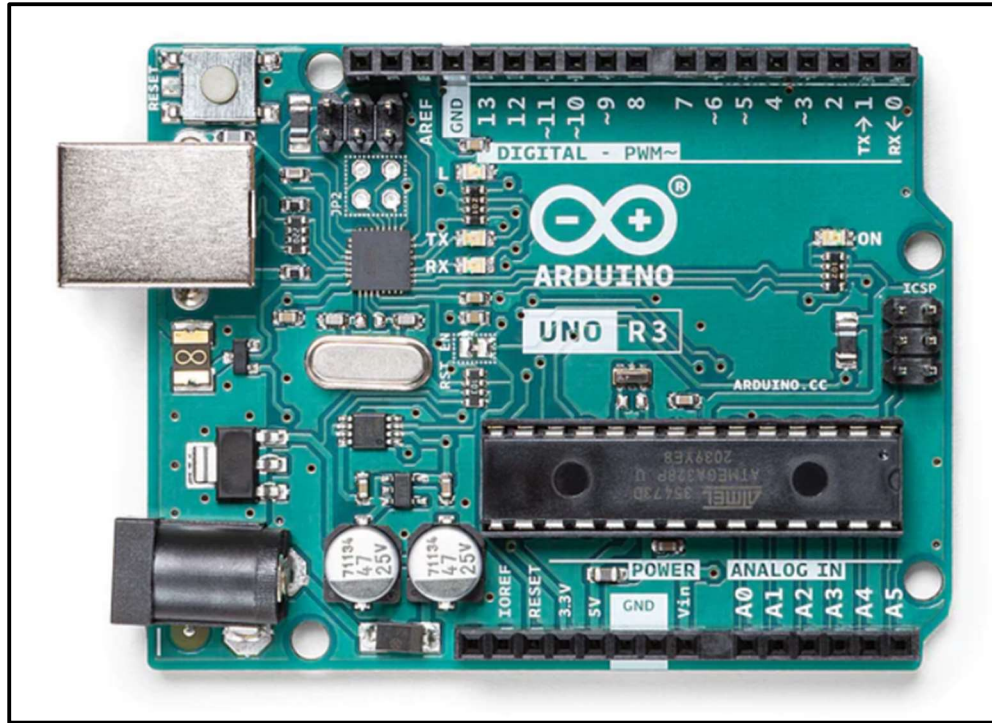
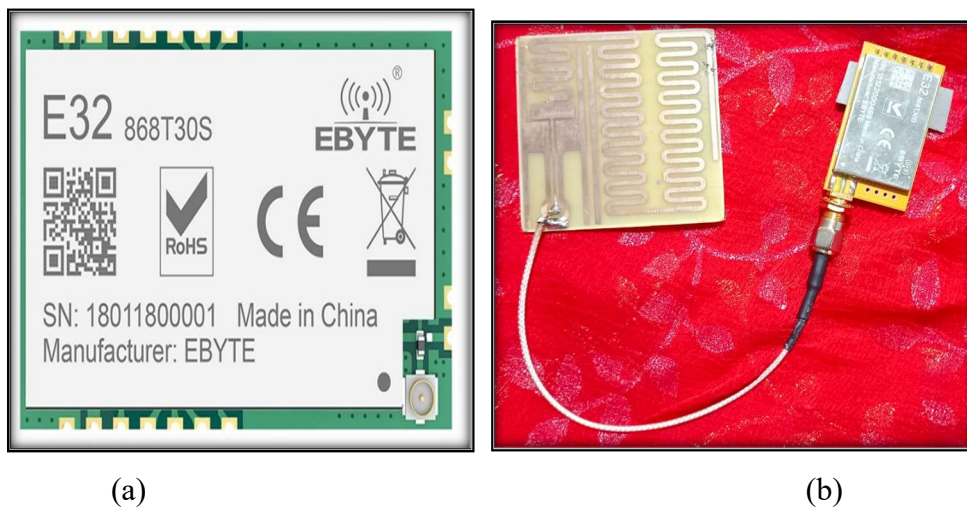


Figure 6.1 Arduino UNO Chip

6.2.3 LoRa Module SX1276

The SX1276 is a LoRa chip manufactured by EByte. The connection between the Arduino and the LoRa Module is shown in Figure 6.2.



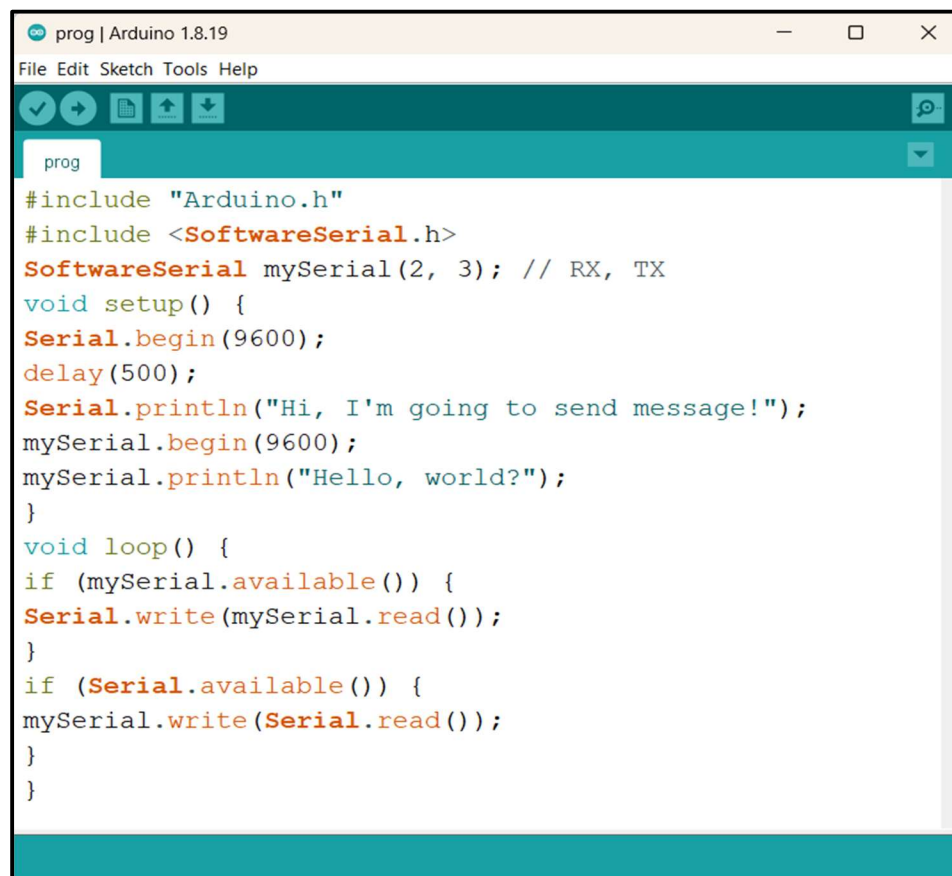
(a)

(b)

Figure 6.2: The LoRa Module (EByte E32-868T30S SX1276 868MHz) (a)Module (b)Module with a proposed antenna.

6.2.4 Software Arduino IDE

The Arduino Integrated Development Environment (IDE) is a user-friendly software platform designed for programming and developing applications for Arduino microcontrollers. It provides a comprehensive set of tools, including a code editor, compiler, and uploader, simplifying the process of writing code and uploading it to Arduino boards. With a user-friendly interface and a vast library of pre-built functions and examples, Arduino IDE is accessible for both beginners and experienced developers. It supports various Arduino boards and shields, making it a versatile choice for creating interactive projects, IoT devices, robots, and more. Arduino IDE empowers users to bring their creative electronic ideas to life effortlessly. It connects to the Arduino and Genuino hardware to upload programs and transmit them.

The image shows a screenshot of the Arduino IDE software window. The window title is "prog | Arduino 1.8.19". The menu bar includes "File", "Edit", "Sketch", "Tools", and "Help". Below the menu bar is a toolbar with icons for checkmark, back, save, upload, and download. A tab labeled "prog" is active. The main text area contains the following C++ code:

```
#include "Arduino.h"
#include <SoftwareSerial.h>
SoftwareSerial mySerial(2, 3); // RX, TX
void setup() {
  Serial.begin(9600);
  delay(500);
  Serial.println("Hi, I'm going to send message!");
  mySerial.begin(9600);
  mySerial.println("Hello, world?");
}
void loop() {
  if (mySerial.available()) {
    Serial.write(mySerial.read());
  }
  if (Serial.available()) {
    mySerial.write(Serial.read());
  }
}
```

Figure 6.3: Arduino Software window with the program used to address the device.

6.3 Implementation of LoRa Connectivity

The final circuit design and assembled version can be seen in Figure 6.4, which depicts all pertinent components, including the proposed antenna, LoRa radio module, microcontroller, sensor antenna, and other passive components. Two sets are prepared so that one is used as a receiver and the other as a LoRa transmitter for the real-time LoRa connectivity experiments. The radio module used is EByte E32-868T30S, SX1276, 868MHz, 30dBm, as shown in Figure 6.2. Therefore, the experiments were conducted to evaluate connectivity. The dimensions of the printed circuit board are 70 mm x 60 mm.

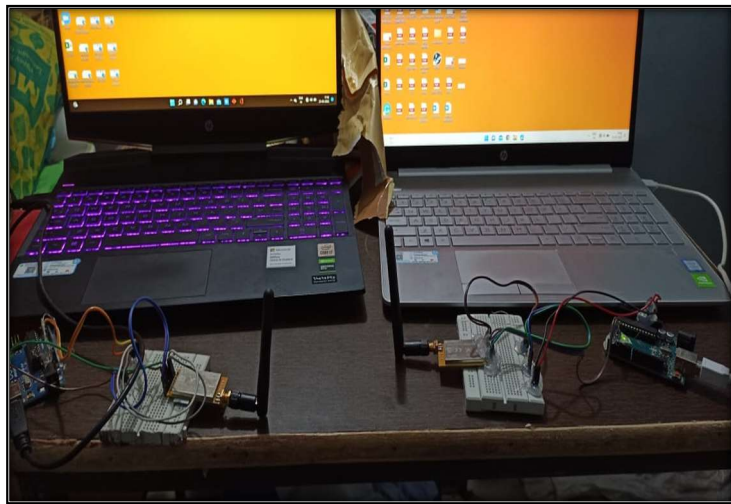


Figure 6.4: Final Circuit assembly with Laptop, LoRa Module, UNO R3 SMD Atmega328P Board, jumping wires, and reference antenna (one is as transmitter and another one as receiver).

The connection between an Arduino Uno board and a LoRa (Long-Range) module typically involves wiring and programming to establish communication between the two as shown in Figure 6.5. The connection between them is as follows:

- **Power Supply:** Both the Arduino Uno and the LoRa module require a power supply. The Arduino Uno can be powered via USB or an external power source (e.g., a battery or a power adapter). The LoRa module also needs a power supply, which may differ based on the specific module used for the connection. Commonly,

they operate at 3.3V, so they may need a voltage regulator if Arduino Uno provides 5V.

- **Serial Communication:** LoRa modules often use UART (Universal Asynchronous Receiver-Transmitter) for communication. To connect the Arduino Uno to the LoRa module, It will typically connect the module's RX (receive) pin to one of the Arduino's TX (transmit) pins and vice versa. This allows data to be transmitted and received between the two.
- **Antenna:** Most LoRa modules require an antenna. So there is a need to connect an appropriate antenna to the module to ensure effective long-range communication. Here the designed LoRa antenna is used.
- **Programming:** To facilitate communication between the Arduino Uno and the LoRa module, there is a need to write and upload a sketch (code) to the Arduino using the Arduino IDE. The sketch will utilize the appropriate libraries for the LoRa module and define how data is transmitted and received.
- **Configuration:** Depending on the specific LoRa module, it may need to configure parameters such as frequency, spreading factor, bandwidth, and coding rate to ensure proper communication within the LoRa network. This configuration is typically done in the Arduino sketch.
- **Serial Monitor:** The Arduino IDE's Serial Monitor is used to monitor and debug the communication between the Arduino Uno and the LoRa module. This can help diagnose issues and verify that data is being transmitted and received correctly.
- **Testing and Deployment:** After the connections are made, the code is uploaded, and the configuration is set, then the communication between the Arduino Uno and the LoRa module is tested. Once everything is working as expected, then the data communication is performed in different scenarios.

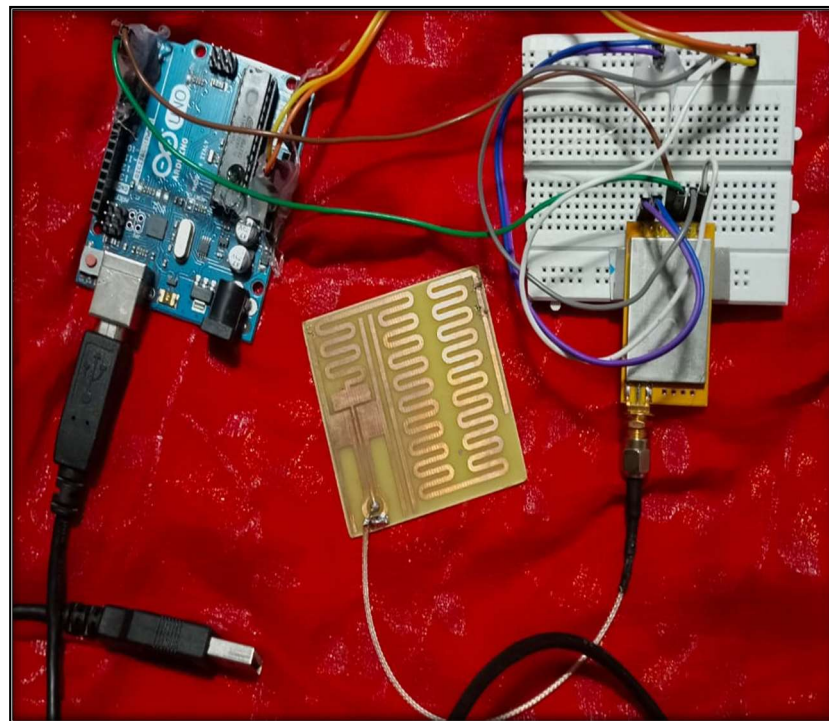
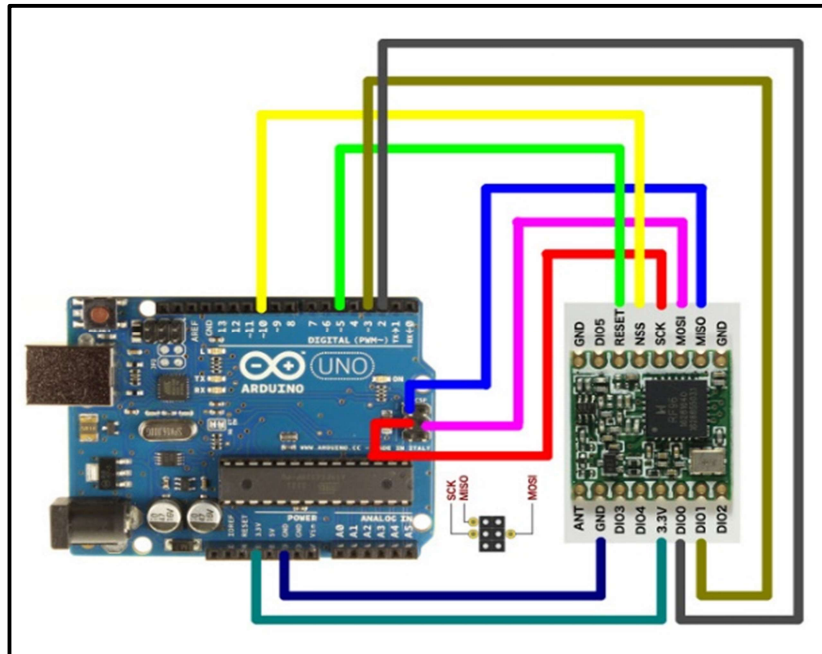


Figure 6.5: The connection between Arduino and LoRa Module (868MHz),

The antenna design has been effectively utilized with LoRa technology, enabling the transmission of data over considerable distances. In ideal conditions with a clear line of

sight, the antenna achieved a remarkable communication range of up to 8 km. Even in urban settings, where obstacles and interference are more prevalent, it managed to maintain a reliable connection for distances exceeding 1 km. Moreover, within building areas, the antenna provided a satisfactory coverage of approximately 250m. To validate its performance, the receiver was mounted on the roof of a vehicle on an express highway, while the transmitter was positioned in a line-of-sight environment. The communication remained consistently stable and connected over the entire 8 km range, as demonstrated in Figure 6.6.

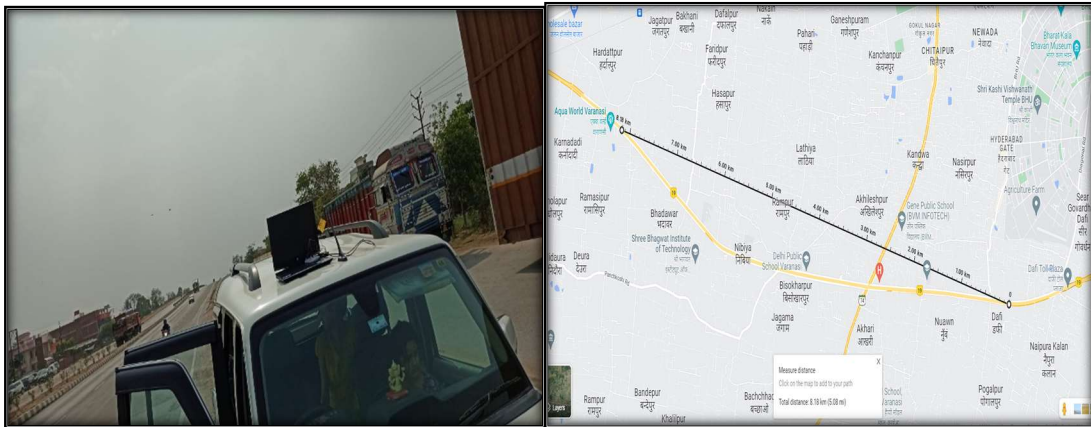


Figure 6.6: First experiment- Connectivity for Line of sight (a)receiver set up (b) Map where the experiment (Tx-Transmitter and Rx-Receiver) performed

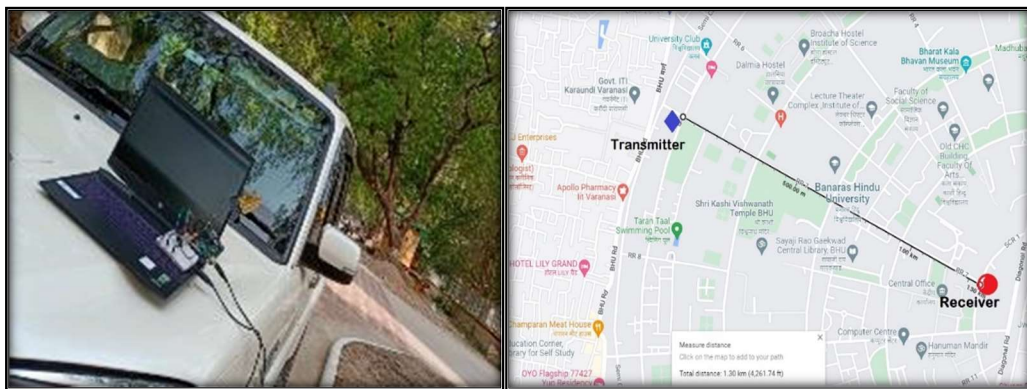


Figure 6.7: Second experiment- Connectivity in the urban environment (a)receiver set up (b) Map where the experiment (Tx-Transmitter and Rx-Receiver) performed

Moving on to the second experiment, the receiver, equipped with a reference antenna, was placed on a vehicle, while the transmitter was located inside another moving car within an urban setting. The proposed antenna was used as the transmitter in this scenario, as illustrated in Figure 6.7. The results indicated that the communication range achieved with the proposed antenna was approximately 1.3 km. However, when the reference antenna was employed instead, the range was limited to only 900 m. This suggests that the proposed antenna provides superior coverage compared to the reference antenna.

In the third experiment, the transmitter was positioned on the balcony of a building, and the receiver antenna was moved to a neighboring building, as shown in Figure 6.8. Using the proposed antenna, the two LoRa devices were able to establish communication with each other within a range of up to 250 m. On the other hand, when the reference antenna was used, the communication range was restricted to a maximum of 150 m.



Figure 6.8: Third experiment- Setup for In-building connectivity (a)receiver set up (b) Map where the experiment (Tx-Transmitter and Rx-Receiver) performed

To summarize, the conducted experiments assessed the performance of the proposed antenna in various scenarios. The first experiment demonstrated that the antenna facilitated well-connected communication over a distance of 8 km on an express highway. The second experiment revealed that the proposed antenna outperformed the reference antenna in an

urban environment, achieving a communication range of 1.3 km compared to only 900 m. Lastly, the third experiment indicated that the proposed antenna enabled communication between two devices at a range of up to 250 m, surpassing the range of 150 m achieved with the reference antenna. These findings highlight the improved coverage capabilities of the proposed antenna in different real-world scenarios.

6.4 Summary

A meandered-dipole planar antenna is proposed for a long-range application, and the antenna is implemented in a real-time environment to verify its performance. The antenna latency is reported to be less than the standard monopole antenna used for LoRa Module devices of the brand Arduino. The designed antenna is successfully implemented with LoRa connectivity and communicates the data up to 8 km in line-of-sight communication, more than 1 km in urban environments, and approximately 250 m of connectivity in building areas. The characteristics of the antenna were analyzed and found suitable for the LoRa applications. In future work, it is anticipated that the presented circuit will be reduced in size and that forms and dimensions will be designed to facilitate building deployment. In this case, the antenna should be redesigned with the new materials and size constraints in mind.

CHAPTER 7

CONCLUSION AND FUTURE SCOPE

7.1 Introduction

Communication has always been a part of human evolution. The ever-changing world of technology has always necessitated the ongoing improvement and refinement of communication systems. The Internet has ushered in a completely new age for communication standards. Connecting individuals to gadgets and devices to other devices on a global scale is part of modern communication. Automation of society with the help of sensors is in demand and it can be fulfilled by using IoT with the help of its data communication network system.

Among all the IoT technologies, “LPWAN is wireless wide-area connectivity for low-powered battery-operated devices, which can communicate with less bitrate over a wide range”. It receives huge demands from researchers and industrialists, as it gives wings to the automation world, which is full of sensors, and it fits perfectly for data communication in a smart world. For our thesis work, the NB-IoT and LoRa technologies were chosen because of their huge demands, their characteristics, and the wide area of application of these technologies in a real-time environment. This thesis explores and intends to construct microstrip patch antennas for communication modules supporting contemporary IoT applications that are small, have a decent range, and have good radiation properties. This chapter's goals are to wrap up the study's work, provide a summary of it, and provide some recommendations for the direction future research in this area should go.

7.2 Conclusion

This chapter provides a comprehensive overview of the proposed antenna configuration and the findings of this thesis, along with a discussion on potential future research directions. The thesis is structured as follows:

The first chapter serves as an introduction to the entire thesis. It sets the stage by presenting the context and significance of the research and establishing the groundwork for the subsequent chapters. The next chapters delve into a thorough examination of existing literature related to IoT (Internet of Things) antennas. This literature review draws from various sources, including books and published papers, guiding the research throughout its entirety. This stage is crucial as it provides a comprehensive understanding of the state-of-the-art in IoT antenna technology. Chapters 3,4 and 5 deal with antenna designs and analysis. In these chapters, we explore the design and analysis of a range of microstrip patch antennas. Initially, the focus is on High-Frequency Structure Simulator (HFSS) software to design and analyze these antennas. Subsequently, the thesis delves into the design of monopole and slotted monopole antennas tailored for narrow-band Internet of Things (NB-IoT) applications. A meandered-dipole antenna optimized for Long Range (LoRa) applications is also discussed. Each antenna design is scrutinized, highlighting their respective characteristics and performance metrics. Chapter 6 brings us to the practical realm, where the real-time implementation of a LoRa antenna is discussed in detail . Here, we validate the LoRa antenna's connectivity and assess its operational range under different conditions, including Line-of-Sight (LOS), indoor, and open-ground scenarios.

The overarching objective of this research is to develop multiband, compact, and lightweight antennas, a critical requirement in the era of automation where seamless sensor communication is paramount. This research specifically targets two low-power wide-area network technologies: narrowband Internet of Things (NB-IoT) and long-range (LoRa). The antenna performance is thoroughly examined, considering factors such as dielectric substrate material, substrate height, and design geometry. This analysis contributes to optimizing the return loss performance, ensuring that the antennas operate at peak efficiency. For both NB-IoT and LoRa technologies, we employ HFSS software to design efficient, planar, and compact antennas. Following the design phase, these antennas are fabricated, and their performance is meticulously measured and cross-verified with simulated results. The LoRa antenna, with its meandered design, operates in the 868 MHz frequency range. It features compact dimensions of $\lambda/6 \times \lambda/6$ and $\lambda/215$, exhibiting an

omnidirectional radiation pattern. In contrast, the monopole antenna caters to NB-IoT bands B1 (2100) and B3 (1800) with dimensions of $\lambda/6.6 \times \lambda/3.3 \times \lambda/125$. Additionally, two more antenna designs, employing slotted and fractal technologies, are explored to achieve broadband characteristics within a compact form factor. It's worth noting that the fractal design, incorporating a two-port feed system, seeks to enhance gain and isolation, marking a notable advancement over existing antenna designs.

In comparison to conventional antennas, the proposed antennas offer several advantages, including a lower profile, reduced weight, compactness, and superior gain and radiation characteristics. The real-world implementation of the LoRa antenna demonstrates its enhanced connectivity compared to the available monopole antenna, further validating its practical utility. LoRa antenna is well implemented in the real-time scenario and found better connectivity than the available monopole antenna. Overcoming isolation and power limitation problems in microstrip patch antennas can be challenging but is crucial for achieving better performance in terms of radiation efficiency, gain, and signal quality. By Optimizing the patch geometry, such as shape, size, and substrate material, to improve radiation efficiency. High dielectric constant substrates can lead to increased efficiency, but care should be taken to avoid losses associated with high dielectric materials. With a good ground plane design beneath the patch antenna. A well-designed ground plane can reduce the losses due to surface waves and improve radiation efficiency.

The limitation with the proposed designs is as: One significant drawback with monopole patches is their size, as they typically require a quarter-wavelength to operate efficiently. This limits their application in compact devices and higher frequency bands where space is constrained. Additionally, monopoles are susceptible to impedance-matching issues and can suffer from low radiation efficiency when not properly tuned. Fractal antennas, on the other hand, offer compact and multiband capabilities, but they also come with limitations. One limitation is their complexity in design and manufacturing, which can increase production costs. Moreover, fractal antennas can be sensitive to the environment and nearby objects, which can affect their performance. They may also exhibit narrower bandwidth compared to traditional antennas, making them less suitable for applications

requiring a broad frequency range. Meandering patch antennas are known for their compact size and versatility, but they too have limitations. The meandering design can introduce additional losses, reducing radiation efficiency. Furthermore, meandering patch antennas can be sensitive to changes in the substrate material or thickness, which makes them less robust in varying environmental conditions. Achieving precise impedance matching across a wide frequency range can also be challenging with these antennas, limiting their use in applications requiring high-frequency agility.

In conclusion, this thesis represents a comprehensive exploration of IoT antenna technology, spanning from theoretical analysis to practical implementation. The innovative designs and performance enhancements achieved in this research contribute to the development of efficient, compact, and multiband antennas, addressing the evolving needs of the automation era's sensor networks. These findings pave the way for future advancements in IoT antenna technology and its broader applications.

7.3 Future Scope

The thesis work presented here revolves around the design of a compact LoRa antenna tailored for use in NB-IoT (Narrowband Internet of Things) applications and LoRa (Long-Range) applications. This section outlines the research conducted in this work and discusses potential avenues for future research expansion.

i. Enhancing LoRa Range in High-Traffic Areas: A promising direction for future studies is to address the challenge of extending the range of LoRa communication in high-traffic areas. This can be achieved by strategically adding more gateways along the LoRa network's route. This approach would help alleviate congestion and improve the overall performance of LoRa-based IoT systems in densely populated regions.

ii. Frequency Diversity with 433MHz: To increase the versatility of the LoRa antenna in the Indian context, future research can explore the integration of the 433MHz frequency band with the existing LoRa antenna design. This would enable the antenna to operate in

multiple frequency bands, making it more adaptable to diverse communication environments and regulatory constraints within India.

iii. Expanding IoT Ecosystem: While the current focus of the LoRa antenna is data transmission, future efforts can explore the integration of this antenna with various sensors to create a more comprehensive and intelligent IoT ecosystem. This could lead to applications such as smart lighting systems or advanced smart agriculture systems, where data collection and control mechanisms can be integrated seamlessly.

iv. Improving Bandwidth: Another promising area for future research is the enhancement of antenna bandwidth. One approach to achieve this could involve incorporating meta-surface ground structures into both the LoRa and multi-band antennas. These structures can help widen the bandwidth, enabling more efficient data transmission and reception.

v. Enhancing MIMO Antenna Isolation: For applications requiring multiple-input, multiple-output (MIMO) antenna systems, future research can focus on improving isolation between the antennas. This might involve the implementation of Electromagnetic Band Gap (EBG) structures or innovative array configurations to reduce interference and crosstalk between MIMO antennas, thereby enhancing overall system performance.

vi. Power Harvesting Techniques: Addressing the power limitations faced by deployed and often inaccessible nodes in IoT networks is crucial. Future studies can delve into various power-harvesting antenna techniques. These techniques can help nodes generate and store energy from their surroundings, reducing their dependence on external power sources and prolonging their operational lifetimes.

vii. Polarization Purity: To enhance the reception quality at the receiver side, future antenna designs could focus on achieving polarization purity. Circular polarization, for instance, can be achieved through the integration of power divider circuits. This approach can help mitigate polarization-related signal losses and improve communication reliability in various scenarios.

BIBLIOGRAPHY

- [1] K. Ashton, "Internet of Things," RFID J., vol. 22, no. 7, pp. 97_114, 2009.
- [2] E. Ahmed, I. Yaqoob, A. Gani, M. Imran, and M. Guizani, "Internet-of-Things-based smart environments: State of the art, taxonomy, and open research challenges," IEEE Wireless Commun., vol. 23, no. 5, pp. 10_16, Oct. 2016.
- [3] Co-operation with the working Group RFID of the ETP EPOSS, Internet of Things in 2020 Roadmap for the Future, Version 1.1, INFSO D.4 Networked Enterprise RFID INFSO G.2 Micro Nanosystems, May 2020.
- [4] L. Atzori, A. Iera, and G. Morabito, "The Internet of Things: A survey," Comput. Netw., vol. 54, no. 15, pp. 2787_2805, Oct. 2010.
- [5] [The Future of IoT: 10 Predictions about the Internet of Things | Norton](#)
- [6] Balanis C. A, "Microstrip Antennas", Antenna Theory, Analysis and Design, Third Edition, John Wiley & Sons, 2010.
- [7] K.D Prasad, "Antenna wave and propagation", Satya Prakashan, 1983.
- [8] Kin-Lu. Wong, "Planar Antennas for Wireless Communications" by Wiley Interscience, 2003.
- [9] Eshita Rastogi a, Navrati Saxena b,* , Abhishek Roy, Dong Ryeol Shin," Narrowband Internet of Things: A Comprehensive Study" Computer Networks 173 (2020) 107209.
- [10] <https://www.i-scoop.eu/internet-of-things-IoT/lpwan/nb-IoT-narrowband-IoT/>
- [11] Technical Specification Group GSM/EDGE Radio Access Network; Cellular system support for ultra-low complexity and low throughput, Internet of things(IoT), Technical Report (TR), 3rd Generation Partnership Project (3GPP), 2015, Version 13.1.0.
- [12] Mads Lauridsen, Istvan Z. Kovacs, Preben Mogensen, Mads Sorensen, Steffen Holst, Coverage and Capacity Analysis of LTE-M and NB-IoT in a Rural Area, IEEE 84th Vehicular Technology Conference (VTC-Fall), pp 1-5, Sept 2016.

- [13] Jun Xu, Junmei Yao, Lu Wang, Zhong Ming, Kaishun Wu, Lei Chen, Narrowband Internet of Things: Evolutions, Technologies, and Open Issues, IEEE Internet of Things Journal (Volume: 5, Issue: 3, June 2018), 1449-1462.
- [14] [5 things to know about the LPWAN market in 2021 \(iot-analytics.com\)](https://www.iot-analytics.com)
- [15] <https://www.data-alliance.net/blog/nb-IoT-narrowband-internet-of-things/>
- [16] M. Centenario, L. Vangelista, A. Zanella, and M. Zorzi, "Long-range communications in unlicensed bands: The rising stars in the IoT and smart city scenarios," IEEE Wireless Communications, vol. 23, pp. 60-67, 2016.
- [17] J. Petäjäjärvi, K. Mikhaylov, M. Hämäläinen, and J. Iinatti, "Evaluation of LoRa LPWAN technology for remote health and wellbeing monitoring," in Medical Information and Communication Technology (ISMICT), 2016 10th International Symposium on, 2016, pp. 1-5.
- [18] D. Bankov, E. Khorov, and A. Lyakhov, "On the Limits of LoRaWAN Channel Access," in Engineering and Telecommunication (EnT), 2016 International Conference on, 2016, pp. 10-14.
- [19] R. S. Sinha, Y. Wei, and S.-H. Hwang, "A survey on LPWA technology: LoRa and NB-IoT," ICT Express, 2017.
- [20] https://lora-alliance.org/wp-content/uploads/2020/11/RP_2-1.0.2.pdf
- [21] D. M. Pozar, "Microstrip Antennas," Proc. IEEE, Vol. 80, No. 1, pp. 79_81, January 1992.
- [22] Bhattacharyya, Arun K. and Rohini Garg. "Generalised transmission line model for microstrip patches." (1985).
- [23] Abhishek K. Chaudhary, Murli Manohar," Design and Analysis of a Compact Wideband Monopole Patch Antenna for Future Handheld Gadgets", Progress In Electromagnetics Research C, Vol. 109, 227–241, 2021
- [24] L. H. Trinh, T. Q. K. Nguyen, H. L. Tran, P. C. Nguyen, N. V. Truong, and F. Ferrero, "Low-profile horizontal Omni-directional antenna for LoRa wearable devices," 2017 International Conference on Advanced Technologies for Communications (ATC), 2017, pp. 136-139, DOI: 10.1109/ATC.2017.8167603.

- [25] Natarajan, R, Gulam Nabi Alsath, M, Kanagasabai, M, Bilvam, S, Meiyalagan, S. Integrated Vivaldi antenna for UWB/diversity applications in a vehicular environment. *Int J RF Microw Comput Aided Eng.* 2020; 30:e21989. <https://doi.org/10.1002/mmce.21989>
- [26] Gurpreet Bharti, Jagtar S. Sivia, "A Design of Multiband Nested Square Shaped Ring Fractal Antenna with Circular Ring Elements for Wireless Applications", *Progress In Electromagnetics Research C*, Vol. 108, 115–125, 2021.
- [27] Lizzi, L., Ferrero, F., Danchesi, C., Boudaud, S., 2018. Miniature Multiband Inverted-F Antenna over an Electrically Small Ground Plane for Compact IoT Terminals. *Wireless Communications and Mobile Computing 2018*, 1–8.
- [28] S. X. Ta, H. Choo, and I. Park, "Broadband printed-dipole antenna and its arrays for 5G applications," *IEEE Antennas and Wireless Propagation Letters*, vol. 16, pp. 2183–2186, 2017.
- [29] S. Katoch, H. Jotwani, S. Pani and A. Rajawat, "A compact dual band antenna for IOT applications," 2015 International Conference on Green Computing and Internet of Things (ICGCIoT), 2015, pp. 1594-1597, doi: 10.1109/ICGCIoT.2015.7380721.
- [30] A. Glisson, "Advances in microstrip and printed antennas [Reviews and Abstracts]," in *IEEE Antennas and Propagation Magazine*, vol. 41, no. 2, pp. 68-69, April 1999, doi: 10.1109/MAP.1999.769694.
- [31] Pozar, D. M.. "A review of bandwidth enhancement techniques for microstrip antennas." In *Microstrip Antennas: The Analysis and Design of Microstrip Antennas and Arrays* , edited by D. M. Pozar and D.H. Schaubert , 157-166. New York: IEEE Press, 1995.
- [32] H. Liu, S. Ishikawa, A. An, S. Kurachi, and T. Yoshimasu, "Miniaturized microstrip meander-line antenna with the very high-permittivity substrate for sensor applications," *Microw. Opt. Technol. Lett.*, vol. 49, no. 10, pp. 2438–2440, 2007.

- [33] Y. Yoshimura, "A microstrip line slot antenna (short papers)," *IEEE Trans. Microw. Theory Tech.*, vol. 20, no. 11, pp. 760–762, Nov. 1972.
- [34] Kaur and P. K. Malik, "Tri-State, T Shaped Circular Cut Ground Antenna for Higher 'X' Band Frequencies," 2020 International Conference on Computation, Automation and Knowledge Management (ICCAKM), Dubai, United Arab Emirates, 2020, pp. 90-94.
- [35] N.P. Agrawall, G. Kumar, and K.P. Ray, "Wideband planar monopole antennas", *IEEE Trans Antennas Propagat.*, vol. AP - 46, pp. 249 - 251, Feb. 1998.
- [36] R. Garg, P. Bhartia, I. Bahl, and A. Ittipiboon, *Microstrip Antenna Design Handbook*. Norwood, MA, USA: Artech House, 2001.
- [37] W. Menzel, D. Pilz, and R. Leberer, "A 77 GHz FM/CW radar front end with a low-profile, low-loss printed antenna," *IEEE Trans. Microw. Theory Tech.*, vol. 47, no. 12, pp. 2237–2241, Dec. 1999.
- [38] Ali, I.; Jamaluddin, M.H.; Gaya, A.; Rahim, H.A. A Dielectric Resonator Antenna with Enhanced Gain and Bandwidth for IoT Applications. *Sensors* 2020, 20, 675. <https://doi.org/10.3390/s20030675>
- [39] Geonyeong Shin, Joomin Park, Tae Rim Park, Ck-Jae Yoon," Sustaining the Radiation Properties of a 900-MHz-Band Planar LoRa Antenna Using a 2-by-2 Thin EBG Ground Plane", *IEEE Access*, Volume 8, 2020, (145586-145592).
- [40] T. Mishra, S. K. Panda, M. F. Karim, L. C. Ong and T. M. Chiam, "SIW-based slot array antenna and power management circuit for wireless energy harvesting applications," *Proceedings of the 2012 IEEE International Symposium on Antennas and Propagation*, 2012, pp. 1-2, doi: 10.1109/APS.2012.6348552.
- [41] G. Li, H. Zhai, T. Li, L. Li and C. Liang, "CPW-Fed S-Shaped Slot Antenna for Broadband Circular Polarization," in *IEEE Antennas and Wireless Propagation Letters*, vol. 12, pp. 619-622, 2013, doi: 10.1109/LAWP.2013.2261652.
- [42] W. A. Khan et al., "Smart IoT Communication: Circuits and Systems," 2020 International Conference on Communication Systems & NetworkS (COMSNETS), 2020, pp. 699-701, doi: 10.1109/COMSNETS48256.2020.9027430.

- [43] L. Su, J. Muñoz-Enano, P. Vélez, J. Martel, F. Medina and F. Martí, "On the Modeling of Microstrip Lines Loaded With Dumbbell Defect-Ground-Structure (DB-DGS) and Folded DB-DGS Resonators," in *IEEE Access*, vol. 9, pp. 150878-150888, 2021, doi: 10.1109/ACCESS.2021.3125775..
- [44] T. T. Le and T. -Y. Yun, "Wearable Dual-Band High-Gain Low-SAR Antenna for Off-Body Communication," in *IEEE Antennas and Wireless Propagation Letters*, vol. 20, no. 7, pp. 1175-1179, July 2021, doi: 10.1109/LAWP.2021.3074641.
- [45] G. Gao, C. Yang, B. Hu, R. Zhang and S. Wang, "A Wearable PIFA With an All-Textile Metasurface for 5 GHz WBAN Applications," in *IEEE Antennas and Wireless Propagation Letters*, vol. 18, no. 2, pp. 288-292, Feb. 2019, doi: 10.1109/LAWP.2018.2889117.
- [46] Vamseekrishna, A., Madhav, B.T.P., Anilkumar, T., Reddy, L.S.S., 2019. An IoT Controlled Octahedron Frequency Reconfigurable Multiband Antenna for Microwave Sensing Applications. *IEEE Sens. Lett.* 3, 1–4.
- [47] Prem P. Singh, Pankaj K. Goswami *, Sudhir K. Sharma, and Garima Goswami, Frequency Reconfigurable Multiband Antenna for IoT Applications in WLAN, Wi-Max, and C-Band, *Progress In Electromagnetics Research C*, Vol. 102, 149–162, 2020.
- [48] A. Shoykhetbrod, D. Nussler and A. Hommes, "Design of a SIW meander antenna for 60 GHz applications," 2012 The 7th German Microwave Conference, 2012, pp. 1-3.
- [49] S. K. V. Das and T. Shanmuganatham, "Design of multiband microstrip patch antenna for IOT applications," 2017 IEEE International Conference on Circuits and Systems (ICCS), 2017, pp. 87-92, doi: 10.1109/ICCS1.2017.8325968.
- [50] S. K. V. Das and T. Shanuganatham, "Design of triple starfish shaped microstrip patch antenna for IoT applications," 2017 IEEE International Conference on Circuits and Systems (ICCS), 2017, pp. 182-185, doi: 10.1109/ICCS1.2017.8325986.

- [51] A. Satheesh, R. Chandrababu and I. S. Rao, "A compact antenna for IoT applications," 2017 International Conference on Innovations in Information, Embedded and Communication Systems (ICIIECS), 2017, pp. 1-4, doi: 10.1109/ICIIECS.2017.8275921.
- [52] Y. Giay and B. R. Alam, "Design and Analysis 2.4 GHz Microstrip Patch Antenna Array for IoT Applications using Feeding Method," *2018 International Symposium on Electronics and Smart Devices (ISESD)*, 2018, pp. 1-3, doi: 10.1109/ISESD.2018.8605455.
- [53] O. M. A. Dardeer, H. A. Elsadek and E. A. Abdallah, "2×2 Circularly Polarized Antenna Array for RF Energy Harvesting in IoT System," *2018 IEEE Global Conference on Internet of Things (GCIoT)*, 2018, pp. 1-6, doi: 10.1109/GCIoT.2018.8620143.
- [54] Awais, Q., Chattha, H. T., Jamil, M., Jin, Y., Tahir, F. A., & Rehman, M. U. (2018). A novel dual ultrawideband CPW-fed printed antenna for Internet of Things (IoT) applications. *Wireless Communications and Mobile Computing*, 2018.
- [55] Shafique, K., Khawaja, B.A., Khurram, M.D., Sibtain, S.M., Siddiqui, Y., Mustaqim, M., Chattha, H.T., Yang, X., "Energy Harvesting Using a Low-Cost Rectenna for Internet of Things (IoT) Applications," in *IEEE Access*, vol. 6, pp. 30932-30941, 2018, doi: 10.1109/ACCESS.2018.2834392
- [56] Lizzi, Leonardo et al. "Miniature Multiband Inverted-F Antenna over an Electrically Small Ground Plane for Compact IoT Terminals." *Hindawi, Wireless Communications and Mobile Computing*. 2018 (2018): 8131705:1-8131705:8 pages.
- [57] Qianyun Zhang and Yue Gao, "Embedded Antenna Design on LoRa Radio for IoT Applications", 12th European Conference on Antennas and Propagation (EuCAP 2018), 2018 page (3 pp.)

- [58] Shi, G., He, Y., Yin, B., Zuo, L., She, P., Zeng, W., Ali, F., 2019. Analysis of Mutual Couple Effect of UHF RFID Antenna for the Internet of Things Environment. *IEEE Access* 7, 81451–81465.
- [59] Shahidul Islam, M., Islam, M.T., Ullah, MD.A., Kok Beng, G., Amin, N., Misran, N., 2019. A Modified Meander Line Microstrip Patch Antenna With Enhanced Bandwidth for 2.4 GHz ISM-Band Internet of Things (IoT) Applications. *IEEE Access* 7, 127850–127861.
- [60] Vamseekrishna, A., Madhav, B.T.P., Anilkumar, T., Reddy, L.S.S., 2019. An IoT Controlled Octahedron Frequency Reconfigurable Multiband Antenna for Microwave Sensing Applications. *IEEE Sens. Lett.* 3, 1–4.
- [61] Mung, S.W.Y., Cheung, C.Y., Wu, K.M., Yuen, J.S.M., 2019. Wideband Rectangular Foldable and Non-foldable Antenna for Internet of Things Applications. *International Journal of Antennas and Propagation* 2019, 1–5.
- [62] Sharif, A., Ouyang, J., Yang, F., Chattha, H.T., Imran, M.A., Alomainy, A., Abbasi, Q.H., 2019. Low-Cost Inkjet-Printed UHF RFID Tag-Based System for Internet of Things Applications Using Characteristic Modes. *IEEE Internet Things J.* 6, 3962–3975.
- [63] A. Sabban, "Small New Wearable Antennas for IOT, Medical and Sport Applications," *2019 13th European Conference on Antennas and Propagation (EuCAP)*, 2019, pp. 1-5.
- [64] P. Van Torre, T. Ameloot and H. Rogier, "Long-range body-to-body LoRa link at 868 MHz," *2019 13th European Conference on Antennas and Propagation (EuCAP)*, 2019, pp.1-5.
- [65] Lopes S.I., Pereira F., Vieira J.M.N., Carvalho N.B., Curado A. (2019) Design of Compact LoRa Devices for Smart Building Applications. In: Afonso J., Monteiro V., Pinto J. (eds) *Green Energy and Networking. GreeNets 2018. Lecture Notes of the Institute for Computer Sciences, Social Informatics and Telecommunications Engineering*, vol 269. Springer, Cham. https://doi.org/10.1007/978-3-030-12950-7_12

- [66] F. Ferrero and M. B. Toure, "Dual-band LoRa Antenna : Design and Experiments," *2019 IEEE Conference on Antenna Measurements & Applications (CAMA)*, 2019, pp. 243-246, doi: 10.1109/CAMA47423.2019.8959760.
- [67] Wazie M. Abdulkawi, Abdel-Fattah A. Sheta, Waqar A. Malik, Sajjad U. Rehman, & Majeed S. Alkanhal. (2019). RF MEMS Switches Enabled H-Shaped Beam Reconfigurable Antenna. *The Applied Computational Electromagnetics Society Journal (ACES)*, 34(09), 1312–1319.
- [68] Birwal, A., Singh, S., Kanaujia, B., & Kumar, S. (2019). Broadband CPW-fed circularly polarized antenna for IoT-based navigation system. *International Journal of Microwave and Wireless Technologies*, 11(8), 835-843. doi:10.1017/S1759078719000461
- [69] Aksha Mushtaq, Sindhu Hak Gupta and Asmita Rajawat, 2020, Design and Performance Analysis of LoRa LPWAN Antenna for IoT Applications, 7th International Conference on Signal Processing and Integrated Networks (SPIN)2020
- [70] Aayush Pandey, M. V. Deepak Nair, Inset Fed Miniaturized Antenna with Defected Ground Plane for LoRa Applications, Science Direct, Procedia Computer Science 171 (2020) 2115–2120
- [71] Turke Althobaiti, Abubakar Sharif, Jun Ouyang, Naeem Ramzan And Qammer H. Abbasi, planar pyramid shaped uhf rfid tag antenna with polarisation diversity for iot applications using characteristics mode analysis , IEEE ACCESS volume 8, 2020
- [72] Prem P. Singh, Pankaj K. Goswami *, Sudhir K. Sharma, and Garima Goswami, Frequency Reconfigurable Multiband Antenna for IoT Applications in WLAN, Wi-Max, and C-Band, Progress In Electromagnetics Research C, Vol. 102, 149–162, 2020
- [73] Yi Yan , Abubakar Sharif , Jun Ouyang , Chu Zhang , And Xiao Ma, UHF RFID Handset Antenna Design With Slant Polarization for IoT and Future 5G Enabled Smart Cities Applications Using CM Analysis, IEEE Access, SPECIAL

SECTION ON ANTENNA AND PROPAGATION FOR 5G AND BEYOND, Volume 8. 2020

- [74] Wang, M.; Yang, L.; Shi, Y. A Dual-port Microstrip Rectenna for Wireless Energy Harvest at LTE Band. *AEU Int. J. Electron. Commun.* 2020, 126, 153451
- [75] Mainsuri *et al.*, "A 923 MHz Steerable Antenna for Low Power Wide Area Network (LPWAN)," *2020 IEEE International Conference on Communication, Networks and Satellite (Commnetsat)*, 2020, pp. 246-250, doi: 10.1109/Commnetsat50391.2020.9328990.
- [76] Sneha, Priyadarshi Suraj, A Metamaterial based Monopole antenna for Satellite-based Navigation Applications, *International Journal of Intelligent Communication, Computing and Networks*, Aug-2020 Open Access Journal (ISSN: 2582-7707).
- [77] Jayshri Kulkarni, "Multi-Band Printed Monopole Antenna Conforming Bandwidth Requirement of GSM/WLAN/WiMAX Standards," *Progress In Electromagnetics Research Letters*, Vol. 91, 59-66, 2020. doi:[10.2528/PIERL20032104](https://doi.org/10.2528/PIERL20032104)
- [78] L. Zhuo, H. Han, X. Shen and H. Zhao, "A U-shaped wide-slot dual-band broadband NB-IoT antenna with a rectangular tuning stub," *2020 IEEE 4th Information Technology, Networking, Electronic and Automation Control Conference (ITNEC)*, 2020, pp. 123-128, doi: 10.1109/ITNEC48623.2020.9084751.
- [79] S. A. Haydhah, F. Ferrero, L. Lizzi, M. S. Sharawi and A. Zerguine, "A Multifunctional Compact Pattern Reconfigurable Antenna With Four Radiation Patterns for Sub-GHz IoT Applications," in *IEEE Open Journal of Antennas and Propagation*, vol. 2, pp. 613-622, 2021, doi: 10.1109/OJAP.2021.3078236.
- [80] R. Hussain, M. Abou-Khousa, M. Umar Khan and M. S. Sharawi, "A Compact Sub-1 GHz IoT Antenna Design with Wide Tuning Capabilities," *2021 15th European Conference on Antennas and Propagation (EuCAP)*, 2021, pp. 1-3, doi: 10.23919/EuCAP51087.2021.9411308.

- [81] Dala A, Arslan T. Design, Implementation, and Measurement Procedure of Underwater and Water Surface Antenna for LoRa Communication. *Sensors*. 2021; 21(4):1337. <https://doi.org/10.3390/s21041337>
- [82] Rohan C, Audet J, Keating A. Small Split-Ring Resonators as Efficient Antennas for Remote LoRa IOT Systems-A Path to Reduce Physical Interference. *Sensors (Basel)*. 2021 Nov 23;21(23):7779. doi: 10.3390/s21237779. PMID: 34883783; PMCID: PMC8659506.
- [83] Ibrahim, N.F.; Dzabletey, P.A.; Kim, H.; Chung, J.-Y. An All-Textile Dual-Band Antenna for BLE and LoRa Wireless Communications. *Electronics* 2021, 10, 2967. <https://doi.org/10.3390/electronics10232967>
- [84] X. Wang, L. Xing and H. Wang, "A Wearable Textile Antenna for LoRa Applications," *2021 IEEE 4th International Conference on Electronic Information and Communication Technology (ICEICT)*, 2021, pp. 613-615, doi: 10.1109/ICEICT53123.2021.9531121.
- [85] Mira, F., Artiga, X., Llamas-Garro, I., Vázquez-Gallego, F., & Velázquez-González, J. S. (2021). Circularly Polarized Dual-Band LoRa/GPS Antenna for a UAV-Assisted Hazardous Gas and Aerosol Sensor. *Micromachines*, 12(4), 377. <https://doi.org/10.3390/mi12040377>
- [86] Abdulkawi WM, Sheta AFA, Elshafiey I, Alkanhal MA. Design of Low-Profile Single- and Dual-Band Antennas for IoT Applications. *Electronics*. 2021; 10(22):2766. <https://doi.org/10.3390/electronics10222766>
- [87] Singh, H.; Mittal, N.; Gupta, A.; Kumar, Y.; Woźniak, M.; Waheed, A. Metamaterial Integrated Folded Dipole Antenna with Low SAR for 4G, 5G and NB-IoT Applications. *Electronics* 2021, 10, 2612. <https://doi.org/10.3390/electronics10212612>
- [88] G. A. Casula, G. Muntoni, G. Montisci and H. Rogier, "An Eighth Mode Wearable Textile SIW Antenna for Lo-Ra and RFID Applications," *2021 6th International Conference on Smart and Sustainable Technologies (SpliTech)*, 2021, pp. 1-4, doi: 10.23919/SpliTech52315.2021.9566365.

- [89] N. A. H. Putra et al., "Design of Cubesat Microstrip Antenna with Metamaterial Structure for LoRa Communication," 2021 IEEE International Conference on Aerospace Electronics and Remote Sensing Technology (ICARES), 2021, pp. 1-5, doi: 10.1109/ICARES53960.2021.9665185.
- [90] Zaheer Ahmed Dayo, Muhammad Aamir, Shoaib Ahmed Dayo, Imran A. Khoso, Permanand Soothar, Fahad Sahito, Tao Zheng, Zhihua Hu, Yurong Guan. A novel compact broadband and radiation efficient antenna design for medical IoT healthcare system[J]. *Mathematical Biosciences and Engineering*, 2022, 19(4): 3909-3927. doi: 10.3934/mbe.2022180
- [91] M. Wagih and P. Birley, "Towards Improved IoT LoRa-WAN Connectivity using Broadband Omnidirectional Antennas," *2022 16th European Conference on Antennas and Propagation (EuCAP)*, 2022, pp. 1-5, doi: 10.23919/EuCAP53622.2022.9768906.
- [92] Hussain, R.; Alhuwaimel, S.I.; Algarni, A.M.; Aljaloud, K.; Hussain, N. A Compact Sub-GHz Wide Tunable Antenna Design for IoT Applications. *Electronics* 2022, 11, 1074. <https://doi.org/10.3390/electronics11071074>
- [93] R. Roges, P. K. Malik and S. Sharma, "A Compact Wideband Antenna with DGS for IoT Applications using LoRa Technology," *2022 10th International Conference on Emerging Trends in Engineering and Technology - Signal and Information Processing (ICETET-SIP-22)*, 2022, pp. 1-4, doi: 10.1109/ICETET-SIP-2254415.2022.9791725.
- [94] Mushtaq, A., Rajawat, A. & Gupta, S.H. Design of Antenna Array Based Beam Repositioning for IoT Applications. *Wireless Personal Communication*, 122, 3205–3225 (2022). <https://doi.org/10.1007/s11277-021-09046-2>
- [95] S. Robee, F. Gallée, J. -P. Coupez, D. Jakonis, V. Beni and S. Rioual, "A 868 MHz compact antenna with no impact of the material support," *2022 16th European Conference on Antennas and Propagation (EuCAP)*, 2022, pp. 1-5, doi: 10.23919/EuCAP53622.2022.9769344.

- [96] Nozha Zalfani, Sabri Beldi, Samer Lahouar, Kamel Besbes, "A miniaturized planar meander line antenna for UHF CubeSat communication", *Advances in Space Research*, Volume 69, Issue 5, 2022, Pages 2240-2247, ISSN 0273-1177, <https://doi.org/10.1016/j.asr.2021.11.043>.
- [97] Wang, Shuqi, and Huan Gao. "A Dual-Band Wearable Conformal Antenna Based on Artificial Magnetic Conductor." *International Journal of Antennas and Propagation* 2022 (2022).
- [98] http://www.mitspcb.com/catalog/mits_12_e.pdf
- [99] <https://www.everythingrf.com/rf-calculators/microstrip-width-calculator>
- [100] Dastranj A, Imani A, Naser-Moghaddasi M. Printed wide-slot antenna for wideband applications [J]. *IEEE Transactions on Antennas and Propagation*, 2008, 56(10): 3097-3102.
- [101] Jha, K.R.; Bukhari, B.; Singh, C.; Mishra, G.; Sharma, S.K. Compact Planar Multistandard MIMO Antenna for IoT Applications. *IEEE Trans. Antennas Propag.* 2018, 66, 3327–3336
- [102] Saghati, A.P.; Azarmanesh, M.; Zaker, R. A Novel Switchable Single- and Multifrequency Triple-Slot Antenna for 2.4-GHz Bluetooth, 3.5-GHz WiMax, and 5.8-GHz WLAN. *IEEE Antennas Wirel. Propag. Lett.* 2010, 9, 534–537.
- [103] Muddineni Raveendra, Saravanakumar U., Venkatesh Choppa, Palivela, Venkata Naga & Ravi Teja, "Design and Analysis of a Tunable Rectangular Microstrip Slot Antenna for Narrow Band Internet of Things Applications at 1800 MHz", In book: *Antenna Design for Narrowband IoT*, January 2022 DOI:10.4018/978-1-7998-9315-8.ch004
- [104] Best S.R and Morrow J.D "Limitations of inductive Circuit model representations of meander line antennas", vol.1, pp852-855, *IEEE Trans..Antennas and Propagation Society International Symposium*, June 2003.
- [105] Warnagiris T.J, and Minardo T.J, "Performance of a meandered line as an electrically small transmitting antennas "Antenna and Propagation , *IEEE Transaction on*, vol.46no.12pp.1797-1801. Dec 1998.

- [106] Shruti Sonawane, Dr. Hetal Patha, Sagar Mistry, “Design and Analysis of FPC (Flexible Printed Circuit) Antenna for LoRa frequency: 865 MHz - 867 MHz Application,” *International Journal of Scientific and Research Publications*, Volume 10, Issue 5, May 2020
- [107] Muhammad Aziz ul-Haq, Sławomir Koziół, —Design optimization and trade-offs of miniaturized wideband antenna for the internet of things applications, *Metrology, and measurement systems*, Vol. 24, No. 3, pp. 463–471, 2017.
- [108] L.H. Trinh, T.Q.K. Nguyen, D.D. Phan, V.Q. Tran, V.X Bui, N. V. Truong, F. Ferrero, Miniature Antenna for IoT Devices Using LoRa Technology, *International Conference on Advanced Technologies for Communications*, pp. 170-173, 2017.
- [109] L. Lizzi and F. Ferrero, — Use of ultra-narrow band miniature antennas for the internet of things applications, *Electronics Letters*, IET Publisher, Vol.51, Issue.24, pp.1964-1966, 2015.
- [110] M. Sharma, Y. K. Awasthi, H. Singh, R. Kumar, and S. Kumari, "Design of Compact Flower Shape Dual Notched-Band Monopole Antenna for Extended UWB Wireless Applications," *Frequent*, vol. 70, no. 11-12, 2016
- [111] Kaur and P. K. Malik, "Tri-State, T-Shaped Circular Cut Ground Antenna for Higher ‘X’ Band Frequencies," 2020 International Conference on Computation, Automation and Knowledge Management (ICCAKM), Dubai, United Arab Emirates, 2020, pp. 90-94.
- [112] Sneha.; Malik, P. K.; Bilandi, N.; Gupta, A. Narrow band-IoT and long-range technology of IoT smart communication: Designs and challenges. *Computers & Industrial Engineering* 2022. 172, 108572. <https://doi.org/10.1016/j.cie.2022.108572>
- [113] P. Syam Sundar, Sarat K Kotamraju, Sri Kavya K Ch, BTP Madhav, Y Srikanth, Narendra Babu,” pentagon shaped microstrip antenna for wireless IoT applications”, *Journal of Critical Reviews*, ISSN- 2394-5125, Vol 7, Issue 14, 2020.

- [114] P. Tiwari and P. K. Malik, "Design of UWB Antenna for the 5G Mobile Communication Applications: A Review," 2020 International Conference on Computation, Automation and Knowledge Management (ICCAKM), Dubai, United Arab Emirates, 2020, pp. 24-30
- [115] Prince Kumar, Girish Chandra Ghivela," Optimized N-Sided Polygon Shaped Microstrip Patch Antenna for UWB Application", IEEE,2019.
- [116] Liu, L.-L., et al., "A compact band-notch ultra-wideband antenna," 2017 International Workshop on Electromagnetics: Applications and Student Innovation Competition (iWEM), IEEE, 2017.
- [117] Ali, J., et al., "Ultra-wideband antenna design for GPR applications: A review," International Journal of Advanced Computer Science and Applications, Vol. 8, No. 7, 392–400, 2017
- [118] Cicchetti, R., E. Miozzi, and O. Testa, "Wideband and UWB antennas for wireless applications: A comprehensive review," International Journal of Antennas and Propagation, Vol. 2017, 2017.
- [119] Ahmed, F., N. Hasan, and M. H. M. Chowdhury, "A compact low-profile ultra wideband antenna for biomedical applications," International Conference on Electrical, Computer and Communication Engineering (ECCE), IEEE, 2017.
- [120] Franchina, V., et al., "A UWB antenna for X-band automotive applications," 2016 IEEE International Symposium on Antennas and Propagation (APSURSI), IEEE, 2016.
- [121] Gogikar S, Chilukuri S. A compact wearable textile antenna with dual band-notched characteristics for UWB applications. Paper presented at: 2019 IEEE-APS Topical Conference on Antennas and Propagation in Wireless Communications (APWC), Sep. 2019, pp. 426–430.
- [122] Ghaffar A, Awan WA, Zaidi A, Hussain N, Rizvi SM, Li XJ. Compact ultra wide-band and tri-band antenna for portable device. Radioengineering. 2020;29(4):601-608

- [123] Bong H-U, Jeong M, Hussain N, Rhee S-Y, Gil S-K, Kim N. Design of an UWB antenna with two slits for 5G/WLAN-notched bands. *Microw Opt Technol Lett.* 2019;61(5):1295-1300
- [124] Lu, Y., Y. Huang, Y. C. Shen, and H. T. Chattha, "A further study of planar UWB monopole antennas," *Proc. Loughbrough Antennas Propag. Conf. 2007*, 353–356, September 2009. *Progress In Electromagnetics Research C*, Vol. 119, 2022 273
- [125] Chan, K. C. L., Y. Huang, and X. Zhu, "A planar elliptical monopole antenna for UWB applications," *Proc. IEEE/ACES Int. Conf. Wireless Commun. Appl. Comput. Electromagn.*, 182–185, April 2005.
- [126] Chen, Z. N., M. J. Ammann, X. Qing, X. H. Wu, T. S. P. See, and A. Cat, "Planar antennas," *IEEE Microw. Mag.*, Vol. 7, No. 6, 63–73, December 2006.
- [127] Liang, J. X., C. C. Chian, X. D. Chen, and C. G. Parini, "Study of a printed circular disc monopole antenna for UWB systems," *IEEE Transactions on Antennas and Propagation*, Vol. 53, No. 11, 3500–3504, November 2005.
- [128] Bekasiewicz, A. and S. Koziel, "Structure and computationally efficient simulation-driven design of compact UWB monopole antenna," *IEEE Antennas and Wireless Propagation Letters*, Vol. 14, 1282–1285, 2015.
- [129] Hossain M, Faruque MRI, Islam MT (2016) Design of a patch antenna for ultra wide band applications. *Microwave Opt Technol Lett* 58(9):2152–2156
- [130] Liang J, Chiau CC, Chen X, Parini CG (2005) Study of a printed circular disc monopole antenna for UWB systems. *IEEE Trans Antennas Propag* 53(11):3500–3504
- [131] Low Z, Cheong J, Law C (2005) Low-cost PCB antenna for UWB applications. *IEEE Antennas Wireless Propag Lett* 4:237–239 7
- [132] Ling C-W, Lo W-H, Yan R-H, Chung S-J (2007) Planar binomial curved monopole antennas for ultrawideband communication. *IEEE Trans Antennas Propag* 55(9):2622–2624

- [133] “Arduino - Introduction.” <https://www.arduino.cc/en/guide/introduction> (accessed Jun. 27, 2020).
- [134] “Arduino Uno,” Wikipedia. Jun. 04, 2020, Accessed: Jun. 27, 2020. [Online]. Available: https://en.wikipedia.org/w/index.php?title=Arduino_Uno&oldid=960701078.
- [135] “Arduino - Environment.” <https://www.arduino.cc/en/guide/environment> (accessed Jun. 28, 2020).

APPENDIX 1

LIST OF ABBREVIATIONS

Abbreviations	Meaning
3GPP	Third-Generation Partnership Project
4G	Fourth Generation
AES	Advanced Encryption Standard
BLE	Bluetooth Low Energy
Cat-NB	Category- Narrow Band
CPW	Coplanar Waveguide
CSRR	Complementary Split Ring Resonator
CSS	Chirp Spread Spectrum
CST	Computer Simulation Technology
D2D	Device To Device
dB	Decibel
EM	Electromagnetic
FDMA	Frequency Division Multiple Access
FEM	Finite Element Method
FR	Frequency Reconfigurability
FR4	Fire-Retardant
FSK	Frequency Shift Keying
GHz	Giga- Hertz
GPS	Global Positioning System
GSM	Global System For Mobile Communication
HFSS	High-Frequency Structure Simulator
IDE	Integrated Development Environment
IoT	Internet Of Things
IP	Internet Protocol

ISM	Industrial, Scientific, And Medical
<u>LDE</u>	Light Emitting Diode
LoRa	Long Range
LPWA	Low Power Wide Area
LPWAN	Low Power Wide Area Network
LTE	Long Term Evolution
MEMS	Micro-Electro-Mechanical Systems
MHz	Mega-Hertz
MIMO	Multiple Input Multiple Output
MPA	Microstrip Patch Antenna
MSPA	Micro-Strip Patch Antenna
MTM	Metamaterial
NB-IoT	Narrow Band -Internet of Things
OFDMA	Orthogonal Frequency Division Multiple Access
OOK	On-Off Keying
PCB	Printed Circuit Board
PER	Packet Error Rate
PIFA	Planar Inverted F Antenna
PLR	Packet Loss Rate
PNA	Power Network Analyzer
QPSK	Quadrature Phase Shift Keying
RF	Radio Frequency
RFID	Radio-Frequency Identification
SBR	Shooting and Bouncing Rays
SMA	Sub Miniature Version A
TV	Television
UHF	Ultra High Frequency
UHF	Ultra High Frequency
USB	Universal Serial Bus

UWB	Ultra-Wide Band
VNA	Vector Network Analyzer
VSWR	Voltage Stand Wave Ratio
WAN	Wide Area Networks
Wi-Fi	Wireless-Fidelity
Wi-MAX	Worldwide Interoperability For Microwave Access
WLAN	Wireless Local Area Network

APPENDIX II

ANTENNA DESIGN AND MEASUREMENT TOOLS

A. Simulation Tool- “HFSS (High-Frequency Structure Simulator)”

The Ansys HFSS-15 is used “for designing and simulating high-frequency electronic structures like antennas, RF components”. It contains versatile solvers and GUI (Graphical User Interface). This tool consists of a combination of simulation, visualization, automation, and solid modeling. This software uses the Finite Element Method (FEM), excellent graphics, and meshing to provide good performance. HFSS solves any geometry with very accuracy of a FEM solver that has an Integral equation that is designed to solve open radiation and scattering problems, it also consists of a Shooting and Bouncing Rays(SBR) Solver and adapts meshing techniques to solve the geometry with accuracy.

HFSS is a very powerful tool, and with time it is upgraded to a better version of itself. Many unlimited capabilities of the HFSS make the designing and simulation process more accurate. Some of its capabilities are as follows:

- i. Complex design problems can be solved easily.
- ii. The export file result data can be used for comparison purposes.
- iii. Flexibility in the addition of material or components is available.
- iv. A variable solution setup is available.
- v. Meshing can be redefined and can be done for a specific area.
- vi. Various tool kits are available in the latest version of HFSS.
- vii. Both far-field and near-field sources are available.

Antenna Designing Steps

- i. Create the ground plane
- ii. Create the substrate and assign dimensions after calculating with mathematical expressions

- iii. Assign dielectric material
- iv. Create the patch and assign dimensions to catch after mathematical calculations
- v. Create a feed line with proper dimensions
- vi. Unite the structure i.e. Patch with feed-line
- vii. Assign perfect boundary conditions to patch, ground plane
- viii. Assign port (Lumped or Wave) to antenna structure to couple electromagnetic energy
- ix. Create a radiation box and assign the Radiation boundary to the radiation box. All the steps are mentioned in the flowchart in Figure II.1.

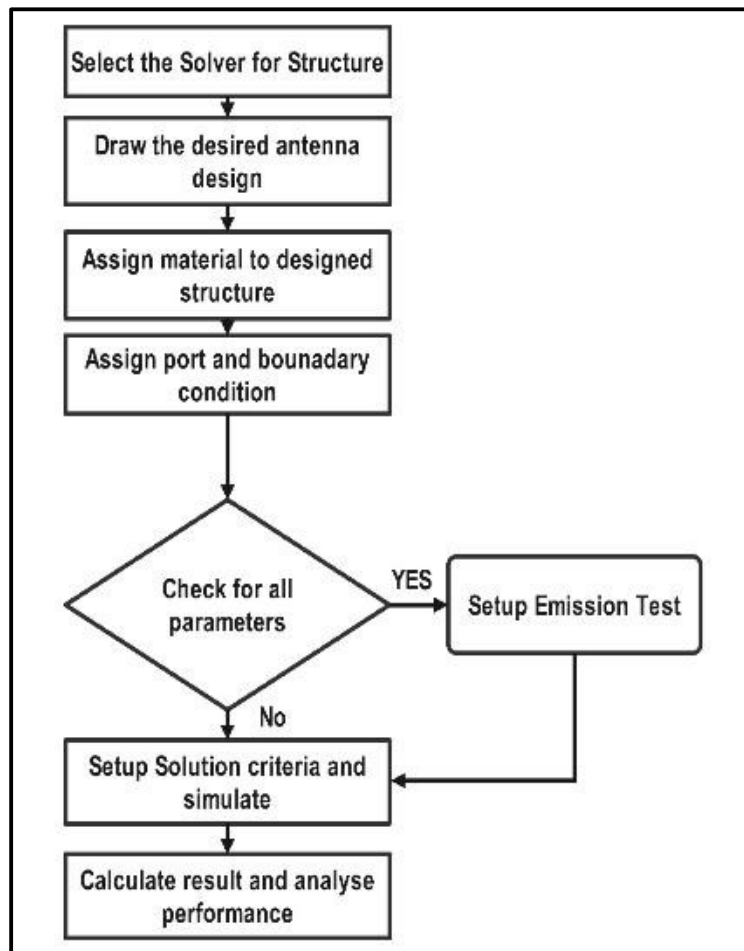


Figure II.1: Ansys HFSS simulation procedure for Antenna designing

B. Fabrication Tool- PCB Prototype Machine

For the fabrication of the designed antenna, a PCB prototyping machine is used, which is manufactured by MITS Eleven Lab as shown in Figure II.2. It offers very cost-effective and easy fabrication of microstrip patch antennas (PCB antennas). It is operated by a desktop with the help of its software PCAM, where anyone can easily upload dxf or Gerber files, verify their design, and command the machine to fabricate the uploaded design. It is equipped with some functions that help in designing patch antennas like drilling, routing, milling, tracking, tracing, and many more. Its working area in terms of the X/Y/Z axis is 229mm X 320mm X 10mm and it has an XYZ axis control system. It has several drilling and milling tools (width) that can be changed as per our requirements. The designing process can be observed accurately using the camera available with the motor. It can also be used to place the drilling pin at the exact position. The spindle speed can vary from 5000 rpm to 41000 rpm. It is outfitted with a higher-quality pressure foot, which improves milling width consistency and vacuum cleaning efficiency.



Figure II.2 PCB prototyping machine by eleven labs [98].

C. Antenna Parameter Measurement Tool

(a) Vector Network Analyser (VNA)

A VNA is used to measure the frequency response of active or passive components or networks; or it is an electronic instrument that is used to measure the frequency-dependent properties of a device under test (DUT), as shown in Figure II.3. This measurement can be carried over a range of frequencies starting from a few kHz to hundreds of GHz. VNA measures power going into and reflected from a component and network at high frequencies. A signal's electrical properties can be analyzed in terms of incident, reflected, and transmitted signals, so the impedance of DUT can be calculated. The ratio of incident and reflected waves is defined in the form of S parameters, also called scattering parameters. Using VNA, both the amplitude and phase of frequency signals can be measured at each frequency point. Also, the insertion loss and return loss of the device under test can be visualized by the computer used in VNA in different formats.

For $|S_{11}|$ (dB) parameter measurement, the following setup as given in Figure II.4 is considered, using a 2-port VNA to measure S-Parameters of the DUT. Before measuring the device under test in VNA, it should be calibrated. Calibration means all the undesired signal reflections that will occur due to connecting cables and end terminals of connectors C1 and C2 as shown in the figure, must be considered and nullified. After calibration, measurement can be done. When Port1 can be used as a source for RF and a_1 is considered as an incident voltage wave on the DUT, then b_1 and b_2 will be the reflected waves and transmitted waves through the DUT, respectively. An incident wave propagates from the analyzer to DUT, and a reflected wave travels in the opposite direction from DUT to an analyzer. As the phase and amplitude of a_1 are known, the phase and amplitude of b_1 and b_2 can be measured using VNA. S-parameters give a very accurate representation of the linear characteristics of the device under test. It describes how the device interacts with other devices when cascaded with them. Reflection coefficient (Γ) or $|S_{11}|$ (dB) is given as follows in Figure II.4 and can be calculated using expressions (II.1) and (II.2);

The equation for the scattering parameter is

$$S_{11} = \left. \frac{b_1}{a_1} \right|_{a_2=0} \quad S_{12} = \left. \frac{b_1}{a_2} \right|_{a_1=0} \quad (\text{II.1})$$

$$S_{21} = \left. \frac{b_2}{a_1} \right|_{a_2=0} \quad S_{22} = \left. \frac{b_2}{a_2} \right|_{a_1=0} \quad (\text{II.2})$$

“ S11 voltage reflection coefficient at the input port., S12 reverse voltage gain,
S21 forward voltage gain, S22 voltage reflection coefficient at the output port ”.



Figure II.3: The photograph of the VNA which is used to measure the return

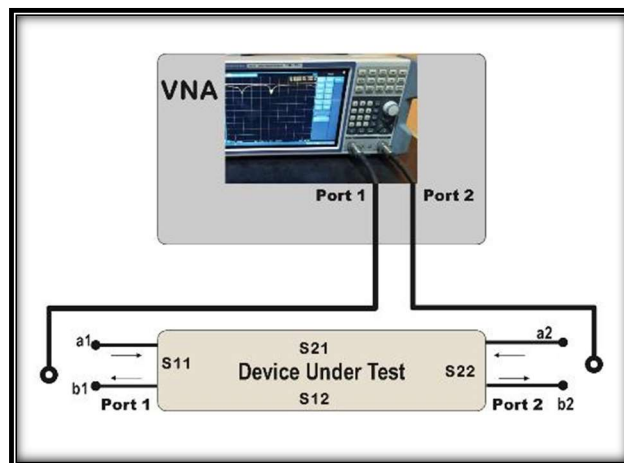


Figure II.4: VNA Setup for $|S_{11}|$ (dB) parameter measurement and $|S_{11}|$ (dB) parameter representation.

(b) Anechoic Chamber

The gain and radiation pattern measurements are done in an anechoic chamber. The anechoic chamber is well equipped with the antenna positioner, pattern recorder, VNA, signal generator, desktop, and one reference antenna with known gain. Here we used a “ridged horn antenna”. “The distance between the antenna under the test and the reference antenna is 5.2m” (size of the anechoic chamber of IIT BHU). The most important parameter of a radiator is the gain that represents the performance of the antenna. Usually, free-space ranges are used to measure the gain above 1 GHz. But as the free space region is not easily available so the anechoic chamber is used as a free space region for gain and pattern measurement of the antenna. “The gain and radiation pattern measurements are done in IIT BHU, under the guidance of Prof. Meshram Sir and Research Scholar Rahul Dubey”. The photograph of the anechoic chamber is shown in Figure II.5.

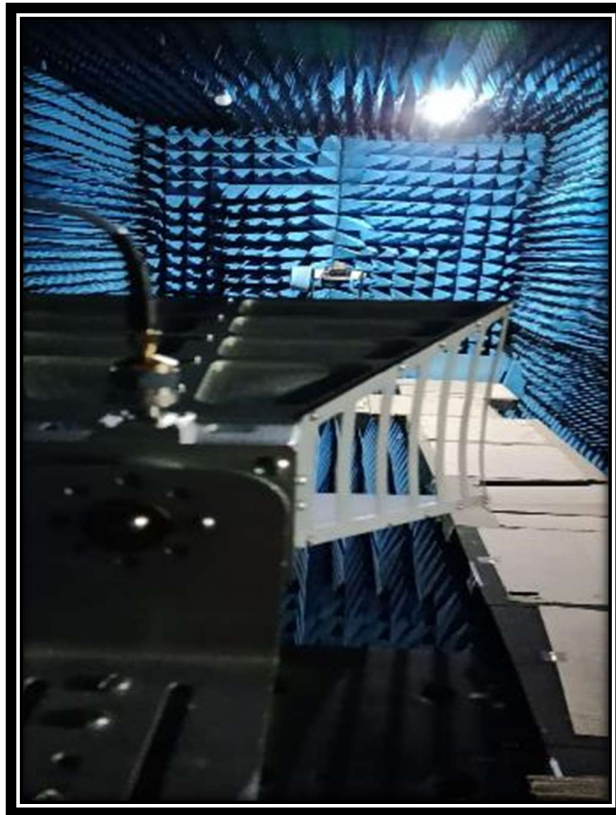


Figure II.5: The photograph of reference antenna and antenna under test in an anechoic chamber.

Here we have used the **Gain Comparison method** for determining the Gain.

Another method to measure gain is the gain comparison method, in which we have one reference antenna whose gain is known and then “ the power received by the standard gain antenna and the test antenna is measured, respectively, under the same conditions” [6]. The block diagram of the typical antenna gains and radiation pattern measurement system is mentioned in Figure II.6. The following relation [II.4] is used from gain can be determined.

$$G_T = \frac{P_T(1-|\Gamma_s|)^2}{P_S(1-|\Gamma_T|)^2} G_S \quad (\text{II.3})$$

$$(G_T)dB = (G_S)dB + 10\log_{10}\left(\frac{P_T}{P_S}\right) - 10\log_{10}\left(\frac{1-|\Gamma_s|^2}{1-|\Gamma_T|^2}\right) \quad (\text{II.4})$$

G_T = Test antenna gain

G_S = Gain of the source antenna

P_T = power received by test antenna

P_S = power received by source antenna

Γ_T = reflection coefficient of the test antenna

Γ_s = reflection coefficient of the source antenna

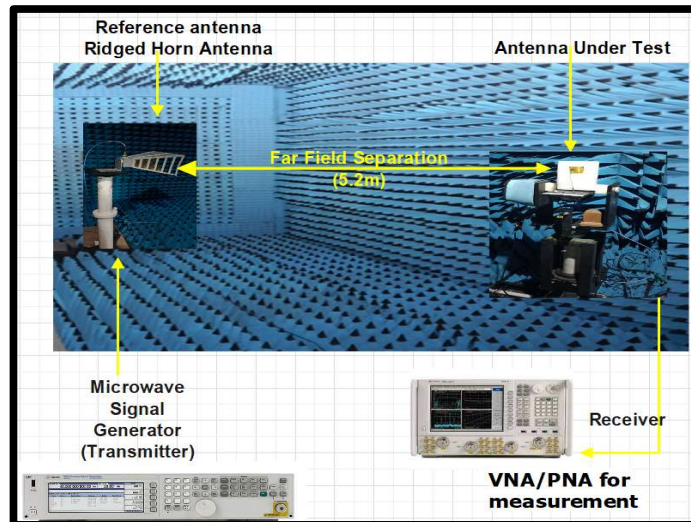


Figure II.6: Representation of Antenna-Measurement System

LIST OF PUBLICATION

1. Sneha, Suraj P, "A Metamaterial based Monopole antenna for Satellite-based Navigation Applications", **International Journal of Intelligent Communication, Computing and Networks**, Vol 1, Issue 1, PP 010-014, Aug 2020, <https://doi.org/10.51735/ijiccn/001/07>
2. Sneha, Praveen Malik, "A Brief Review Analysis on NB-IoT Antenna", **Test Engineering and Management**, Vol 83, PP 27288-27292, March-April 2020.
3. Sneha, Praveen Malik, Naveen Bilandi, Anish Gupta, "Narrow Band-IoT and Long-Range Technology of IoT Smart Communication: Designs and Challenges", **Computers & Industrial Engineering**, 2022, 108572, ISSN 0360-8352, <https://doi.org/10.1016/j.cie.2022.108572>.
4. Sneha, Praveen Malik, Sudipta Das, Syed Inthiyaz "Long-Range Technology-Enabled Smart Communication: Challenges and Comparison", **Journal of Circuits, Systems, and Computers**, Dec, 2022, <https://doi.org/10.1142/S021812662350161X>
5. Sneha, Praveen Malik, Rohit Sharma, Uttam Ghosh, Waleed S Alnumay, "Internet of Things and Long-Range Antenna's; Challenges, Solutions and Comparison in Next Generation Systems", **Microprocessors and Microsystems**, Sep 2023, 104934, ISSN 0141-9331, <https://doi.org/10.1016/j.micpro.2023.104934>.

LIST OF CONFERENCE

1. Sneha, Dr. Praveen Kumar Malik, and Rashmi Roges, "A Symmetric Slotted Microstrip Patch Antenna for NB-IoT Technology", 7th International Conference on Nanoelectronics, Circuits & Communication Systems (NCCS-2021) published by Springer, Ranchi, Jan 29-30, 2022. UNDER PROCEEDING
2. Sneha, Dr. Praveen Kumar Malik, "A study and design of flexible planar antenna with different substrates for Long Range Applications", 6th International Conference on Micro-Electronics and Telecommunication Engineering (ICMETE-2022), 23-24 Sep 2022, under proceeding
3. Sneha, Dr. Praveen Kumar Malik, Dr. Anita Gehlot, "A key-shaped ultra-wideband antenna for IoT applications", Artificial Intelligence and Smart Communication (AISC-2023), 27-29 Jan 2023.
4. H. Bedi, R. Roges, P. K. Goel, Sneha, P. K. Malik and S. V. Akram, "Artificial Intelligence-based Recommendations in Wildlife Sustainability," 2023 4th International Conference on Electronics and Sustainable Communication Systems (ICESC), Coimbatore, India, 2023, pp. 1670-1675, doi: 10.1109/ICESC57686.2023.10192970.
5. P. Malik, Sneha, D. Garg, H. Bedi, A. Gehlot and P. K. Malik, "An Improved Agriculture Farming Through the Role of Digital Twin," 2023 4th International Conference on Electronics and Sustainable Communication Systems (ICESC), Coimbatore, India, 2023, pp. 667-671, doi: 10.1109/ICESC57686.2023.10193522.
6. A. Singhal, Sneha, H. Kaur, A. S. Duggal, P. K. Malik and R. Singh, "Emerging Technologies in the Fish Farming by Deploying Artificial Intelligence," 2023 4th International Conference on Electronics and Sustainable Communication Systems (ICESC), Coimbatore, India, 2023, pp. 1666-1669, doi: 10.1109/ICESC57686.2023.10193206.

LIST OF PATENTS

1. **Patent Title-** Key Shaped Broadband Microstrip Antenna for Wireless Applications.

Patent ID- 202111052709

Filing Date - 17th Nov2021 and Publishing Date- 26th Nov 2021

2. **Patent Title-** A meandered patch antenna for long-range (LoRa) application.

Patent ID- 202211034193

Filing Date- 15th June 2022 and Publishing Date- 24th June 2022